AD-A130 824 FINDING EDGES AND LINES IN IMAGES(U) MASSACHUSETTS INST 1/2
OF TECH CAMBRIDGE ARTIFICIAL INTELLIGENCE LAB
J F CANNY JUN 83 AI-TR-720 N00014-80-C-0505
UNCLASSIFIED F/G 20/6 NL

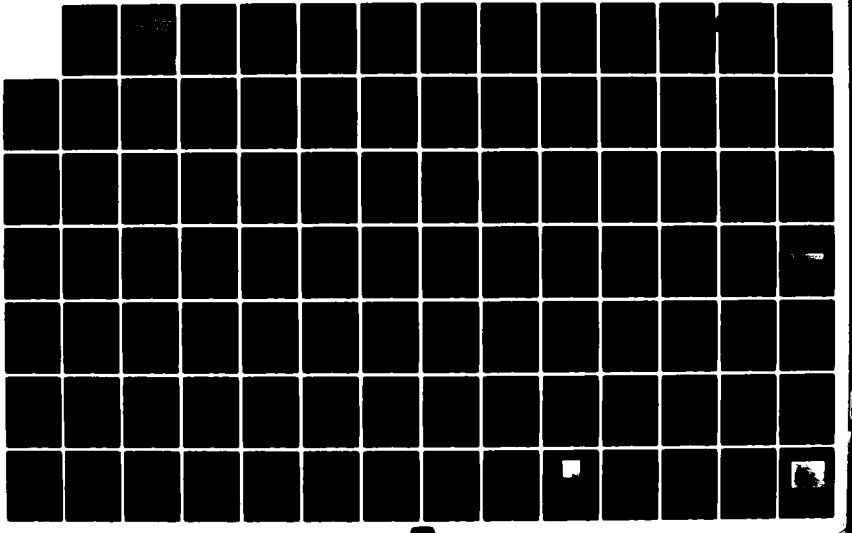

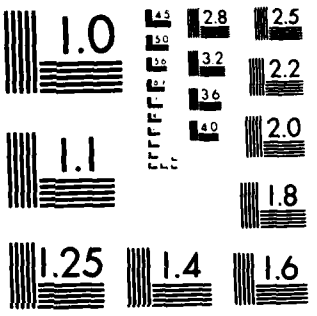

Technical Report No. 720

Finding Edges and Lines in Images

John Francis Canny

MIT Artificial Intelligence Laboratory

UNCLASSIFIED

SECURITY CLASSIFICATION OF THIS PAGE *(When Data Entered)*

REPORT DOCUMENTATION PAGE		READ INSTRUCTIONS BEFORE COMPLETING FORM
1. REPORT NUMBER AI-TR-720	2. GOVT ACCESSION NO. AD-A130 824	3. RECIPIENT'S CATALOG NUMBER
4. TITLE *(and Subtitle)* Finding Edges and Lines in Images		5. TYPE OF REPORT & PERIOD COVERED Technical Report 6. PERFORMING ORG. REPORT NUMBER
7. AUTHOR(s) John Francis Canny		8. CONTRACT OR GRANT NUMBER(s) N00014-80-C-0505
9. PERFORMING ORGANIZATION NAME AND ADDRESS Artificial Intelligence Laboratory 545 Technology Square Cambridge, Massachusetts 02139		10. PROGRAM ELEMENT, PROJECT, TASK AREA & WORK UNIT NUMBERS
11. CONTROLLING OFFICE NAME AND ADDRESS Advanced Research Projects Agency 1400 Wilson Blvd Arlington, Virginia 22209		12. REPORT DATE June 1983 13. NUMBER OF PAGES 146
14. MONITORING AGENCY NAME & ADDRESS*(if different from Controlling Office)* Office of Naval Research Information Systems Arlington, Virginia 22217		15. SECURITY CLASS. *(of this report)* UNCLASSIFIED 15a. DECLASSIFICATION/DOWNGRADING SCHEDULE

16. DISTRIBUTION STATEMENT *(of this Report)*

Distribution of this document is unlimited.

17. DISTRIBUTION STATEMENT *(of the abstract entered in Block 20, if different from Report)*

18. SUPPLEMENTARY NOTES

None

19. KEY WORDS *(Continue on reverse side if necessary and identify by block number)*

Edge Detection
Machine Vision
Feature Extraction
Image Processing
Image Understanding

20. ABSTRACT *(Continue on reverse side if necessary and identify by block number)*

The problem of detecting intensity changes in images is canonical in vision. Edge detection operators are typically designed to optimally estimate first or second derivative over some (usually small) support. Other criteria such as output signal to noise ratio or bandwidth have also been argued for. This thesis is an attempt to formulate a set of edge detection criteria that capture as directly as possible the desirable properties of an edge operator. Variational techniques are used to find a solution over the space of all →(over)

DD FORM 1 JAN 73 1473 EDITION OF 1 NOV 65 IS OBSOLETE
S/N 0102-014-6601

UNCLASSIFIED

SECURITY CLASSIFICATION OF THIS PAGE *(When Data Entered)*

linear shift invariant operators. The first criterion is that the detector have low probability of error i.e. failing to mark edges or falsely marking non-edges. The second is that the marked points should be as close as possible to the centre of the true edge. The third criterion is that there should be low probability of more than one response to a single edge. The technique is used to find optimal operators for step edges and for extended impulse profiles (ridges or valleys in two dimensions). The extension of the one dimensional operators to two dimensions is thendiscussed. The result is a set of operators of varying width, length and orientation. The problem of combining these outputs into a single description is discussed, and a set of heuristics for the integration are given.

This report describes research done in the Artificial Intelligence Laboratory of the Massachusetts Institute of Technology. Support for the laboratory's artificial intelligence research is provided in part by the Advanced Research Projects Agency of the Department of Defense under Office of Naval Research contract N00014-80-C-0505 and in part by the System Development Foundation.

FINDING EDGES AND LINES IN IMAGES

by

John Francis Canny

Massachusetts Institute of Technology

June 1983

Revised version of a thesis submitted to the Department of Electrical Engineering and Computer Science on May 12, 1983 in partial fulfillment of the requirements for the Degree of Master of Science.

Abstract

The problem of detecting intensity changes in images is canonical in vision. Edge detection operators are typically designed to optimally estimate first or second *derivative over some* (usually small) *support*. Other criteria such as output signal to noise ratio or bandwidth have also been argued for. This thesis is an attempt to formulate a set of edge detection criteria that capture as directly as possible the desirable properties of an edge operator. Variational techniques are used to find a solution over the space of all linear shift invariant operators. The first criterion is that the detector have low probability of error i.e. failing to mark edges or falsely marking *non*-edges. The second is that the marked points should be as close as possible to the centre of the true edge. The third criterion is that there should be low probability of more than one response to a single edge. The technique is used to find optimal operators for step edges and for extended impulse profiles (ridges or valleys in two dimensions). The extension of the one dimensional *operators* to two dimensions is then discussed. The result is a set of operators of varying width, length and orientation. The problem of combining these outputs into a single description is discussed, and a set of heuristics for the integration are given.

Thesis Supervisor: Dr. J. Michael Brady

Title: Senior Research Scientist

Acknowledgements

First of all I must thank my supervisor, Mike Brady, whose enthusiasm for this work was almost infinite, and who compensated for my reluctance to consult the literature. Mike also contributed valuable feedback as the major user of the system.

Thanks to the readers Eric Grimson and Rod Brooks, and especially to Berthold Horn for his extensive comments on the thesis proposal.

I would also like to thank all of the "vision" people, especially Tommy Poggio, Alan Yuille and Ellen Hildreth for discussions at various times.

I thank the Macsyma Consortium for the complexity of equations I was able to produce, and for the speed with which I was able to try new ideas.

My thanks to Patrick Winston and to the System Development Foundation for their current support, and to ITT for providing the Fellowship support which enabled me to be here.

Table of Contents

1. Introduction

Edge detection forms the first stage in a very large number of vision modules, and any edge detector should be formulated in the appropriate context. However, the requirements of many modules are similar and it seems as though it should be possible to design one edge detector that performs well in several contexts. The crucial first step in the design of such a detector should be the specification of a set of performance criteria that capture these requirements. The specification of these criteria and the derivation of optimal operators from them forms the subject of this report.

The operation of the edge detector is best illustrated by the example in figure (1.1), which was produced by the detector described in this report. The detector accepts discrete digitized images and produces an "edge map" as its output. The edge map includes explicit information about the position and strength of edges, their orientation, and the "scale" at which the change took place. Although they are not made explicit, it is also possible to compute the uncertainty in position or strength of an edge from the quantites in the edge map. The example in figure (1.1) includes position information only.

A digitized image contains a great deal of redundancy. There is redundancy in the information theoretic sense (it is possible to compress the sampled data into fewer bits without changing the reconstructed image significanty). Even after efficient encoding, much of the what remains is not useful to later vision modules. These modules typically require structural information, i.e. details of surface orientation and the material of which the visible surfaces comprise. Where the surfaces are smooth and of uniform reflectance, shape from shading (Horn 1975) may be applied to obtain surface orientation. In many other modules such as shape from motion (Ullman 1979 and Hildreth 1983), shape from contour (Stevens 1980), shape from texture (Witkin 1980), and Stereo (Marr and Poggio 1979, Grimson 1981) structural properties of underlying surfaces are inferred from edge contours. In particular, step changes in intensity are important because they typically correspond to sharp changes in orientation or material, or to object boundaries. Edge detection is a

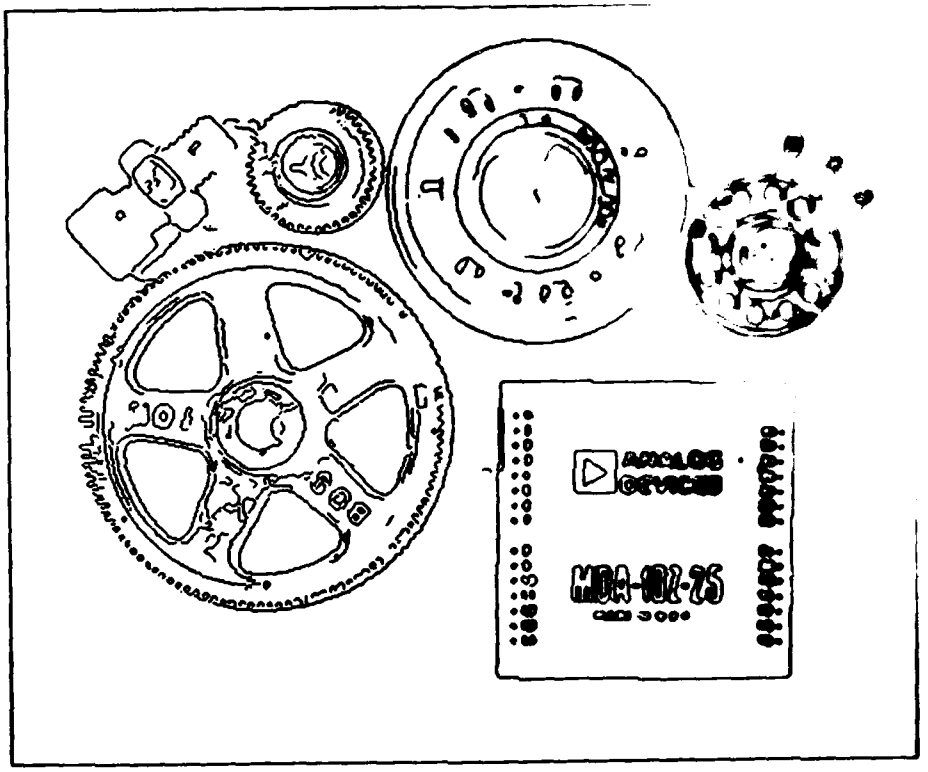

Figure 1.1. Positional information provided by the edge detector applied to an image of some mechanical parts

... space descriptions which preserve most of the structural ... image.

... formulations have chosen the first or second derivative as the ... step edges, and have formed optimal estimates ... Examples of first derivative operators are the ... Macleod (1970), while Modestino and Fries (1977) ... the two dimensional Laplacian over a large support. ... suggested the Laplacian of a broad Gaussian since it ... and bandwidth. There are problems with the ... concept of derivative estimation seems to have ... this will be made specific in chapter 7.

... class of formulations in which the image surface is ... basis functions and the edge parameters are estimated ... surface. Examples of this technique include the work of ... 1971 and Haralick (1982). These methods allow more ... edge properties such as position and orientation, but since the ... are usually not complete, the properties apply only to a projection ... image surface on to the subspace spanned by the basis functions. ... basis functions are a major factor in operator performance, especially ... to localize edges.

... this report we begin with a traditional model of a step edge in white Gaussian noise and try to formulate precisely the criteria for effective edge detection. We assume that detection is performed by convolving the noisy edge with a spatial function $f(x)$ (which we are trying to find) and by marking edges at the maxima in the output of this convolution. We then specify three performance criteria on the output of this operator.

(i) Good detection. There should be a low probablity of failing to mark real edge points, and low probability of falsely marking non-edge points. Since both these probabilities are monotonically decreasing functions of the output signal to noise ratio, this criterion corresponds to maximizing signal to noise ratio.

(ii) Good localization. The points marked as edges by the operator should be as close as possible to the centre of the true edge.

(iii) Only one response to a single edge. This is implicitly captured in (i) since when two nearby operators respond to the same edge, one of them must be considered a false edge. However, the mathematical form of the first criterion did not capture the multiple response requirement and it had to be made explicit.

The first result of the analysis for step edges is that (i) and (ii) are conflicting and that there is a trade-off or uncertainty principle between them. Broad operators have good signal to noise ratio but poor localization and vice-versa. A simple choice of the mathematical form for the localization criterion gives a product of a localization term and signal to noise ratio that is constant. Spatial scaling of the function $f(x)$ will change the individual values of signal to noise ratio and localization but not their product. Given the analytic form of a detection function, we can theoretically obtain arbitrarily good signal to noise ratio or localization from it by scaling, but not simultaneously. From the analysis we can conclude that there is a single best shape for the function f which maximizes the product and that if we scale it to achieve some value of one of the criteria, it will simultaneously provide the maximum value for the other. To handle a wide variety of images, an edge detector needs to use several different widths of operator, and to combine them in a coherent way. By forming the criteria for edge detection as a set of functionals of the unknown operator f, we can use variational techniques to find the function that maximizes the criteria.

The second result is that the criteria (i) and (ii) by themselves are inadequate to produce a useful edge detector. It seems that we can obtain maximal signal to noise ratio and *arbitrarily* good localization by using a difference of boxes operator. The difference of boxes (see figure 2.2) was suggested by Rosenfeld and Thurston (1971) and was used by Herskovits and Binford (1970). If we look closely at the response of such an operator to a noisy step edge we find that there is an output maximum close to the centre of the edge, but that there may be many others nearby. We have not achieved good localization because there is no way of telling

which of the maxima is closest to the true edge. The addition of criterion (iii) gives an operator that has very low probability of giving more than one maximum in response to a single edge, and it also leads to a finite limit for the product of localization and signal to noise ratio.

The third result is an analytic form for the operator. It is the sum of four complex exponentials and can be approximated by the first derivative of a Gaussian. A numerical finite dimensional approximation to this function was first found using a stochastic hill-climbing technique. This was done because it was much easier to write the multiple response criterion in deterministic form for a numerical optimization than as a functional of f. Specifically, the numerical optimizer provides candidate outputs for evaluation, and it is a simple matter to count the number of maxima in one of the outputs. To express this constraint analytically we need to find the expectation value of the number of maxima in the response to an edge, and to express this as a functional on f, which is much more difficult. The first derivative of a Gaussian has been suggested before (Macleod 1970). It is also worth noting that in one dimension the maxima in the output of this first derivative operator correspond to zero-crossings in the output of a second derivative operator.

Several further results relate to the extension of the operator to two (or more) dimensions. They can be summarized roughly by saying that the detector should be directional, and if the image permits, the more directional the better. The issue of non-directional (Laplacian) versus directional edge operators has been the topic of debate for some time, compare for example Marr (1976) with Marr and Hildreth (1980). To summarize the argument presented here, a directional operator can be shown to have better localization than the Laplacian, signal to noise ratio is better, the computational effort required to compute the directional components is slight if efficient algorithms are used, and finally the problem of combining operators of several orientations is difficult but not intractable. It is, for example, much more difficult to combine the outputs of operators of different sizes, since their supports differ markedly. For a given operator width, both signal to noise ratio and localization improve as the length of the operator (parallel to the edge) increases, provided of course that the edge does not deviate from a straight line. When

the image does contain long approximately straight contours, highly directional operators are the best choice. This means several operators will be necessary to cover all possible edge orientations, and also that less directional operators will also be needed to deal with edges that are locally not straight.

The problem of combining the different operator widths and orientations is approached in an analogous manner to the operator derivation. We begin with the same set of criteria and try to choose the operator that gives good signal to noise ratio and best localization. We set a minimum acceptable error rate and then choose the smallest operator with greater signal to noise than the threshold determined by the error rate. In this way the global error rate is fixed while the localization of a particular edge will depend on the local image signal to noise ratio. The problem of choosing the best operator from a set of directional operators is simpler, since only one or two will respond to an edge of a particular orientation. The problem of choosing between a long directional operator and a less directional one is theoretically simple but difficult in practice. Highly directional operators are clearly preferable, but they cannot be used for locally curved edges. It is necessary to associate a goodness of fit measure with each operator that indicates how well the image fits the model of a linearly extended step. When the edge is good enough the directional operator output is used and the output of less directional neighbours is suppressed.

While the detection of step edges is the primary goal of the report, chapter 4 gives a general form for the optimality criteria. Using this general form, it is possible to design optimal operators for arbitrary features. A numerical optimization is used to find the impulse response of the operator given an input waveform to be detected. The technique is illustrated by the derivation of operators for ridge, roof and step edges. Of these the ridge and step detectors have been tested on real images. The particular problems of extending the one-dimensional ridge operator to two dimensions, and the problem of integrating the step and ridge detector outputs are discussed.

Following the analysis we outline some simple experiments which seem to indicate that the human visual system is performing similar selections (at some

computational level), or at least that the computation that it does perform has a similar set of goals. We find that adding noise to an image has the effect of producing a blurring of the image detail, which is consistent with there being several operator sizes. More interestingly, the addition of noise may enable perception of changes at a large scale which, even though they were present in the original image, were difficult to perceive because of the presence of sharp edges. Our ability to perceive small fluctuations in edges that are approximately straight is also reduced by the addition of noise, but the impression of a straight edge is not.

As a guide to the reader, chapters 2 and 3 form the core of the analysis for step edges. They also contain most of the signal theory, and the general reader may wish to skim over them. The first section of chapter 3 should be read however, as it includes the translation of the theoretical operator into a practical algorithm. Chapter 4 is easier going and contains a more general form for the optimality criteria. It gives examples of the solution of the variational problem for roof and ridge edges. Chapter 5 is titled "details of implementation" and it may be tempting to avoid it as being too low-level. However it contains several efficient algorithms for Gaussian convolution, and may have applications outside the scope of the present work. Finally, chapters 6 and 7 give weight to the analysis by showing the performance of the operator on real images and by comparing it both experimentally and theoretically with some other edge detectors.

2. One-Dimensional Formulation for Step Edges

The basic design problem is illustrated in figure (2.1). We are trying to detect a step edge which is bathed in Gaussian noise, figure (2.1a). We convolve with some spatial function (2.1b) and mark edges at maxima in the result of this convolution (2.1c). The objective is to find the spatial function (call it f) which gives the "best" output, where best is defined by a precise set of criteria on step edge detection.

Some preliminaries on notation ; when we speak of an edge detection "operator" we mean a mapping from a one or two dimensional intensity function (the image or a linear slice through it) to an intensity function of the same dimension. If the operator is linear and shift invariant, then it can be represented by a convolution of the intensity function with the "impulse response" (one dimension) or "point-spread function" (two dimensions) of the operator, which is the result of applying the operator to a unit impulse at the origin. Shift invariance is clearly a desirable property of an edge operator. To begin with we will consider only linear shift invariant operators and later we will apply decision procedures to their outputs, which will lead to shift invariant non-linear operators. The operator that describes the mapping from an image to the final representation of edge contours is called the "edge detector".

The key to the design of an effective edge operator is the accurate evaluation of its performance. If we can write down the evaluation function in closed mathematical form, we can apply standard tools such as the calculus of variations to find the operator that maximizes it. As with many optimization problems, the key to obtaining a useful answer is to ask the right questions. The edge detection problem is no exception, as should become apparent in the course of the derivation. Several passes at the evaluation function had to be made before one was found that closed all the "loopholes" and excluded operators that were impractical for "obvious" reasons. This is not to say that the problem became one of finding a question to fit a proposed solution, but rather that the question was always the same, it was just very difficult to express in a closed form that was simple enough to yield a variational problem that could be solved. By way of contrast, it was relatively easy to obtain a similar solution using a Monte Carlo optimization, because the

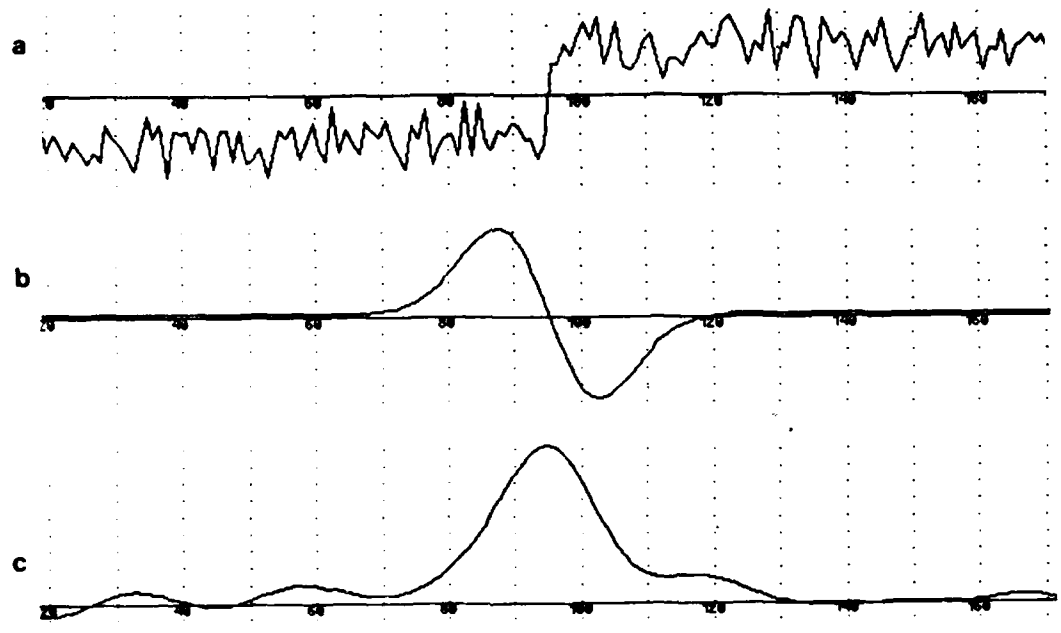

Figure 2.1. (a) The step edge model, (b) The detection function to be derived, (c) The result of the convolution of this function with the edge.

---

evaluation could be done directly on the output of a candidate operator. The real problem then, was the translation of the intuitive performance goals to functionals that depended directly on the form of the operator. This section describes the main stages in the translation process.

2.1. An Uncertainty Principle

We consider first the one dimensional edge detection problem. The goal is to detect and mark step changes in a signal that contains additive white noise. We assume that the signal is flat on both sides of the discontinuity, and that there are no other edges close enough to affect the output of the operator (see figure 2.1). We need to somehow combine the two goals of accurate detection and localization into a single evaluation functional. The detection criterion is simple to express in terms of the signal to noise ratio in the operator output, i.e. the ratio of the output in response to the step input to the output in response to the noise only. The localization criterion is more difficult, but a reasonable choice is the inverse of the distance between the true edge and the edge marked by the detector. For the distance measure we will use the standard deviation in the position of the maximum of the operator output. By using local maxima we are making what seems to be an arbitrary choice in the mapping from linear operator output to detector output. But the mapping must involve some local predicate, and since we are designing a linear operator that will respond strongly to step edges, the maxima in its response are a logical choice.

Let the amplitude of the step be A, and let the noise be $n(x)$. Then the input signal $I(x)$ can be represented as

$$I(x) = Au_{-1}(x) + n(x) \tag{2.1}$$

where $u_{-1}(x)$ is the unit step function defined as

$$u_{-1}(x) = \begin{cases} 0, & \text{for} \quad x < 0 \\ 1, & \text{for} \quad x \geq 0 \end{cases}$$

Let the impulse response of the operator we are seeking be represented by the function $f(x)$. Then the output $O(x_0)$ of the application of the operator to the input $I(x)$ is given by the convolution integral,

$$O(x_0) = \int_{-\infty}^{+\infty} I(x) f(x_0 \qquad dx \tag{2.2}$$

We can use the linearity of convolution to split this integral into contributions due to the step and to noise only. The output due to the step only is (at the centre of the step, i.e. at $x_0 = 0$)

$$\int_{-\infty}^{+\infty} f(x) A u_{-1}(-x)\, dx = A \int_{-\infty}^{0} f(x)\, dx \tag{2.3}$$

While the mean squared response to the noise component only will be

$$E\left[\int_{-\infty}^{+\infty} f(x) n(-x)\, dx\right]^2$$

where $E[y]$ is the expectation value of y. If the noise is white the above simplifies to

$$E\left[\int_{-\infty}^{+\infty} f^2(x) n^2(-x)\, dx\right] = n_0^2 \int_{-\infty}^{+\infty} f^2(x)\, dx$$

where $n_0^2 = E[n^2(x)]$ for all x, i.e. n_0^2 is the variance of the input noise. We define the output signal-to-noise ratio as the quotient of the response to the step only and the *square root* of the mean squared noise response.

$$S.N.R. = \frac{A \int_{-\infty}^{0} f(x)\, dx}{n_0 \sqrt{\int_{-\infty}^{+\infty} f^2(x)\, dx}}$$

From this expression we can define a measure Σ of the signal to noise performance of the *operator* which is independent of the input signal

$$S.N.R. = \frac{A}{n_0}\Sigma \qquad \text{and} \qquad \Sigma = \frac{\int_{-\infty}^{0} f(x)\, dx}{\sqrt{\int_{-\infty}^{+\infty} f^2(x)\, dx}} \tag{2.5}$$

This then is the first part of our dual criterion, and finding the impulse response f which maximizes it corresponds to finding the best operator for detection only.

For the localization criterion we proceed as follows. Recall that we chose to mark edges at maxima in the output of the operator. For an ideal step we would

expect a single maximum at the centre of the edge. Since the signal $I(x)$ contains noise we would expect this maximum to be displaced from the true position of the edge (at the origin in this case). To obtain a performance measure which improves as the localizing ability of the operator improves, we use the reciprocal of the standard deviation of the distance of the actual maximum from the centre of the true edge. This is not an arbitrary choice, as it gives a composite performance criterion which is scale independent, as we shall see.

A maximum in the output $O(x_0)$ of the operator corresponds to a zero-crossing in the spatial derivative of this output. We wish to find the position x_0 where

$$O'(x_0) = \frac{d}{dx_0}\int_{-\infty}^{+\infty} f(x)I(x_0 - x)\,dx = 0$$

Which by the differentiation theorem for convolution can be simplified to

$$\int_{-\infty}^{+\infty} f'(x)I(x_0 - x)\,dx = 0$$

To find x_0 we again split the derivative of the output $O'(x_0)$ into components due to the step and due to noise only (call these O'_s and O'_n respectively).

$$O'_s(x_0) = \int_{-\infty}^{+\infty} f'(x)Au_{-1}(x_0 - x)\,dx = \int_{-\infty}^{x_0} Af'(x)\,dx = Af(x_0) \qquad (2.6)$$

The response of the derivative filter to the noise only (at any output point) will be a Gaussian random variable with mean zero and variance equal to the mean-squared output amplitude

$$E[O'^2_n(x)] = n_0^2\int_{-\infty}^{+\infty} f'^2(x)\,dx \qquad (2.7)$$

We now add the constraint that the function f should be antisymmetric. An arbitrary function can always be split into symmetric and antisymmetric components, but it should be clear that the symmetric component adds nothing to

the detection or localizing ability of the operator but will contribute to the noise components that affect both. The Taylor expansion of $O'_s(x_0)$ about the origin gives

$$O'_s(x_0) = Af(x_0) \approx x_0 Af'(0) \tag{2.8}$$

For a zero-crossing in the output O' we require

$$O'(x_0) = O'_s(x_0) + O'_n(x_0) = 0 \tag{2.9}$$

i.e. $O'_s(x_0) = -O'_n(x_0)$ and $E[O'^2_s(x_0)] = E[O'^2_n(x_0)]$. Substituting for the two outputs from (2.7) and (2.8) we obtain

$$E[x_0^2] \approx \frac{\int_{-\infty}^{+\infty} n_0^2 f'^2(x)\,dx}{A^2 f'^2(0)} = \delta x_0^2 \tag{2.10}$$

where δx_0 is an approximation to the standard deviation of the distance of the actual maximum from the true edge. The localization is defined as the reciprocal of δx_0

$$Localization = \frac{A}{n_0} \frac{|f'(0)|}{\sqrt{\int_{-\infty}^{+\infty} f'^2(x)\,dx}}$$

Again we define a performance measure Λ which is a property of the *operator* only

$$Localization = \frac{A}{n_0}\Lambda \qquad \Lambda = \frac{|f'(0)|}{\sqrt{\int_{-\infty}^{+\infty} f'^2(x)\,dx}} \tag{2.11}$$

Having obtained both our desired criteria, we now have the problem of combining them in a meaningful way. It turns out that if we use the product of the two criteria we obtain a measure which is both amplitude and scale independent. This measure is a property of the *shape* of the impulse response f only, and will be the same for all functions f_w obtained from f by spatial scaling. In fact the choice of the combination will not affect the form of the solution since the variational

equations depend only on the individual terms in the criteria. The product of the two criteria is

$$\Sigma(f)\Lambda(f) = \frac{\int_{-\infty}^{0} f(x)\,dx}{\sqrt{\int_{-\infty}^{+\infty} f^2(x)\,dx}} \frac{|f'(0)|}{\sqrt{\int_{-\infty}^{+\infty} f'^2(x)\,dx}} \tag{2.12}$$

To illustrate the invariance of this criterion under changes of scale, we consider the performance of an operator whose impulse response is f_w where $f_w(x) = f(\frac{x}{w})$. The performance of the scaled operator is

$$\Sigma(f_w)\Lambda(f_w) = \left[\sqrt{w}\frac{\int_{-\infty}^{0} f(x)\,dx}{\sqrt{\int_{-\infty}^{+\infty} f^2(x)\,dx}}\right]\left[\frac{1}{\sqrt{w}}\frac{|f'(0)|}{\sqrt{\int_{-\infty}^{+\infty} f'^2(x)\,dx}}\right] \tag{2.13}$$

where the bracketed terms correspond in order to the detection and localization criteria. We see from this form that the signal to noise performance of the operator varies as $\sqrt{w}$, while the localization varies as the reciprocal of $\sqrt{w}$. An operator with a broad impulse response will have good signal to noise ratio but poor localization and vice versa. With this form of the composite criterion though, the product of detection and localization terms is the same for all f_w.

This result suggests that there is a *class of operators* that have optimal performance and that they are related by spatial scaling. In fact this result is independent of the choice of combination of the criteria. To see this we assume that there is a function f which gives the best localization Λ for a particular Σ. That is, we find f such that

$$\Sigma(f) = c_1 \qquad \text{and} \qquad \Lambda(f) \qquad \text{is maximized} \tag{2.14}$$

Now suppose we seek a second function f_w which gives the best possible localization while its signal to noise ratio is fixed to a different value. i.e.

$$\Sigma(f_w) = c_2 \qquad \text{while} \qquad \Lambda(f_w) \qquad \text{is maximized} \tag{2.15}$$

If we define f_w as before, $f_w(x) = f(\frac{x}{w})$, and further if we set

$$w = c_2^2/c_1^2$$

Then the constraint on f_w in (2.15) translates to constraint on f which is identical with (2.14). So to solve (2.15) we find f such that

$$\Sigma(f) = c_1 \qquad \text{and} \qquad \frac{1}{\sqrt{w}}\Lambda(f) \qquad \text{is maximized}$$

Which has the same solution as (2.14). So if we find a single such function f, we can obtain maximal localization for any fixed signal to noise ratio by scaling f. Thus our choice of the composite criterion was not arbitrary but highlighted a natural constraint or "uncertainty principle" for detection of step edges in noise. We can obtain arbitrarily good localization or detection by scaling but not both simultaneously.

We will find (eventually) that the above analysis is valid but that the criterion as given is still underspecified. While it does lead to a plausible class of solutions, performance will be poor because we have so far ignored an important aspect of the detection process. Namely the detector should not produce multiple outputs in response to a single edge. In the next section we find the solutions to the above optimization problem, and highlight their weakness with regard to multiple edge responses.

2.2. The Optimal Operator for Steps

The optimal edge detection operator has now been defined implicitly by equation (2.12). All that remains is to find a function which maximizes this large expression. We must make some simplifications before a solution can be found using the calculus of variations. We cannot directly find a function which maximizes the quotient of integrals in equation (2.12) since each depends on $f(x)$. Instead we set all but one of the integrals to undetermined constant values in an analogous manner to the method of Lagrange multipliers. We then find the extreme value of the

remaining integral (since it will correspond to the maximum in the total expression) as a function of the undetermined constants. The values of the constants are then chosen so as to maximize the value of the remainder of the expression, which is now a function only of the three constants. Given these constants, we can completely uniquely specify the function $f(x)$ which gives the global maximum of the criterion.

The second simplification involves the limits of the integrals. The two integrals in the denominator of (2.12) have limits at plus and minus infinity, while the integral in the numerator has one limit at zero and the other at minus infinity. Since the function f should be antisymmetric, we can use the latter limit for all integrals. The denominator integrals will have half the value over this subrange that they would have had over the full range. Also, this enables the value of $f'(0)$ to be set as a boundary condition, rather than expressed as an integral of f''. The lower limit of all the integrals at minus infinity should be set to some finite negative value, say $-W$ since we will be dealing with an operator of finite extent. These simplifications allow us to exploit the *isoperimetric constraint* condition (see Courant and Hilbert 1953). This allows us to combine a set of constraint integrals that share the same limits as the integral being extremized into a single variational equation.

So the problem of finding the maximum of equation (2.12) reduces to that of finding the minimum of the integral in the denominator of the S.N.R. term, subject to the constraint that the other integrals remain constant. By the principle of reciprocity, we could have chosen to extremize any of the integrals while keeping the others constant, but the solution should be the same. We seek some function f chosen from a space of *admissible* functions that minimizes the integral

$$\int_{-W}^{0} f^2(x)\,dx \tag{2.16}$$

subject to

$$\int_{-W}^{0} f(x)\,dx = c_1$$

$$\int_{-W}^{0} f'^2(x)\,dx = c_2$$

$$f'(0) = c_3 \tag{2.17}$$

The space of admissible functions in this case will be the space of all continuous functions that satisfy certain boundary conditions, namely that $f(0) = 0$ and $f(-W) = 0$. These boundary conditions are necessary to ensure that the integrals evaluated over finite limits accurately represent the infinite convolution integrals. That is, if the nth derivative of f appears in some integral, the function must be continuous in its (n-1)st derivative over the range $(-\infty, +\infty)$. This implies that the values of f and its first (n-1) derivatives must be zero at the limits of integration, since they must be zero outside this range.

The functional to be minimized is of the form $\int_a^b F(x, f, f')$ and we have a series of constraints that can be written in the form $\int_a^b G_i(x, f, f') = c_i$. Since the constraints are isoperimetric, i.e. they share the same limits of integration as the integral being minimized, we can form form a composite functional $\Psi(x, f, f')$ as a linear combination of the functionals that appear in the expression to be minimized and in the constraints (Courant and Hilbert 1953). Finding a solution for this unconstrained problem is equivalent to finding the solution to the constrained problem. The composite functional is

$$\Psi(x, f, f') = F(x, f, f') + \lambda_1 G_1(x, f, f') + \lambda_2 G_2(x, f, f') + \ldots$$

Substituting,

$$\Psi(x, f, f') = f^2 + \lambda_1 f'^2 + \lambda_2 f \tag{2.18}$$

It may be seen from the form of this equation that the choice of which integral is extremized and which are constraints is arbitrary, the solution will be the same.

This is an example of what is known as *reciprocity* in variational problems. The choice of an integral from the denominator is simply convenient since the standard form of the Euler equations applies to minimization problems. The Euler equation that corresponds to this functional is

$$\frac{d}{dx}\Psi_{f'} - \Psi_f = 0$$

Where Ψ_f denotes the partial derivative of Ψ with respect to f. This gives

$$2f(x) - 2\lambda_1 f''(x) + \lambda_2 = 0 \tag{2.19}$$

The general solution of this differential equation is

$$f(x) = -\frac{\lambda_2}{2} + a_1 e^{\alpha x} + a_2 e^{-\alpha x} \tag{2.20}$$

Where $\alpha = \lambda_1^{-\frac{1}{2}}$ and the constants a_1 and a_2 are determined by the boundary conditions $f(0) = 0$ and $f(-W) = 0$. When these constraints are added the function f can be written in the form

$$f(x) = -\frac{\lambda_2}{2}\left(1 - \frac{\cosh \alpha(x + \frac{W}{2})}{\cosh \alpha \frac{W}{2}}\right) \tag{2.21}$$

From this we can obtain expressions for the signal-to-noise ratio and localization as a function of the parameters λ_1 and λ_2. To simplify the expressions we will assume a width W of 2 and make use of the scaling properties from equation (2.13). This gives

$$\Sigma = \frac{2\alpha \cosh \alpha - 2 \sinh \alpha}{\sqrt{2\alpha^2 \cosh 2\alpha - 3\alpha \sinh 2\alpha + 4\alpha^2}} \tag{2.22}$$

$$\Lambda = \frac{\alpha \sinh \alpha}{\sqrt{\alpha \sinh 2\alpha - 2\alpha^2}} \tag{2.23}$$

Both these expressions are functions only of α, and we can investigate the behaviour of f as α tends to its limiting values 0 and $+\infty$. As α tends to zero we find that function f tends to a parabola whose equation is

$$f(x) = -\lambda_2 \alpha^2 (1 - x^2) \tag{2.24}$$

The corresponding values of signal-to-noise ratio and localization are

$$\Sigma = \sqrt{\frac{5}{6}} \qquad \Lambda = \sqrt{\frac{3}{4}} \tag{2.25}$$

When the value of α approaches infinity, we find that the function approaches a constant over the range (-2,0) (recalling that $W = 2$), and that the signal-to-noise ratio tends to 1. This is a very small increase over the corresponding value as α tended to zero. However, the localization term, $\frac{1}{\delta x}$, increases without bound. From this result it would seem that a difference of boxes function (the antisymmetric extension of the derived function over the range [-2,2]) gives the best possible *signal-to-noise ratio with arbitrarily good localization*. This function is in fact the optimal Wiener filter for the step edge.

This operator has been used quite extensively because of its simplicity and because it is easy to compute, as in the work of Rosenfeld and Thurston (1971), and in conjunction with lateral inhibition in Herskovits and Binford (1970). However it has a very high bandwidth and tends to exhibit many maxima in its response to noisy step edges, which is a serious problem when the imaging system adds noise or when the image itself contains textured regions. These extra edges should be considered erroneous according to the first of our criteria. However, the analytic form of this criterion was derived from the response at a single point (the centre of the edge) and did not consider the interaction of the responses at several nearby points. We need to make this explicit by adding a further constraint to the solution.

2.3. Eliminating Multiple Responses

If we examine the output of a difference of boxes edge detector we find that the response to a noisy step is a roughly triangular peak with numerous sharp maxima

in the vicinity of the edge (see figure 2.2). These maxima are so close together that it is not possible to select one as the response to the step while identifying the others as noise. We need to add to our criteria the requirement that the function f will not have "too many" responses to a single step edge in the vicinity of the step. We need to limit the number of peaks in the response so that there will be a low probability of declaring more than one edge. Ideally, we would like to make the distance between peaks in the noise response approximate the width of the response of the operator to a single step. This width will be about the same as the operator width W.

In order to express this as a functional constraint on f, we need to obtain an expression for the distance between adjacent noise peaks. We first note that the mean distance between adjacent maxima in the output is twice the distance between adjacent zero-crossings in the derivative of the operator output. Then we make use of a result due to Rice (1944, 1945) that the average distance between zero-crossings of the response of a function g to Gaussian noise is

$$x_{ave} = \pi\left(\frac{-R(0)}{R''(0)}\right)^{\frac{1}{2}} \tag{2.26}$$

Where $R(\tau)$ is the autocorrelation function of g. In our case we are looking for the mean zero-crossing spacing for the function f'. Now since

$$R(0) = \int_{-\infty}^{+\infty} g^2(x)\,dx \qquad \text{and} \qquad R''(0) = -\int_{-\infty}^{+\infty} g'^2(x)\,dx$$

The mean distance between zero-crossings of f' will be

$$x_{zc} = \pi\left(\frac{\int_{-\infty}^{+\infty} f'^2(x)\,dx}{\int_{-\infty}^{+\infty} f''^2(x)\,dx}\right)^{\frac{1}{2}} \tag{2.27}$$

The distance between adjacent maxima in the noise response of f, denoted x_{max}, will be twice x_{zc}. We set this distance to be some fraction k of the operator width.

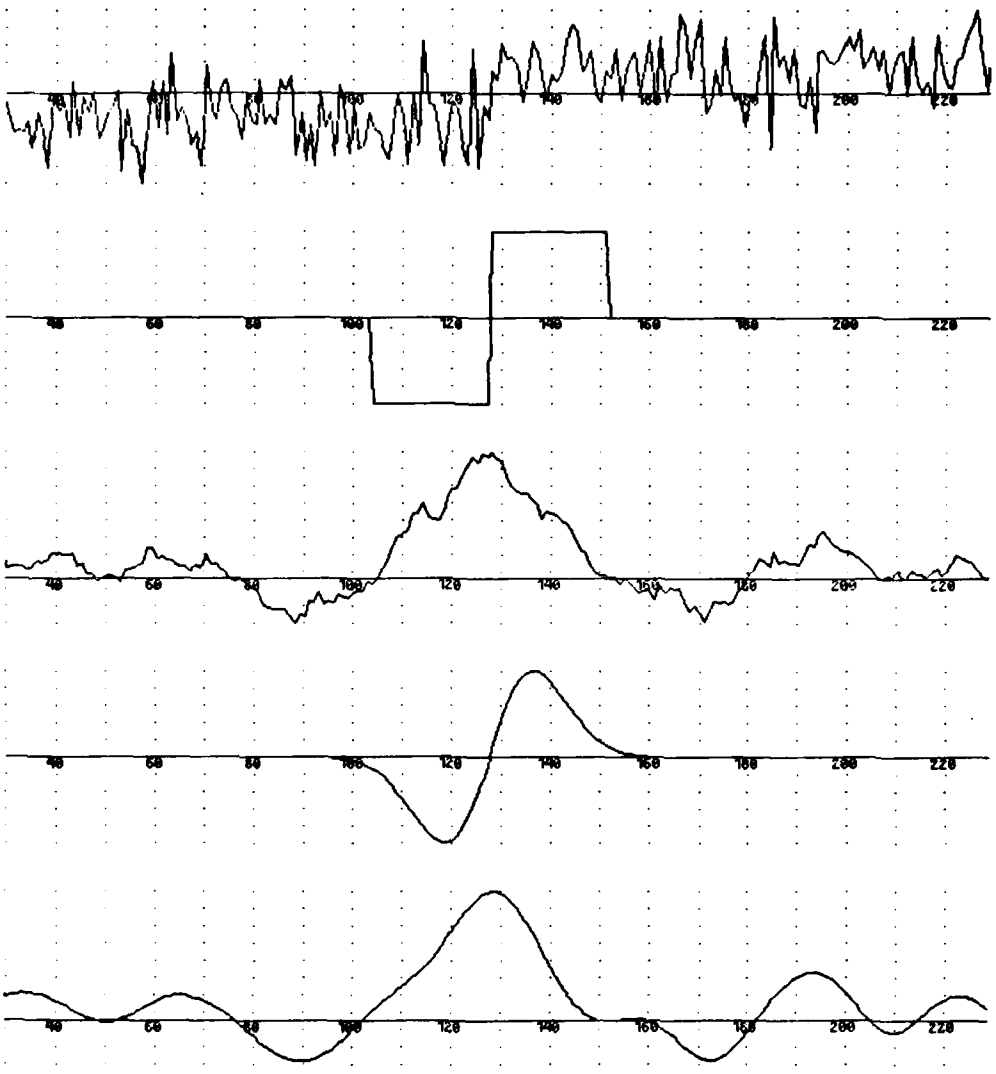

Figure 2.2. Responses of difference of boxes and first derivative of Gaussian operators to a noisy step edge

---

$$x_{max} = 2x_{zc} = kW$$

This new constraint adds only one term to the composite functional Ψ since the integral of f'^2 already appears in Ψ from the localization criterion. While in the original functional this integral appeared in the denominator of a quantity to be maximized, (i.e. the localization criterion) it now appears in the numerator of

the mean distance between maxima, which is a constraint on the solution. It is now no longer clear what the sign of its Lagrange multiplier should be. This leads to several possible solutions for f as we shall see. The new functional is given by

$$\Psi(x, f, f', f'') = f^2 + \lambda_1 f'^2 + \lambda_2 f''^2 + \lambda_3 f \tag{2.28}$$

The Euler equation corresponding to a functional of second order is

$$\Psi_f - \frac{d}{dx}\Psi_{f'} + \frac{d^2}{dx^2}\Psi_{f''} = 0$$

When the above Ψ is substituted into the Euler equation we get

$$2f(x) - 2\lambda_1 f''(x) + 2\lambda_2 f''''(x) + \lambda_3 = 0 \tag{2.29}$$

The solution of this differential equation is the sum of a constant and a set of four exponentials of the form $e^{\gamma x}$ where γ derives from the solution of the corresponding homogeneous differential equation. Now

$$2 - 2\lambda_1\gamma^2 + 2\lambda_2\gamma^4 = 0$$

$$\gamma^2 = \frac{\lambda_1}{2\lambda_2} \pm \sqrt{\left(\frac{\lambda_1}{2\lambda_2}\right)^2 - \frac{1}{\lambda_2}} \tag{2.30}$$

This equation may have roots that are purely imaginary, purely real or complex depending on the values of λ_1 and λ_2. From the composite functional Ψ we can infer that λ_2 is positive (since f''^2 is to be minimized) but it is not clear what the sign or magnitude of λ_1 should be. The Euler equation supplies a necessary condition for the existence of a minimum, but it is not a sufficient condition. By formulating such a condition we can resolve the ambiguity in the value of λ_1. To do this we must consider the second variation of the functional. Let

$$J[f] = \int_{x_0}^{x_1} \Psi(x, f, f', f'')\, dx$$

Then by Taylor's theorem,

$$J[f + \epsilon g] = J[f] + \epsilon J_1[f, g] + \frac{1}{2}\epsilon^2 J_2[f + \rho g, g]$$

where ρ is some number between 0 and ϵ, and g is chosen from the space of admissible functions, and where

$$J_1[f, g] = \int_{x_0}^{x_1} \Psi_f g + \Psi_{f'} g' + \Psi_{f''} g''\, dx$$

$$\begin{aligned} J_2[f, g] = \int_{x_0}^{x_1} & \Psi_{ff} g^2 + \Psi_{f'f'} g'^2 + \Psi_{f''f''} g''^2 \\ & + 2\Psi_{ff'} g g' + 2\Psi_{f'f''} g' g'' + 2\Psi_{ff''} g g''\, dx \end{aligned} \tag{2.31}$$

Note that J_1 is nothing more than the integral of g times the Euler equation for f (transformed using integration by parts) and will be zero if f satisfies the Euler equation. We can now define the second variation $\delta^2 J$ as

$$\delta^2 J = \frac{\epsilon^2}{2} J_2[f, g]$$

The necessary condition for a minimum is $\delta^2 J \geq 0$. We can substitute for the second partial derivatives of Ψ from (2.29) and we get

$$\int_{x_0}^{x_1} g^2 + \lambda_1 g_x^2 + \lambda_2 g_{xx}^2\, dx \geq 0 \tag{2.32}$$

which we transform using integration by parts to

$$\int_{x_0}^{x_1} g^2 - \lambda_1 g g_{xx} + \lambda_2 g_{xx}^2\, dx \geq 0$$

which can be written as

$$\int_{x_0}^{x_1}\left(g-\frac{\lambda_1}{2}g_{xx}\right)^2+\left(\lambda_2-\frac{\lambda_1^2}{4}\right)g_{xx}^2\,dx\geq 0$$

The integral is guaranteed to be positive if the expression being integrated is positive for all x, so if

$$\lambda_2>\frac{\lambda_1^2}{4}$$

then the integral will be positive for all x and for arbitrary g, and the extremum will certainly be minimum. If we refer back to (2.28) we find that this condition is precisely that which gives complex roots for γ, so we have both guaranteed the existence of a minimum and resolved a possible ambiguity in the form of the solution. We can now proceed with the derivation and assume four complex roots of the form $\gamma=\pm\alpha\pm i\omega$ With α, ω real, such that

$$\alpha^2-\omega^2=\frac{\lambda_1}{2\lambda_2}\qquad\text{and}\qquad 4\alpha^2\omega^2=-\frac{\lambda_1^2-4\lambda_2}{4\lambda_2^2}\tag{2.33}$$

The general solution may now be written

$$f(x)=a_1e^{\alpha x}\sin\omega x+a_2e^{\alpha x}\cos\omega x+a_3e^{-\alpha x}\sin\omega x+a_4e^{-\alpha x}\cos\omega x+c\tag{2.34}$$

This function is subject to the boundary conditions

$$f(0)=0\qquad f(-W)=0\qquad f'(0)=s\qquad f'(-W)=0$$

Where s is an unknown constant equal to the slope of the function f at the origin. These four boundary conditions enable us to solve for the quantities a_1 through a_4 in terms of the unknown constants α, ω, c and s. The boundary conditions may be rewritten

$$a_2+a_4+c=0$$

$$a_1 e^{\alpha} \sin\omega + a_2 e^{\alpha} \cos\omega + a_3 e^{-\alpha} \sin\omega + a_4 e^{-\alpha} \cos\omega + c = 0$$

$$a_1\omega + a_2\alpha + a_3\omega - a_4\alpha = s$$

$$\begin{aligned} &a_1 e^{\alpha}(\alpha \sin\omega + \omega\cos\omega) + a_2 e^{\alpha}(\alpha\cos\omega - \omega\sin\omega) \\ &+a_3 e^{-\alpha}(-\alpha\sin\omega + \omega\cos\omega) + a_4 e^{-\alpha}(-\alpha\cos\omega - \omega\sin\omega) = 0 \end{aligned} \tag{2.35}$$

These equations are linear in the four unknowns a_1, a_2, a_3, a_4 and when solved they yield

$$\begin{aligned} a_1 = c\Big(&\alpha(\sigma-\alpha)\sin 2\omega - \alpha\omega\cos 2\omega + (-2\omega^2\sinh\alpha + 2\alpha^2 e^{-\alpha})\sin\omega \\ &+2\alpha\omega\sinh\alpha\cos\omega + \omega e^{-2\alpha}(\alpha+\sigma) - \sigma\omega\Big)/4\Big(\omega^2\sinh^2\alpha - \alpha^2\sin^2\omega\Big) \end{aligned}$$

$$\begin{aligned} a_2 = c\Big(&\alpha(\sigma-\alpha)\cos 2\omega + \alpha\omega\sin 2\omega - 2\alpha\omega\cosh\alpha\sin\omega - 2\omega^2\sinh\alpha\cos\omega \\ &+2\omega^2 e^{-\alpha}\sinh\alpha + \alpha(\alpha-\sigma)\Big)/4\Big(\omega^2\sinh^2\alpha - \alpha^2\sin^2\omega\Big) \end{aligned}$$

$$\begin{aligned} a_3 = c\Big(&-\alpha(\sigma+\alpha)\sin 2\omega + \alpha\omega\cos 2\omega + (2\omega^2\sinh\alpha + 2\alpha^2 e^{\alpha})\sin\omega \\ &+2\alpha\omega\sinh\alpha\cos\omega + \omega e^{2\alpha}(\sigma-\alpha) - \sigma\omega\Big)/4\Big(\omega^2\sinh^2\alpha - \alpha^2\sin^2\omega\Big) \end{aligned}$$

$$\begin{aligned} a_4 = c\Big(&-\alpha(\sigma+\alpha)\cos 2\omega - \alpha\omega\sin 2\omega + 2\alpha\omega\cosh\alpha\sin\omega + 2\omega^2\sinh\alpha\cos\omega \\ &-2\omega^2 e^{\alpha}\sinh\alpha + \alpha(\alpha+\sigma)\Big)/4\Big(\omega^2\sinh^2\alpha - \alpha^2\sin^2\omega\Big) \end{aligned} \tag{2.36}$$

where σ is the slope s at the origin divided by the constant c. On inspection of these expressions we can see that a_3 can be obtained from a_1 by replacing α by $-\alpha$, and similarly for a_4 from a_2.

The function f is now parametrized in terms of the constants α, ω, σ and c. We have still to find the values of these parameters which maximize the quotient of integrals that forms our composite criterion. To do this we first express each of the integrals in terms of the constants. Since these integrals are very long and uninteresting, they are not given here but for the sake of completeness they are included in Appendix I. We have reduced the problem of optimizing over an infinite-dimensional space of functions to a non-linear optimization in three variables α, ω and σ (as expected, the combined criterion does not depend on c). Unfortunately the resulting criterion, which must still satisfy the multiple response constraint, is probably too complex to be solved analytically, and numerical methods must be used to provide the final solution.

In fact there is really no best function f for a given W because the shape of f will depend on the multiple response constraint, i.e. it will depend on how far apart we force the adjacent responses. Figure (2.3) shows the operators that result from particular choices of this distance. Recall that there was no single best function for arbitrary w, but a class of functions which were obtained by scaling a prototype function by w. We will want to force the responses further apart as the signal to noise ratio in the image is lowered, and it is not clear what the value of signal to noise ratio will be for a single operator. However, this design is based on the use of multiple widths of operator and on a decision procedure which selects the smallest operator that has an output signal to noise ratio above a given threshold. This means that all operators will spend most of their time operating close to their output Σ thresholds. We should therefore try to choose a spacing which gives acceptable multiple response behaviour under these conditions.

A rough estimate for the probability of a spurious maximum in the neighbourhood of the true maximum can be formed as follows. Recall that maxima in an operator output correspond to zero-crossings in the derivative of this output. If we look at the first derivative of the response to an ideal step we find that it is approximately linear near the centre of the step. There will be only one zero-crossing if the slope of this response is greater than the slope of the response to noise only. This latter slope is just the second derivative of the response to noise

only, and is a Gaussian random variable with standard deviation

$$\sigma_s = n_0\left(\int_{-\infty}^{+\infty} f''^2(x)\,dx\right)^{\frac{1}{2}}$$

while the slope of the zero-crossing at the centre of the edge is $Af'(0)$. The probability $p_m$that the former slope exceeds the latter is given in terms of the normal distribution function Φ

$$p_m = 1 - \Phi\left(\frac{Af'(0)}{\sigma_s}\right)$$

We can choose a value for this probability as an acceptable error rate and this will determine the ratio of $f(0)$ to σ_s. Rearranging we obtain.

$$\frac{A|f'(0)|}{n_0\sqrt{\int_{-\infty}^{+\infty} f''^2(x)\,dx}} = \Phi^{-1}(1-p_m) \tag{2.37}$$

And we can see the explicit dependence of this constraint on the image signal to noise ratio. We can eliminate this dependence by relating the probability of a multiple response p_m to the probability of falsely marking an edge p_f where we define

$$p_f = 1 - \Phi(\Sigma)$$

and we have finally that

$$\frac{|f'(0)|}{\sqrt{\int_{-\infty}^{+\infty} f''^2(x)\,dx}} = k\frac{\int_{-\infty}^{0} f(x)\,dx}{\sqrt{\int_{-\infty}^{+\infty} f^2(x)\,dx}} \tag{2.38}$$

where k is a constant determined by the values of the two probabilities. If we choose to set p_m equal to p_f then the value of k is one. Unfortunately, the largest value of k that could be obtained using the constrained numerical optimization was about .58. This corresponds to an inter-maximum spacing of 1.2 (in units of W). This is

the final form of linear operator that we will use. It is illustrated in the last of the series of graphs in figure (2.3). Its performance is given by the product of Σ and Λ and it has the value

$$\Sigma\Lambda = 1.12 \tag{2.39}$$

Inspection of the shape of this operator in figure (2.3) suggests that it may be possible to approximate it using a first derivative of a Gaussian G' where

$$G(x) = \exp\left(-\frac{x^2}{2\sigma^2}\right)$$

The reason for doing this is that there are very efficient ways to compute the two dimensional extension of the filter if it can be represented as some derivative of a Gaussian. This will be discussed in detail in chapter 5. We now compare the performance of a first derivative of a Gaussian filter with the optimal operator. The impulse response of the filter is now given by

$$f(x) = -\frac{x}{\sigma^2}\exp\left(-\frac{x^2}{2\sigma^2}\right) \tag{2.40}$$

and the terms in the performance criteria have the values

$$|f'(0)| = \frac{1}{\sigma^2}$$

$$\int_{-\infty}^{0} f(x)\,dx = 1$$

$$\int_{-\infty}^{+\infty} f^2(x)\,dx = \frac{\sqrt{\pi}}{2\sigma}$$

$$\int_{-\infty}^{+\infty} f'^2(x)\,dx = \frac{3\sqrt{\pi}}{4\sigma^3}$$

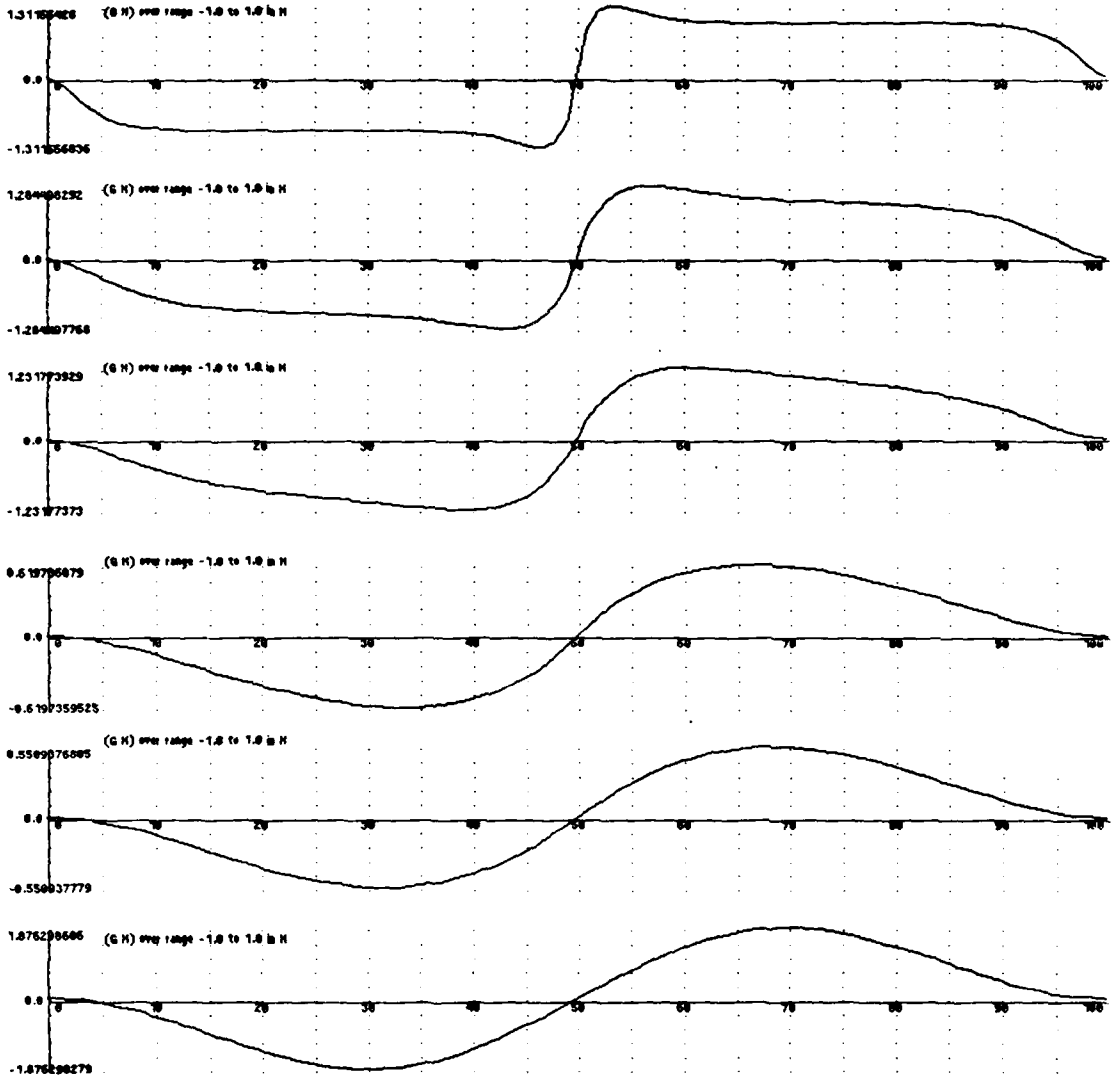

Figure 2.3. Optimal step edge operators for various values of k, from top to bottom they are k = 0.075, 0.15, 0.25, 0.5, 0.65, 0.7

$$\int_{-\infty}^{+\infty} f''^2(x)\,dx = \frac{15\sqrt{\pi}}{8\sigma^5} \tag{2.41}$$

The overall performance index for this operator is

$$\Sigma\Lambda = \sqrt{\frac{8}{3\pi}} \approx 0.92 \tag{2.40}$$

While the k value for this filter is, from (2.38)

$$k = \sqrt{\frac{4}{15}} \approx 0.51$$

The performance of this operator is worse than the optimal operator by about 20%, and its multiple response measure k, is worse by about 10%. It would probably be difficult to detect a difference of this magnitude by looking at the performance of the two operators on real images, and because the first derivative of Gaussian operator can be computed with much less effort in two dimensions (but see section 5.2), it has been used exclusively in experiments. The impulse responses of the two operators can be compared in figure (2.4).

2.4. Finding an Operator by Stochastic Optimization

The previous section contained the derivation of a "closed form" for an optimal edge detector for step edges. Even in the derivation of this closed form for the operator, a numerical optimization was necessary to obtain the coefficients that appear in its analytic form. We saw that this method required the solution of very complex simultaneous systems of non-linear equations. It is likely that if the technique were applied to other problems it would seldom be possible to find closed form solutions for the operators. However, this does *not* mean that a useful operator cannot be derived using these techniques. There are two alternative approaches, both of which were used in the derivation of the step edge operator, and which can be applied when the expressions become too complex to be solved.

(i) The first of these was used in the previous section and involves the use of numerical methods for the determination of some finite number of parameter

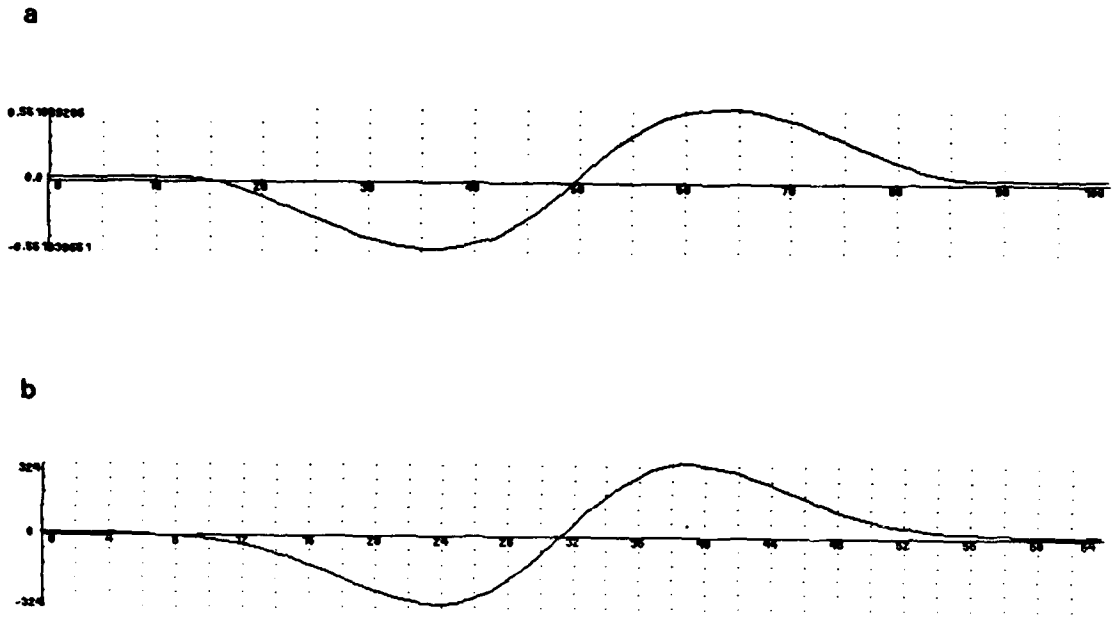

Figure 2.4. (a) The optimal step edge operator, (b) The first derivative of a Gaussian

---

values once the solution has been reduced to a parametric form. In fact even infinite dimensional objects, e.g. the impulse response of a filter, can be approximated by a finite dimensional discrete filter if appropriate constraints on the bandwidth (of the infinite filter) are met. All that is required is a deterministic criterion which can be applied to the parametric form of the operator and which measures the "goodness" of the operator with respect to that criterion.

(ii) The second method is necessary when it is not even possible to write down a closed form for the criterion of optimality. This problem arises when the image model contains some random component (e.g. Gaussian noise) and it is then necessary to form criteria that reflect some meaningful statistics on

the behaviour of operator on an ensemble of images. Gaussian independent random processes are particularly easy to analyse, but even with Gaussian statistics, the closed form criteria for step edges led to very complex solutions. However, in the further work section of this thesis we will propose a method for transforming problems that involve certain stationary processes into equivalent probelms involving only Gaussian independent processes.

In fact in the work leading up to this report, the second method was used successfully before a closed form solution using the first method was obtained. This is almost certainly the rule rather than the exception. While at best the stochastic method leads to an approximate solution, and may not be feasible if the parameter space is poorly conditioned, it is still felt that it is a useful technique and may guide the search for an analytic solution.

The stochastic method begins, as did the analytic method, with a model of the image. Again we consider a step edge with superimposed white Gaussian noise. We seek a filter f which maximizes some criterion but in this case we cannot characterize the filter by its (infinite) impulse response. Instead we consider a discrete filter i.e. we represent the filter by its impulse response sampled at positions 0, τ, 2τ etc. Provided that the bandwidth of the corresponding continuous impulse response filter is less than the Nyquist frequency, $\frac{1}{2\tau}$, the continuous filter is completely described by its discrete approximation. It turns out that for the step edge operators, which have small bandwidth, only about 12 samples are necessary. This was not known before the optimization was done and 32 samples were used for the discrete filter.

The optimization algorithm is essentially a hill-climbing search over the space of possible filters. It proceeds by continuously iterating through the following steps

(i) Create a (discrete) noisy edge by adding Gaussian random numbers to the sampled values of a step edge.

(ii) Convolve the filter with this edge, and evaluate the response.

(iii) Perturb the filter coefficients (sampled values) by a small amount

(iv) Convolve this new filter with the edge, and evaluate the new response.

(v) Change the filter based on the effects of the perturbation in (iii).

Note that this procedure is not guaranteed to lead to a solution even in the case where the analytic solution space is convex. It differs from deterministic hill-climbing procedures in that the "hills" (the contours of constant evaluation in parameter space) are not fixed but vary from iteration to iteration. There is a random component in any particular evaluation caused by the presence of noise in the modelled image. We can only say that the limit of the mean of a number of such evaluations will be the contours that would be obtained from the deterministic criteria. In fact the magnitude of the changes caused by image variations greatly overshadowed the magnitude of the changes due to the perturbations in the filter coefficients. It was therefore important to apply the perturbed and original filters to the same image.

To see when this method should converge, we assume that there exists a deterministic evaluation function F over the parameter space, and such that we can locally estimate the evaluation of an n-tuple of parameters $\vec{p}$ as

$$E_1 = F(\vec{p}) + r$$

where r is a random variable from some unknown distribution which models the effects of the image noise. If we now perturb the filter coefficients by some small $\delta\vec{p}$, we obtain the new evaluation

$$E_2 = F(\vec{p} + \delta\vec{p}) + r$$

assuming that the value of r is constant (the image has not changed) over some small neighbourhood of $\vec{p}$. If we subtract E_1 from E_2 and divide by $|\delta\vec{p}|$ we obtain

$$\frac{E_2 - E_1}{|\delta\vec{p}|} = \frac{F(\vec{p} + \delta\vec{p}) - F(\vec{p})}{|\delta\vec{p}|} \tag{2.43}$$

Now

$$\lim_{|\delta\vec{p}|\to 0} \frac{F(\vec{p}+\delta\vec{p}) - F(\vec{p})}{|\delta\vec{p}|} = \nabla F(\vec{p}) \cdot \vec{u}$$

where $\vec{u}$ is a unit vector in the direction of $\delta\vec{p}$. By using n normal perturbations $\delta\vec{p}_i$ with n corresponding unit vectors $\vec{u}_i$ and forming the sum

$$\sum_{i=1}^{n} \frac{(E_2 - E_1)\delta\vec{p}_i}{|\delta\vec{p}_i|^2} \approx \sum_{i=1}^{n} (\nabla F(\vec{p}) \cdot \vec{u}_i)\vec{u}_i = \nabla F(\vec{p}) \tag{2.44}$$

we have formed an estimate of the gradient of the evaluation function at the point $\vec{p}$ in parameter space. Another way of forming an estimate of ∇F is to use perturbations which are randomly distributed. By randomly distributed we mean that each component of $\delta\vec{p}$ is an independent random variable with zero mean and variance σ_p^2. Then the expectation value of the perturbation weighted by the change in evaluation is

$$E[(E_2 - E_1)\delta\vec{p}] = \nabla F(\vec{p})\sigma_p^2 \tag{2.45}$$

So we can also achieve an estimate of the gradient of F by making random perturbations in the filter coefficients and weighting those perturbations by the change in evaluation. This method provides a more uniform coverage of the neighbourhood around a single parameter space point than does a particular choice of orthonormal perturbations. The implementation uses random perturbations and a short term averaging filter to obtain an estimate of the gradient of F over several iterations. The filter used has a single pole (i.e. its response to an impulse is an exponentially decaying sequence), and can be described by the difference equation

$$\vec{g}_j = \frac{(E_{2j} - E_{1j})\delta\vec{p}_j}{\sigma_p^2} + \beta\vec{g}_{j-1} \tag{2.46}$$

where $\vec{g}_j$ is the estimate of the gradient of f at the j^{th} iteration, and the subscripted quantities E_{2j}, E_{1j} and $\delta\vec{p}_j$ are the values of these quantities at the j^{th} iteration. β is a time constant between 0 and 1, and it determines the "inertia" of the system.

The algorithm performs a simple hill-climbing by taking the estimate of the gradient at each iteration and adding a multiple of it to the current value of $\vec{p}$. However we have (necessarily) added a time constant in the estimator for ∇F so that we can obtain a continuously updating estimate while simultaneously climbing using the existing estimate. We now have a system with both "inertia" from the average over the previous iterations and a "viscosity" caused by the fact that this average decays with time (assuming β is less than 1). Therefore it is possible for it to overshoot a minimum, or even to oscillate several times before settling at the minimum. It was necessary to set the time constant empirically in order to obtain accurate estimates of gradient without excessive overshoot. The behaviour of the system is roughly analogous to a ball rolling along a contoured surface under the influence of gravity, with perfectly viscous drag.

The major reason for resorting to stochastic methods for the optimization was that the evaluation criterion is a function of a particular response, rather than an estimate of the behaviour of the filter on a large set of inputs. But the abstract criteria should be the same. The heuristic criterion should evaluate both the error rate and the localizing abili_, of the operator. The criterion actually used is

$$E_v = -50|1 - n_{max}| - d^2_{max} \tag{2.47}$$

where n_{max} is the number of local maxima that occur in a fixed neighbourhood of the edge, and d_{max} is the distance of the strongest maximum from the centre of the true edge. Note that the two terms in the expression are "penalty" measures, hence the two negations.

Figure (2.5) shows the algorithm converging to a solution after the filter has been initialized to a difference of boxes. In figure (2.6) the initial filter coefficients are random and independent. It is worth comparing figure (2.5) with figure (2.3), which showed the best analytic form of the operator for various inter-maximum distances. It seems that the stochastic method moves through parameter space in such a way that it passes through several of these analytic optimal forms before reaching a global extremum. The two methods produce similar solutions even though their

criteria are slightly different. This is strong evidence that the form of the optimal detector is robust with respect to the actual choice of criteria, so long as the criteria *depend on both error rate and localizing ability*. We will see further evidence of this in the work of Shanmugam et al (1979) in a later chapter.

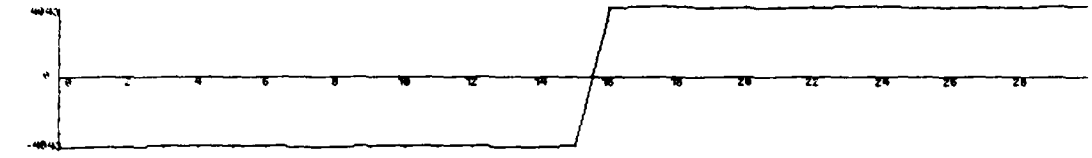

```
# ART-HALF-FIX-32. 5740642>

;; after 200 iterations, performance index is 393
```

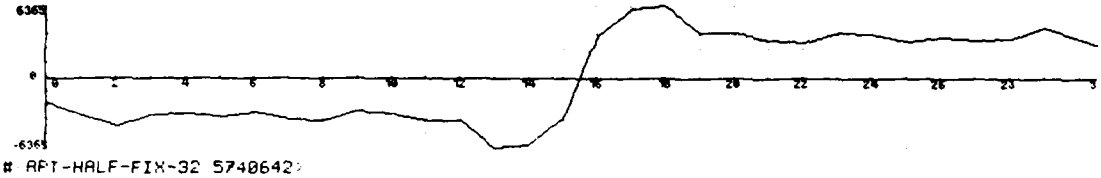

```
# ART-HALF-FIX-32 5740642>

;; after 3300 iterations, performance index is 312
```

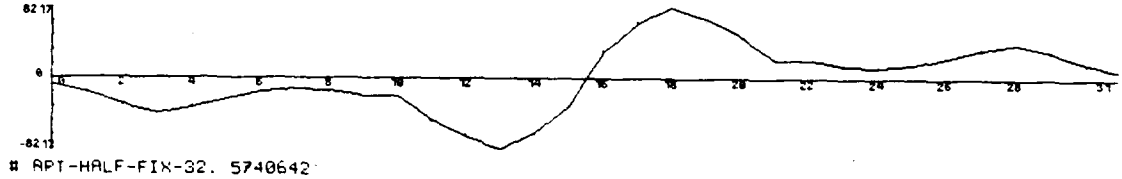

```
# ART-HALF-FIX-32. 5740642>

;; After 14100 iterations, performance index is 204
```

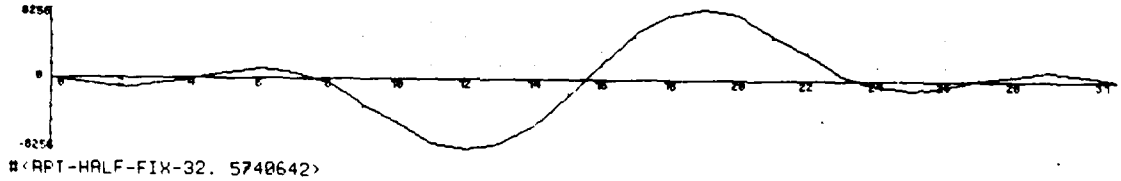

```
#<ART-HALF-FIX-32. 5740642>

;; After 43500 iterations, performance index is 136
```

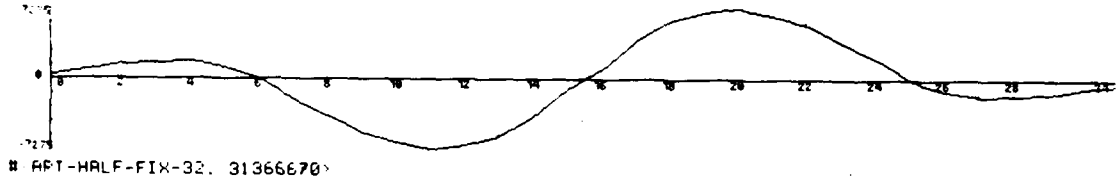

```
# ART-HALF-FIX-32. 31366670>

;; After 120,000 iterations, performance index is 119
```

Figure 2.5. Convergence of the stochastic optimization procedure after initialization to a difference of boxes

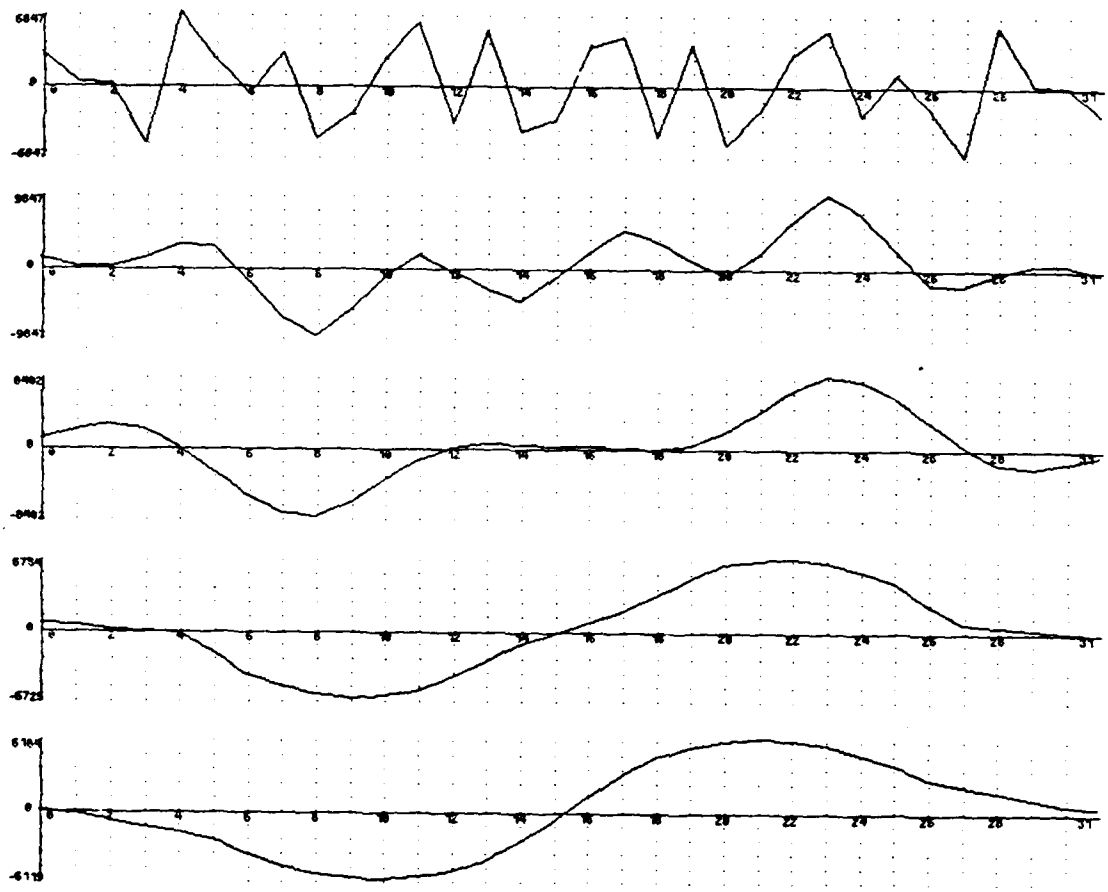

Figure 2.6. Convergence of the stochastic optimization procedure after initialization to random values

3. Two or More Dimensions

In one dimension we can characterise the step edge in space with one position coordinate. In two dimensions an edge also has an orientation. In this chapter we will use the term "edge direction" to mean the direction of the tangent to the contour that the edge defines in two dimensions. Suppose we wish to detect edges of a particular orientation. We create a two-dimensional mask for this orientation by convolving a linear edge detection function aligned normal to the edge direction with a projection function parallel to the edge direction. A substantial saving in computational effort is possible if the projection function is a Gaussian with the same σ as the (first derivative of the) Gaussian used as the detection function. It is possible to create such masks by convolving the image with a symmetric two-dimensional Gaussian and then differentiating normal to the edge direction. In fact we do not have to differentiate normal to every possible edge direction because the slope of a smooth surface in any direction can be determined exactly from its slope in two directions. The simplest form of the detector uses this method.

After the image has been convolved with a symmetric Gaussian, the edge direction is estimated from the gradient of the smoothed image intensity surface. The gradient magnitude is then non-maximum suppressed in that direction. The directional non-maximum suppression is equivalent to the application of the following non-linear differential predicate

$$\frac{\partial^2}{\partial \mathbf{n}^2} G * I = 0$$

where $\mathbf{n} = \frac{\nabla G * I}{|\nabla G * I|}$, which has the same zero-crossings as

$$\nabla S \cdot \nabla (\nabla S \cdot \nabla S) = 0 \tag{3.1}$$

where $S = G * I$ and where I is the image and G is a symmetric Gaussian. This is readily varified by using the substitution

$$\frac{\partial}{\partial \mathbf{n}} S = \frac{\mathbf{n} \cdot \nabla S}{|\mathbf{n}|}$$

The form of non-linear second derivative operator used in (3.1) turns out to be the same as that proposed by Havens and Strikwerda (1983), Torre and Poggio (1983), and Yuille (1983). It also appears in Prewitt (1970) in the context of edge enhancement.

This operator actually locates either maxima or minima, by locating the zero-crossings in the second derivative in the edge direction. In principle this operator could be used to implement an edge detector in an arbitrary number of dimensions, by first convolving the image with a symmetric n-dimensional Gaussian. The convolution with an n-dimensional Gaussian is highly efficient because the Gaussian is decomposable into n linear filters.

There are other more pressing reasons for using a smooth projection funct ı such as a Gaussian. When we apply a linear operator to a two dimensional image, we form at every point in the output a weighted sum of some of the input values. For the edge detector described here, this sum will be a difference between local averages of the different sides of the edge. This output, before non-maximum suppression, represents a kind of moving average of the image. Ideally we would like to use an infinite projection function, but real edges are of limited extent. It is therefore necessary to window the projection function (see Hamming 1983). If the window function is abruptly truncated, e.g. if it is rectangular, the filtered image will not be smooth because of the very high bandwidth of this window. This result is analogous to the Gibbs phenomenon in Fourier theory. When non-maximum suppression is applied these variations will tend to produce edge contours that "wander" or that in severe cases are not even continuous.

The solution is to use a smooth window function. In signal processing, typical windows used are the Hamming and Hanning windows. The Gaussian is a reasonable approximation to both of these, and it certainly has very low bandwidth for a given spatial width (The Gaussian is the unique function with minimal product of bandwidth and frequency). The effect of the window function becomes very

marked for large operator sizes and it is probably the biggest single reason why operators with large support were not practical until the work of Marr and Hildreth on the Laplacian of Gaussian. The perceptive reader will probably see the similarity between these smoothness constraints in the projection function to preserve continuity of contours in the edge direction, and the smoothness of the detection function implied by the addition of the multiple response constraint.

It is worthwhile here to compare the performance of this kind of directional second derivative operator with the Laplacian. First we note that the two-dimensional Laplacian can be decomposed into components of second derivative in two arbitrary orthogonal directions. If we choose to take one of the derivatives in the direction of principal gradient, we find that the operator output will contain one contribution that is essentially the same as the operator described above, and also a contribution that is aligned along the edge direction. This second component contributes nothing to localization or detection, (the surface is roughly constant in this direction) but increases the output noise. This will be verified analytically in chapter 7.

A version of the detector which used the Gaussian convolution followed by directional non-maximum suppression has been implemented and performed very well. Examples of its output will be given in chapter 6. While the complete detector includes multiple operator widths, orientations and aspect ratios, they are a superset of the operators used in the simple detector. In typical images, most of the edges are marked by the operators of the smallest width, and most of these by non-elongated operators. However, as we shall see in the following sections, there are cases when larger or more directional operators should be used, and that they offer considerably better performance when they are applicable. The key to making such a complicated detector produce a coherent output is in the design of effective decision procedures for choosing between operator outputs at each point in the image.

3.1. The Need for Multiple Widths

Having determined the optimal shape for the operator,we now face the problem

of choosing the width of the operator so as to give the best detection/localization trade-off in a particular application. In general the signal to noise ratio will be different for each edge within an image, and so it will be necessary to incorporate several widths of operator in the scheme. The decision as to which operator to use must be made dynamically by the algorithm and this requires a local estimate of the noise energy in the region surrounding the candidate edge. Once the noise energy is known, the signal to noise ratios of each of the operators will be known. If we then use a model of the probability distribution of the noise, we can effectively calculate the probability of a candidate edge being a false edge (for a given edge, this probability will be different for different operator widths).

Since the a-priori penalty associated with a falsely detected edge is independent of the edge strength, it is appropriate to threshold the detector outputs on probability of error rather than on magnitude of response. Once the probability threshold is set, the minimum acceptable signal to noise ratio is determined. However, there may be several operators with signal to noise ratios above the threshold, and in this case the smallest operator should be chosen, since it gives the best localization. We can afford to be conservative in the setting of the threshold since edges missed by the smallest operators may be picked up by the larger ones. Effectively the trade-off between error rate and localization remains, since choosing a high signal to noise ratio threshold leads to a lower error rate, but will tend to give poorer localization since fewer edges will be recorded from the smaller operators.

In summary then, the first heuristic for choosing between operator outputs is that *small operator widths should be used whenever they have sufficient* Σ. This is similar to the selection criterion proposed by Marr and Hildreth (1980) for choosing between different Laplacian of Gaussian channels. In their case the argument was based on the observation that the smaller channels have higher resolution, i.e. there is less possibilty of interference from neighbouring edges. That argument is also very relevant in the present context, as to date there has been no consideration of the possibility of more than one edge in a given operator support. Interestingly, Rosenfeld and Thurston (1971) proposed exactly the opposite criterion in the choice of operator for edge detection in texture. The argument given was

that the larger operators give better averaging and therefore (presumably) better signal to noise ratio.

Taking this hueristic as a starting point, we need to form a local decision procedure that will enable us to decide whether to mark one or more edges when several operators in a neighbourhood are responding. If the operator with the smallest width responds to an edge and if it has a signal to noise ratio above the threshold, we should immediately mark an edge at that point. We now face the problem that there will almost certainly be edges marked by the larger operators, but that these edges will probably not be exactly coincident with the first edge. A possible answer to this would be to suppress the outputs of all nearby operators. This has the undesirable effect of preventing the large channels from responding to "fuzzy" edges that are superimposed on the sharp edge.

Instead we use a "feature synthesis" approach. We begin by marking all the edges from the smallest operators. From these edges, we synthesize the large operator outputs than would have been produced if these were the only edges in the image. We then compare the actual operator outputs to the synthetic outputs. We mark additional edges only if the large operator has significantly greater response that what we would predict from the synthetic output. The simplest way to produce the synthetic outputs is to take the edges marked by a small operator in a particular direction, and convolve with a Gaussian normal to the edge direction for this operator. The σ of this Gaussian should be the same as the σ of the large channel detection filter.

This procedure can be applied repeatedly to first mark the edges from the second smallest scale that were not marked by at the first, and then to find the edges from the third scale that were not marked by either of the first two etc. Thus we build up a cumulative edge map by adding those edges at each scale that were not marked by smaller scales. It turns out that in many cases the majority of edges will be picked up by the smallest channel, and the later channels mark mostly shadow and shading edges, or edges between textured regions.

3.2. The Need for Directional Operators

So far we have assumed that the projection function is a Gaussian with the same σ as the Gaussian used for the detection function. In fact both the detection and localization of the operator improve as the length of the projection function increases. We now prove this for the operator signal to noise ratio. The proof for localization is similar. We will consider a step edge in the x direction which passes through the origin. This edge can be represented by the equation

$$I(x,y) = Au_{-1}(y)$$

where u_{-1} is the unit step function, and A is the amplitude of the edge as before. Suppose that there is additive Gaussian noise of mean squared value n_{00}^2 per unit area. If we convolve this signal with a filter whose impulse response is $f(x,y)$, then the response to the edge (at the origin) is

$$\int_{-\infty}^{0}\int_{-\infty}^{+\infty} f(x,y)\,dx\,dy$$

The root mean squared response to the noise only is

$$n_{00}\Big(\int_{-\infty}^{+\infty}\int_{-\infty}^{+\infty} f^2(x,y)\,dx\,dy\Big)^{\frac{1}{2}}$$

The signal to noise ratio is the quotient of these two integrals, and will be denoted by Σ. We have already seen what happens if we scale the function normal to the edge (equation 2.13). We now do the same to the projection function by replacing $f(x,y)$ by $f(x,\frac{y}{l})$. The integrals become

$$\int_{-\infty}^{0}\int_{-\infty}^{+\infty} f(x,\frac{y}{l})\,dx\,dy = \int_{-\infty}^{0}\int_{-\infty}^{+\infty} f(x,y_1)\,l\,dx\,dy_1$$

$$n_{00}\Big(\int_{-\infty}^{+\infty}\int_{-\infty}^{+\infty} f^2(x,\frac{y}{l})\,dx\,dy\Big)^{\frac{1}{2}} = n_{00}\Big(\int_{-\infty}^{+\infty}\int_{-\infty}^{+\infty} f^2(x,y_1)\,l\,dx\,dy_1\Big)^{\frac{1}{2}}$$

And the ratio of the two is now $\sqrt{l}\Sigma$. The localization Λ also improves as $\sqrt{l}$. It is clearly desirable that we use as large a projection function as possible. There are obviously practical limitations on this, in particular all edges in an image are of limited extent, and few are perfectly linear. However, most edges continue for some distance, in fact much further than the 3 or 4 pixel supports of most edge operators. Even curved edges can be approximated by linear segments at a small enough scale. Considering the advantages, it is obviously preferable to use the directional operators whenever they are applicable. The only proviso is that the detection scheme must ensure that they are used only when the image fits a linear edge model.

The present algorithm tests for applicability of each directional mask by forming a goodness of fit estimate. It does this at the same time as the mask itself is computed. An efficient way of forming long directional masks is to sample the output of non-elongated masks with the same direction. This output is sampled at regular intervals in a line parallel to the edge direction. If the samples are close together (less than 2σ apart), the resulting mask is essentially flat over most of its range in the edge direction and falls smoothly off to zero at its ends. Two cross sections of such a mask are shown in figure (3.1). In this diagram (as in the present implementation) there are five samples over the operator support.

Simultaneously with the computation of the mask, it is possible to establish goodness of fit by a simple squared-error measure. Since the quantity being estimated to produce the mask is the average of some number of values, the squared error is just the variance of these values. We then eliminate those operator outputs whose variance is greater than some fraction of the squared output. Where no directional operator has sufficient goodness of fit at a point, the algorithm will test the outputs of less directional operators. This simple goodness of fit measure is sufficient to eliminate the problems that traditionally plague directional operators, such as false responses to highly curved edges and extension of edges beyond corners, see Hildreth (1980).

This particular form of projection function, that is a function with constant value over some range which decays to zero at each end with two roughly half-

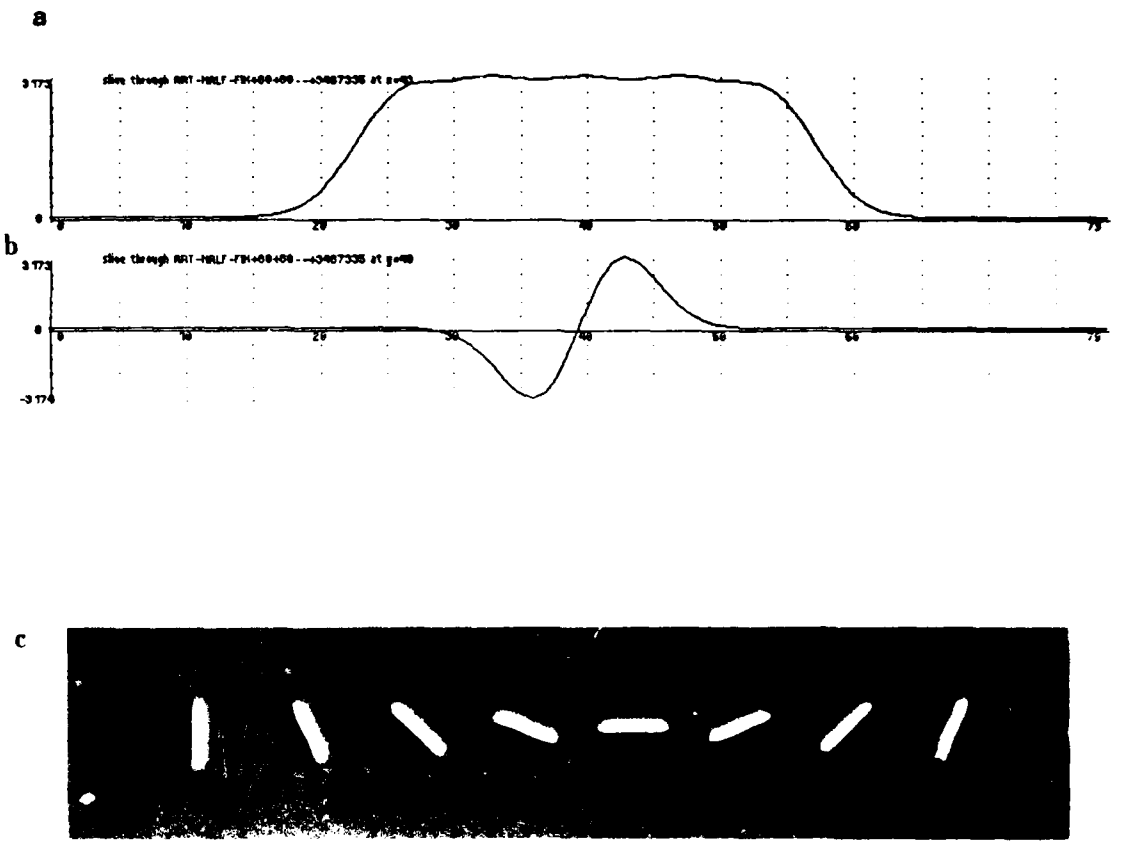

Figure 3.1. Directional step edge mask (a) Cross section parallel to the edge direction, (b) Cross section normal to edge direction (c) Two-dimensional impulse responses of several masks.

Gaussians, is very similar to a commonly used extension of the Hanning window. This latter function is flat for some distance and decays to zero at each end with two half-cosine bells (Bingham, Godfrey and Tukey 1967). We can therefore expect it to have good properties as a moving average estimator, which as we saw at the start of the chapter, is an important role fulfilled by the projection function.

All that remains to be done in the design of directional operators is the specification of the number of directions, or equivalently the angle between two

adjacent directions. To determine the latter, we need to determine the angular selectivity of a directional operator as a function of the angle θ between the edge direction and the preferred direction of the operator. Assume that we form the operator by taking an odd number $2N+1$ of samples. Let the number of a sample be n where n is in the range $-N \ldots +N$. Recall that the directional operator is formed by convolving with a symmetric Gaussian, differentiating normal to the preferred edge direction of the operator, and then sampling along the preferred direction. The differentiated surface will be a ridge which makes an angle θ to the preferred edge direction. Its height will vary as $\cos\theta$, and the distance of the n^{th} sample from the centre of the ridge will be $nd\sin\theta$ where d is the distance between samples. The normalized output will be

$$O_n(\theta) = \frac{\cos\theta}{2N+1}\left[\sum_{n=-N}^{N} \exp\left(-\frac{(nd\sin\theta)^2}{2\sigma^2}\right)\right]$$

If there are m operator directions, then the angle between the preferred directions of two adjacent operators will be $180/m$. The worst case angle between an edge and the nearest preferred operator direction is therefore $90/m$. In the current implementation the value of d/σ is about 1.4 and there are 6 operator directions. The worst case for θ is 15 degrees, and for this case the operator output will fall to about 85% of its maximum value.

3.3. Noise Estimation

To estimate noise from an operator output, we need to be able to separate its response to noise from the response due to step edges. Since the performance of the system will be critically dependent on the accuracy of this estimate, it should also be formulated as an optimization. Wiener filtering is a method for optimally estimating one component of a two-component signal, and can be used to advantage in this application. It requires knowledge of the autocorrelation functions of the two components and of the combined signal. Once the noise component has been optimally separated, it is squared and locally averaged. In fact we can further improve the separation in the smoothing phase, since when we use the noise estimate we will be comparing it to the response of the edge detection operator at a local

maximum. We know that there is an edge near the centre of the detection operator, and that this edge will be producing a known response in the noise separation filter (the noise separation will not be perfect). We can use the positional correspondence of the two responses to make the local averaging filter orthogonal to the output due to a step edge at its centre. Ideally it should give zero output at the centre of an edge when there is no noise present.

Let $g_1(x)$ be signal we are trying to detect (in this case the noise output), and $g_2(x)$ be some disturbance (the edge response), then denote the autocorrelation function of g_1 as $R_{11}(\tau)$ and that of g_2 as $R_{22}(\tau)$, and their cross-correlation as $R_{12}(\tau)$, where the correlation of two real functions is defined as follows

$$R_{ij}(\tau) = \int_{-\infty}^{+\infty} g_i(x) g_j(x+\tau)\, dx$$

We assume in this case that the signal and disturbance are uncorrelated, so $R_{12}(\tau) = 0$. The optimal filter is $K(x)$ where K is defined as follows (Wiener 1949)

$$R_{11}(\tau) = \int_{-\infty}^{+\infty} (R_{11}(\tau - x) + R_{22}(\tau - x)) K(x)\, dx$$

Since the autocorrelation of the output of a filter in response to white noise is equal to the autocorrelation of its impulse response, we have

$$R_{11}(x) = k_3\left(\frac{x^2}{2\sigma^2} - 1\right)\exp\left(-\frac{x^2}{4\sigma^2}\right)$$

If g_2 is the response of the operator derived in (2.38) to a step edge then we will have $g_2(x) = k\exp\left(-\frac{x^2}{2\sigma^2}\right)$ and

$$R_{22}(x) = k_2\exp\left(-\frac{x^2}{4\sigma^2}\right)$$

In the case where the amplitude of the edge is large compared to the noise, $R_{22} + R_{11}$ is approximately a Gaussian and R_{11} is the second derivative of a Gaussian of the same σ. Then the optimal form of K is the second derivative of a delta function.

The filter K above is convolved with the output of the edge detection operator and the result is squared. The next step is the local averaging of the squared noise values. The averaging filter is basically a broad Gaussian, but its accuracy can be improved in this application by orthogonalizing it to the step edge response. Let the averaging filter be expressed as $A_1(x) - A_2(x)$ where

$$A_1(x) = a_1 \exp\left(-\frac{x^2}{2\sigma_a^2}\right)$$

$$A_2(x) = a_2 \exp\left(-\frac{x^2}{\sigma^2}\right)$$

and the σ in the expression for A_2 is the same as for the detection filter. (Actually, the optimal shape for A_2 is the square of the second derivative of a Gaussian, but the use of this function makes the scheme very sensitive to small variations in the position of the detection filter maximum). The constants a_1 and a_2 are chosen so that the net response to the squared filtered step response is zero, i.e.

$$\int_{-\infty}^{+\infty} \Big(A_1(-x) + A_2(-x)\Big)\left(\frac{x^2}{\sigma^2} - 1\right)^2 \exp\left(-\frac{x^2}{\sigma^2}\right) dx = 0$$

Having formed an estimate of the local noise energy at every point, we can now deal with the problem of setting operator thresholds to achieve minimal error rate. This is the subject of the next section.

3.4. Thresholding with Hysteresis

Virtually all edge detection schemes to date use some form of thresholding. If the thresholds are not fixed a priori but are determined in some manner by the algorithm, the detector is said to employ adaptive thresholding. The solitary exception is the Marr Hildreth scheme, where edges are marked at any zero-crossing in the output of a Laplacian of Gaussian filter. This is not a practical proposition because there is a very high density of zero-crossings in the response to pure noise even if the noise has vanishing energy. Most practical implementations of this scheme use thresholding based on the slope of the zero-crossing.

The present algorithm sets thresholds based on local estimates of image noise and therefore falls into the class of adaptive thresholding algorithms. It has the additional complexity that it makes use of two thresholds to deal with the problem of streaking. Streaking is the breaking up of an edge contour caused by the operator output fluctuating above and below the threshold along the length of the contour. Suppose we have a single threshold set at A_{th}, and that there is an edge in the image such that an operator responds to it with mean output amplitude of A_{th}. There will be some fluctuation of the output amplitude due to noise, even if the noise is very slight. We expect the contour to be above threshold only about half the time. This leads to a broken edge contour. While this is a pathological case, streaking is a very common problem with thresholded edge detectors. It is very difficult to set such a threshold so that there is small probability of marking noise edges while retaining high sensitivity. An example of the effect of threholding with hysteresis is given in figure (3.2).

One possible solution to this problem, used by Pentland (1982) with Marr-Hildreth zero-crossings, is to average the amplitude of a contour over part of its length. If the average is above the threshold, the entire segment is marked. If the average is below threshold, no part of the contour appears in the output. The contour is segmented by breaking it at maxima in curvature. This segementation is necessary in the case of zero-crossings since the zero-crossings always form closed contours, which obviously do not always correspond to contours in the image.

In the current algorithm, no attempt is made to pre-segment contours. Instead the thresholding is done with hysteresis. If any part of a contour is above a high threshold, that point is immediately output, as is the entire connected segment of the contour which contains the point and which lies above a low threshold. The probability of streaking is greatly reduced because for a contour to be broken it must now fluctuate above the high threshold and below the low threshold. Also the probability of false edges is reduced because the high threshold can be raised without risking streaking. The ratio of the high to low threshold is usually in the range two or three to one.

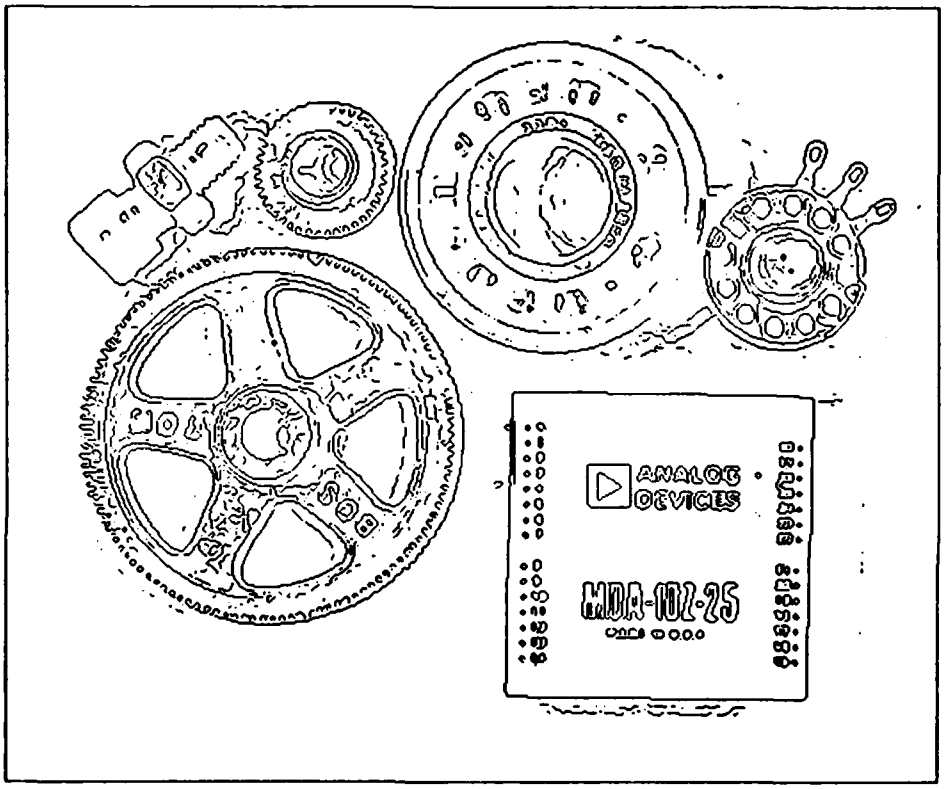

Figure 3.2a. Image thresholded at Th_1

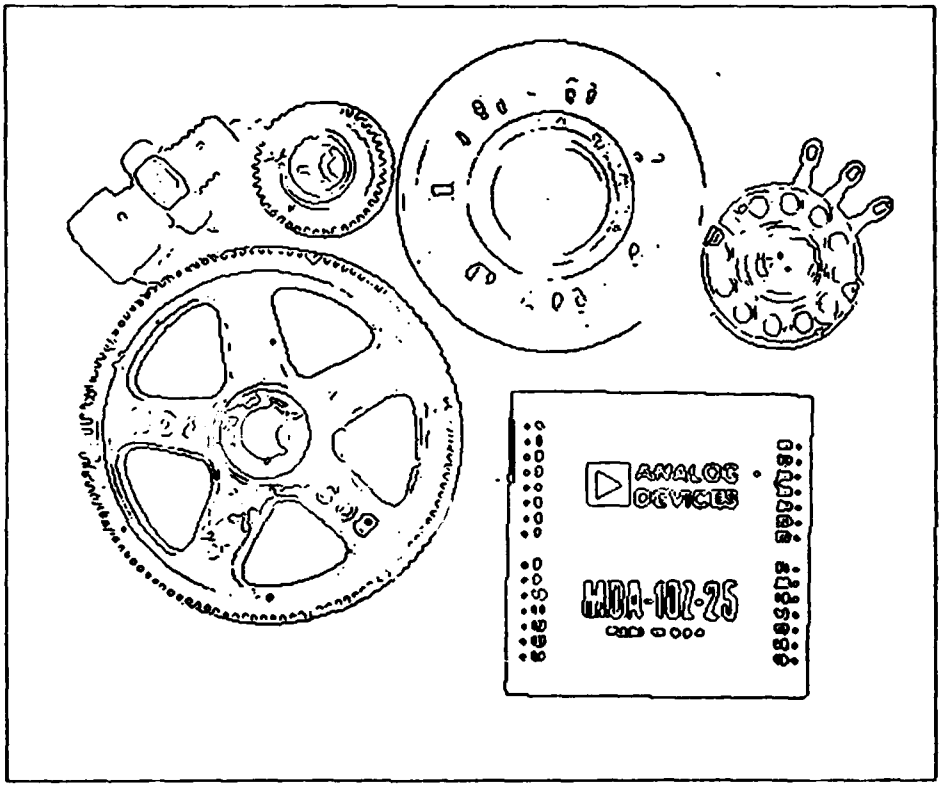

Figure 3.2b. Image thresholded at 2 Th_1

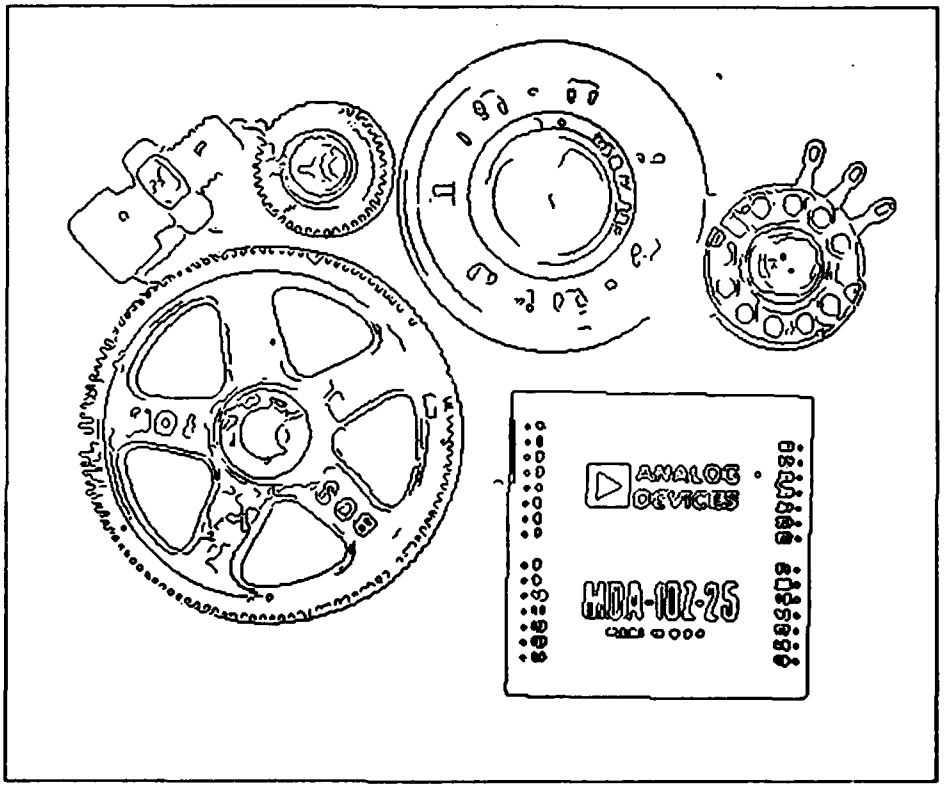

Figure 3.2c. Image thresholded using both the thresholds in figures 3.2a and 3.2b

3.5. Sensitivity to Smooth Gradients

It has been pointed out in Binford-Horn (1973) that images frequently contain slow gradients, and that edge detectors which are sensitive to these gradients are prone to mark multiple edges in regions where the gradient is high. The edge operator derived in the last chapter will be sensitive to image gradients and we should now ask if it is possible to eliminate this sensitivity without prejudicing performance. One possibility would be to use an operator which is a linear combination of two different widths of the optimal operator, such that the resulting operator is insensitive to gradients. Suppose the function f is given by

$$f(x) = \frac{x}{\sigma_1^3}\exp\Big(-\frac{x^2}{2\sigma_1^2}\Big) - \frac{x}{\sigma_2^3}\exp\Big(-\frac{x^2}{2\sigma_2^2}\Big)$$

Then we find that

$$\int_{-\infty}^{+\infty} x\, f(x)\, dx = \sqrt{2\pi} - \sqrt{2\pi} = 0$$

So this function will certainly be insensitive to gradients, and its performance will be given by equation (2.12). The signal to noise ratio and localization are now

$$\Sigma = \left[\frac{2\sigma_1\sigma_2\big(\sigma_1^2+\sigma_2^2\big)^{\frac{3}{2}}(\sigma_2-\sigma_1)^2}{\sqrt{\pi}\sqrt{\sigma_1^2+\sigma_2^2}\big(\sigma_1^5+\sigma_1^3\sigma_2^2+\sigma_1^2\sigma_2^3+\sigma_2^5\big)-4\sqrt{2\pi}\sigma_1^3\sigma_2^3}\right]^{\frac{1}{2}}$$

$$\Lambda = \left[\frac{\sqrt{\sigma_1^2+\sigma_2^2}\big(4\sigma_2^4+8\sigma_1^2\sigma_2^2+4\sigma_1^4\big)\big(\sigma_2^3-\sigma_1^3\big)^2}{\sqrt{\pi}\sigma_1\sigma_2\sqrt{\sigma_1^2+\sigma_2^2}\big(3\sigma_1^9+6\sigma_1^7\sigma_2^2+3\sigma_1^5\sigma_2^4+3\sigma_1^4\sigma_2^5+6\sigma_1^2\sigma_2^7+3\sigma_2^9\big)-24\sqrt{2\pi}\sigma_1^6\sigma_2^6}\right]^{\frac{1}{2}}$$

Asymptotically as σ_2 tends to infinity, the above expressions tend to the limiting values

$$\Sigma = \left[\frac{2\sigma_1}{\sqrt{\pi}}\right]^{\frac{1}{2}} \qquad \text{and} \qquad \Lambda = \left[\frac{4}{3\sqrt{\pi}\sigma_1}\right]^{\frac{1}{2}}$$

Which gives the same overall performance as a simple first derivative of Gaussian as given by equation (2.40). In practice a value of σ_2 of around $3\sigma_1$ is used to reduce the computational expense and to prevent the operator becoming too sensitive to nearby edges because of its large support. The overall performance $\Sigma\Lambda$ is reduced by about 30% in this case. Note also that as σ_2 approaches σ_1 we obtain a third derivative of a Gaussian, which is similar to the operator sometimes used to estimate the strengths of Marr-Hildreth zero-crossings. But the performance is reduced in this case, as will be shown in chapter 7.

The fact that f is insensitive to gradients implies that f may be expressed as the derivative of a function g which has zero mean value, and which is symmetric because f is antisymmetric. A symmetric function g with zero mean value may be thought of as a lateral inhibition operator as described by Binford (1981). Lateral inhibition was proposed as a mechanism for reducing sensitivity to gradients. But the form of the lateral inhibition operator was not determined analytically when in fact it has a direct effect on the performance.

4. Finding Lines and Other Features

Chapters two and three described in some detail the derivation of an optimal operator for step edges in Gaussian noise. The derivation of the analytic form of this operator was rather tedious and in the end, we arrived at a parametric form and had to resort to numerical methods to find the best values for the parameters. The alternative method of finding an operator was by a brute force stochastic optimization which did not even use an analytic expression for the criteria of optimality. The latter method was simpler to implement, but took much longer to arrive at a solution. It is in theory more general, because to find an operator for a different input waveform, only its edge model has to be be changed. This has not been tried, and the time expenditure necessary to modify the stochastic optimizer and arrive at a solution did not seem justified.

It would be very useful if there were a more general method which gave a fast solution and was simple to adapt to new waveforms. There are several reasons for considering optimal detectors for other features. Firstly, it has been pointed out (Herskovits and Binford 1970, Marr 1976) that step edges are not the only kind of intensity change that occur and are important. In particular they mention "roof" and "bar" profiles as being common in real images. Each of these poses a new problem in finding an optimal detector.

Even if we are considering step edge profiles, a strong case can be made for the use of non-white Gaussian noise models. We can remove the spectral flatness constraint and still use the same design technique as long as the noise can be modelled as the output of some filter in response to white Gaussian noise. In fact if we know the autocorrelation of the random process, it is possible to derive a causal filter (linear predictor) which has the same autocorrelation. By applying the inverse of this filter to the noisy waveform to be detected, we obtain a different waveform, but it is now bathed in *white* Gaussian noise. We can apply the same design techniques to this new waveform, and the optimal detector for the original waveform is the convolution of the detector for the filtered waveform and the inverse noise filter. So we have mapped the problem of finding step edges in non-white Gaussian noise to that of finding other edge profiles in white noise.

4.1. General Form for the Criteria

When we derived the analytic criteria for step edges in chapter 2, there were only two places where the form of the input waveform actually affected the criteria. By inserting a general feature in place of the step edge we can readily obtain a general criterion. Recall that the definition of the signal to noise ratio Σ was the quotient of the responses of the operator to the input waveform and to noise only. The response to noise for an operator with impulse response $f(x)$ will be given by equation (2.4), and is

$$n_0\left[\int_{-\infty}^{+\infty} f^2(x)\,dx\right]^{\frac{1}{2}}$$

The response of this operator at the "centre" of an arbitrary waveform $F(x)$ is similar to equation (2.3) and is just

$$\int_{-\infty}^{+\infty} F(-x)f(x)\,dx$$

So the signal to noise ratio for f and any feature F is (assuming $n_0 = 1$)

$$\Sigma = \frac{\int_{-\infty}^{+\infty} F(-x)f(x)\,dx}{\sqrt{\int_{-\infty}^{+\infty} f^2(x)\,dx}} \tag{4.1}$$

The method for determining the localization of the operator is also similar to that used in chapter 2, and we will not describe it fully here. Recall that localization was defined as the reciprocal of the standard deviation in the position of the marked edge relative to the true edge. To find maxima in the operator response we actually locate zero-crossings in the derivative of its response. Localization was defined as the quotient of the slope of the zero-crossing and the root mean squared noise in the differentiated response. The latter is given by equation (2.7) and has the value

$$n_0\left[\int_{-\infty}^{+\infty} f'^2(x)\,dx\right]^{\frac{1}{2}}$$

The slope of the differentiated operator reponse is

$$\left[\frac{d^2}{dx_0^2}\right]_{x_0 x=0} \int_{-\infty}^{+\infty} F(x_0 - x) f(x)\, dx \;=\; \int_{-\infty}^{+\infty} F(-x) f''(x)\, dx$$

And so the localization Λ becomes (assuming $n_0 = 1$)

$$\Lambda \;=\; \frac{\int_{-\infty}^{+\infty} F(-x) f''(x)\, dx}{\sqrt{\int_{-\infty}^{+\infty} f'^2(x)\, dx}} \tag{4.2}$$

The final form of the composite criterion can now be written as the product of (4.1) and (4.2) thus

$$\Sigma\Lambda \;=\; \frac{\int_{-\infty}^{+\infty} F(-x) f(x)\, dx}{\sqrt{\int_{-\infty}^{+\infty} f^2(x)\, dx}} \frac{\int_{-\infty}^{+\infty} F(-x) f''(x)\, dx}{\sqrt{\int_{-\infty}^{+\infty} f'^2(x)\, dx}} \tag{4.3}$$

Thus finding an arbitrary feature detector requires the maximization of this functional, subject possibly to some subsidiary constraints such as the multiple response constraint (2.25). This is difficult in general, even if the feature F is particularly simple, like a step edge. However the form of the functional (4.3) is simple *enough* that given a candidate feature detector we can readily evaluate its performance analytically. If the operator impulse response f and the feature F are both represented as sampled sequences, evaluation of (4.3) requires only the calculation of four inner products between sequences.

This suggests that numerical optimization can be done directly on the sampled operator impulse response. This method can be expected to be much faster than the stochastic optimization since the evaluation of performance is exact, and the gradient at each point in function space can be accurately estimated. At the same time it is very general in that optimization for any waveform only requires a sampled version of the waveform.

The output will not be an analytic form for the operator, but an implementation of a detector for the feature of interest will require discrete point-spread functions anyway. It is also possible to add additional subsidiary constraints by using a *penalty*

method (see Luenberger 1973). In this method the constrained optimization is reduced to one (or possibly several) unconstrained optimization. For each constraint we define a penalty function which has a non-zero value when one of the constraints is violated. We then find the maximum of

$$\Sigma(f)\Lambda(f) - \mu_i P(f)$$

Where P is a function which has a positive value only when a constraint is violated. The larger the value of μ_i the greater the likelihood that the constraints will be satisfied, but at the same time there is a better chance that the method will become ill-conditioned. A sequence of values of μ_i may need to be used, with the final value from each optimization used as the starting value for the next. The μ_i are increased at each iteration so that the value of $P(f)$ will be reduced, until the constraints are "almost" satisfied.

An example of the method applied to the problem of detecting "ridge" profiles is shown in figure (4.1). The function F for a ridge is defined to be a flat plateau of width w, with step transitions to zero at the ends. The auxiliary constraints are

(i) The multiple response constraint. This constraint is taken directly from equation (2.25), since it does not depend on the form of the feature.

(ii) The operator should have zero DC component. That is it should have zero output to constant input.

Since the optimal operator for ridges is also symmetric, it will have zero response to a constant gradient. This means that it can be represented as the second derivative of a function of finite extent, which in turn suggests that there may be economical ways of computing operators for several orientations in two dimensions.

The figure shows two different operators derived for the same feature. The two operators differ in the size of their possible support. The second is constrained to lie within a region twice the width of the ridge, while the second has a support three times the ridge width. The performance of the second operator is very slightly worse than the first. However the fact that it requires a smaller support means that

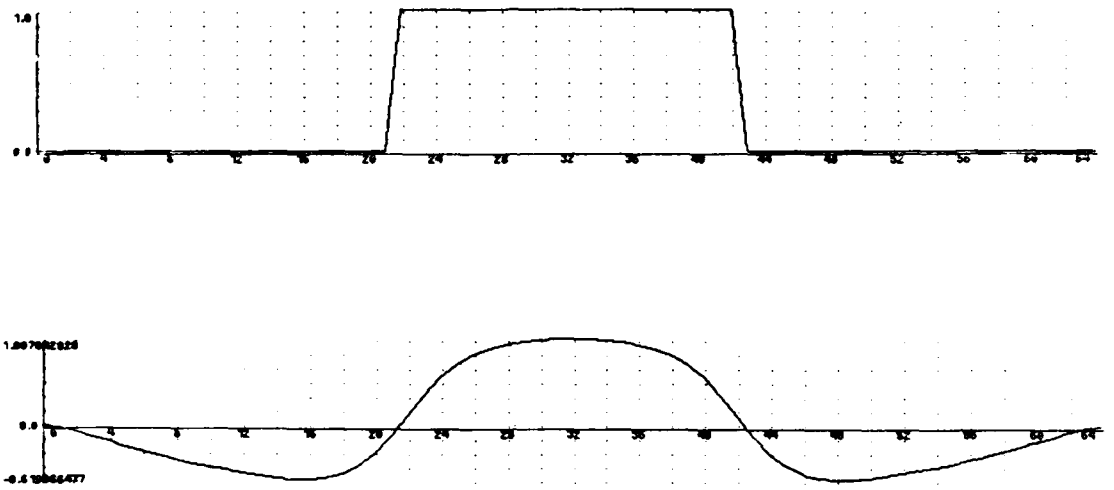

Figure 4.1. A ridge profile and the optimal operator for it

it is likely to be less susceptible to interference from adjacent features. This aspect of performance depends strongly on the width of the support, but performance in other respects does not. We therefore choose the operator support to be three times the ridge width, since at this width there will be no interference if the distance between ridges equals the ridge width, i.e. if the ridges and valleys have the same width.

Since the width of the operator is determined directly by the width of the ridge, there is a suggestion that several widths of operators should be used. This has not been done in the present implementation however. With this ridge model a wide ridge can be considered to be two closely spaced edges, and the implementation already includes detectors for these The only reason for using a ridge detector is that there are ridges in images that are too small to be dealt with effectively by the

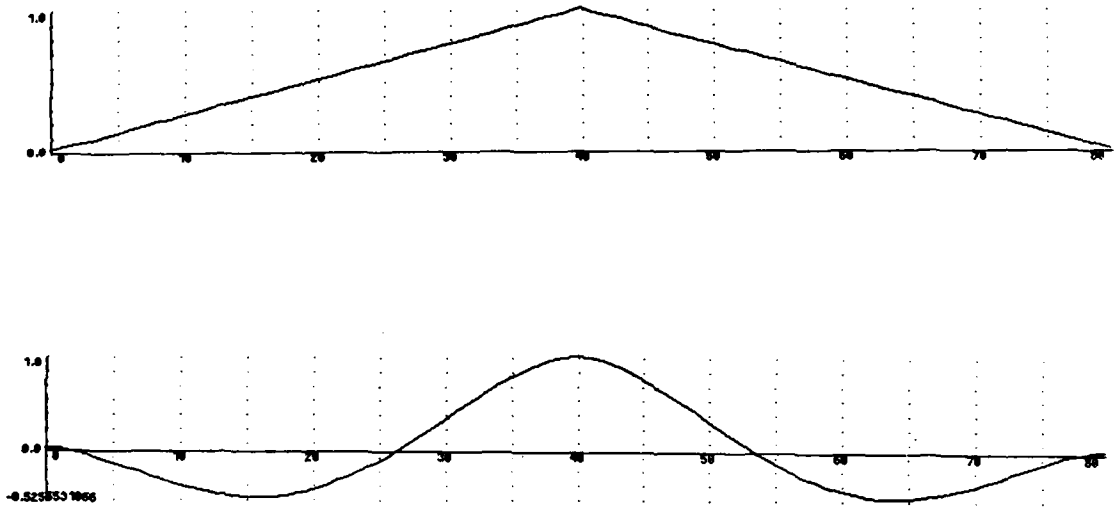

Figure 4.2. A roof profile and an optimal operator for roofs

narrowest edge operator. These occur frequently because there are many features (e.g. scratches and cracks or printed matter) which result in discrete contours only a few pixels wide.

A similar procedure was used to find an optimal operator for roof edges. These features typically occur at the concave junctions of two planar faces of an object. The results are shown in figure (4.2). Again there are two subsidiary constraints, one for multiple responses and one for zero response to constant input. Note that the difference between the two operators is essentially their "resemblance" to their respective inputs. We would expect this from the theory of Wiener filtering. The optimal Wiener filter for a signal in white Gaussian noise is just the time-reversed signal. Wiener filtering considers only signal to noise ratio however, and the localization and multiple response criteria impose effective smoothness constraints

on the operator.

A roof edge detector has not been incorporated into the current edge detector because it was found that ideal roof edges were relatively rare. In any case the ridge detector is an approximation to the ideal roof detector, and is adequate to cope with them. The situation may be different in the case of an edge detector designed explicitly to deal with images of polyhedra, like the Binford-Horn line-finder (1971). Here several width of roof operator may be desirable to deal with different signal to noise ratios in the image.

The method described above has been used to find optimal operators for both ridge and roof profiles and in addition it successfully finds the optimal step edge operator derived in chapter 2. It should be possible to use it to find operators for arbitrary features, and for optimal step operators to deal with non-white noise. For example, the problem of detecting step edges in "blue" noise (uncorrelated noise that has been passed through a perfect differentiator) reduces to the problem of detecting roof edges in white noise. So the optimal detector for step edges in this case is the derivative of an optimal roof operator. Note that it is not the same roof operator which we derived here because the latter includes the zero DC response constraint, which does not translate to something useful for the step operator.

4.2. In Two Dimensions

We now face the problem of extending the one-dimensional ridge operator to two dimensions. As in the case with step edges, the extension is an operator composed of a detection function normal to the ridge direction and a projection function parallel to it. As before we non-maximum suppress the output of the convolution of the image with this mask normal to the edge direction. The maximal points can then be thresholded (with hysteresis) and the marked ridge contours can be combined with the edge map.

In the case of ridges however it is much harder to obtain an accurate estimate of the ridge direction. There is no simple measure like the gradient direction which aligns with the normal. While it is true that the larger principal curvature will be normal to the ridge direction, this is a much less reliable quantity to measure from

even a smoothed image. Remember that the ridge detector will be operating below the resolution of the smallest step edge operator, so the degree of smoothing will be slight. This suggests that it will be necessary to use several oriented masks at each point and to choose the one which best fits the ridge locally. This has been found to be an inadequate solution because it performs so poorly when the ridge is highly curved, as is generally the case for printed text. While the highly directional masks have advantages for long straight ridges, they are not adequate as general ridge detectors.

In practice a measure similar to the curvature must be used. The direction of principal curvature cannot be used directly, and not merely because it is a noisy measure. The peak of a ridge should be approximately flat in the ridge direction but highly curved normal to this direction. But there are points on the sides of the ridge that are approximately planar. Here the direction of greatest curvature will be arbitrary. It is quite possible that it will happen to be parallel to the ridge direction and that there may be a slight maximum in this direction, and hence a ridge point will be marked.

To prevent these erroneous points from being marked it is necessary to modify the ridge direction estimate so that it takes into account the slope of the ridge normal to the direction of greatest curvature. This slope will be approximately zero if the point is at the top of the ridge, but for points on the side of the ridge where the greatest curvature may lie parallel to the ridge direction, the slope normal to this direction (which is the slope of the ridge face at that point) is large. So instead of non-maximum suppressing in the direction of maximum curvature, we use the direction $\mathbf{n}$ which maximizes

$$\frac{\partial^2 I}{\partial \mathbf{n}^2} + \alpha \mathrm{abs}\left[\frac{\partial I}{\partial \mathbf{n}^{\perp}}\right]$$

where $\mathbf{n}^{\perp}$ is the normal to $\mathbf{n}$, and α is some positive constant.

So in regions of low curvature, the above measure chooses a direction in which the slope is large, which is the correct behaviour for points on the sides of a ridge. This method has been used and seems to behave quite well even on difficult ridge

data e.g. finely printed text. An example of its performance on some text images is given in chapter 6.

A second problem with using non-maximum suppression with the ridge operator is that its response to an ideal ridge has two side lobes of opposite sign to its main peak. These will lead to negative ridges or valleys being marked on either side of a true ridge, and vice-versa. In fact there will also be maxima in the ridge detector output on either side of a step edge, and clearly these points should not be marked as ridges. We are starting to run into the problem of integrating descriptions of different features, which is much more difficult than the integration of data about the same kind of feature from different operators. Typical features in an image will lead to responses from several different kind of feature detector, and some decision must be made as to which feature best represents the image.

The question of feature integration was addressed in some detail by Marr (1976) who stressed the importance of producing a single coherent representation of intensity changes called the "Primal Sketch". This incorporated descriptions of several kinds of feature including edges and wide and thin bars. The development of effective algorithms for the combination of arbitrary features was not carried very far by Marr, who rather applied a selection criterion to the feature detector outputs at each point. In practice the responses of two feature detectors may not be exactly coincident in space, and it is not clear how the selection criterion is to be modified. In cases like these surface fitting is a useful technique as in the "topographic primal sketch" of Haralick (1983). Here each possible interpretation has associated with it an error measure that mirrors the difference between the true image and the modelled surface. The best feature to describe each image point is the one with lowest error.

The problem of integrating the ridge description with the edge detector output has not been satisfactorily solved to the present time. A generalization of the feature synthesis approach described in section 3.1 has been implemented and gives acceptable results on some images, but is not robust enough to be used generally. In the case of combination of operator outputs, preference was always given to the smaller operators, and the feature synthesis always proceeded in one direction. For

merging feature descriptions, where there is no a priori reason to prefer one feature to another, it should be symmetric.

For example, suppose a ridge detector and a step edge detector both respond to a feature that is roughly a step edge. From the edge points marked by the edge detector, we synthesize the ridge detector output that would have occurred had the image actually contained a step edge. Then the ridge detector output is compared with the synthetic output and if it is not significantly greater, no ridge point will be marked. Similarly from the ridge detector output, we reconstruct the edge detector output that would have occurred if the ridge detector accurately described the image. The edge detector output will (in this example) be much stronger than the synthesized output and so an edge point will be marked. This method has the advantage that it is possible to mark the occurrence of more than one type of feature at a point in an image. It has been found that such points do occur in images (Herskovits and Binford 1970) in particular roof edges are often superimposed on step changes and "edge effects" which are similar to ridges also often accompany step changes.

It is necessary to consider ridges and valleys as different features as the detector may output both kinds of interpretation near a single feature in the image. Some form of integration technique such as feature synthesis or goodness of fit testing must be used. This has not been done in the present implementation, which only integrates one of these features with the step edge map. This is one area where a lot of work still remains to be done, and several feature integration techniques need to be tried.

5. Implementation Details

The ultimate test of any edge detector is its performance in some application on real images. The translation of a derived operator into a program is non-trivial. While the running version of the program is actually very small, it is still the result of much refinement. The refinements are as much a part of the design of the edge detector as is the theoretical analysis presented in the first four chapters. It is not the intent of this chapter to describe any such program. It will describe in an abstract way several algorithms for implementing some of the processing required by the edge detector. The author feels that this is necessary for several reasons

(i) Since the edge detector involves a considerable amount of computation, especially convolution, it is important that efficient algorithms be used if it is to run in a reasonable amount of time.

(ii) Because images may contain very fine detail it is important that local operations involve the minimum number of pixels, but provide the best accuracy from them. This applies in particular to operations such as the calculation of directional derivatives and non-maximum suppression.

(iii) Edge detectors are not vision programs. The implementor should bear in mind that the detector is only the first stage in a much larger system, and should give consideration to the choice of representation of its output.

This chapter will not describe in detail all the aspects of the present edge detection scheme, in fact some of the algorithms presented do not even form part of the scheme, but may be used in future implementions. Instead it will focus on two or three of the more critical aspects of the implementation, in particular on efficient methods for convolution with Gaussians, and on the details of the non-maximum suppression scheme. It will close with details of a control abstraction for the programming of local parallel operations which are used extensively by the scheme.

5.1. Effects of Discretization

All of the analysis to date has assumed that the image was a continuous differentiable surface and that the edge operators were likewise continuous functions. Since most implementations of the detector on digital computers will employ discrete filters applied to sampled image data, it is necessary to find accurate discrete approximations to the continuous filters. It is also important to consider the effect of the smoothing filter (if any) which was applied to the image before it was sampled. Smoothing filters are necessary to prevent aliasing of high frequency components in the sampled signal. Suppose an image is smoothed, sampled and convolved with a discrete filter. By the associativity of convolution, this is equivalent to convolving the image with a filter that is the result of the convolution of the smoothing filter and the discrete filter. If the image can be smoothed with a Gaussian smoothing function, no convolution is necessary at that scale.

The simplest way to approximate a continuous filter with a discrete filter is to sample the former. If this method is to succeed, we must ensure that the sampling does not introduce aliasing. Consider a continuous first derivative of Gaussian filter of the form

$$f(x) = -\frac{x}{\sigma^2}\exp\left(-\frac{x^2}{2\sigma^2}\right)$$

Suppose that the image is sampled at intervals of τ, (the filter must also be sampled at this rate for discrete convolution) then the Nyquist frequency is $\frac{1}{\tau}$. The effective bandwidth of the filter should be less than half this frequency to prevent aliasing. The Fourier transform of this filter is

$$F(\omega) = \sqrt{2\pi}\mathrm{i}\omega\exp\left(-\frac{\omega^2\sigma^2}{2}\right)$$

The cutoff frequency is $\frac{\pi}{\tau}$, and substituting we find that the amplitude at cutoff is

$$\sqrt{2\pi}\mathrm{i}\frac{\pi}{\tau}\exp\left(-\frac{\pi^2\sigma^2}{2\tau^2}\right) \tag{5.1}$$

This function never reaches zero amplitude for large ω, but it does approach zero very rapidly. We can set the effective cutoff frequency at the point where this function falls to 0.01 of its maximum value. This limits the smallest value of σ that we can use for a given sampling rate. The minimum value of σ is approximately τ. This is in fact the smallest operator size used in the present implementation.

A second problem arises when we try to approximate infinite Gaussians with finite impulse response filters. Once again we can exploit the fact that the Guassian decays to zero very rapidly in the spatial domain. In the current implementation, the Gaussian is truncated at about 0.001 of its peak value. This constrains the ratio of the number of samples in the (discrete) impulse response to the width σ of the filter. This ratio is typically 8, e.g. to approximate a filter with a σ of 2.0 it is necessary to use at least 16 samples.

Finally, it should be mentioned that it is sometimes possible to dispense with the convolution step entirely. If the desired value of σ is much less than τ, discrete convolution is not practical. However, an equivalent convolution may be performed with a continuous filter (the smoothing filter) before the image is sampled. Since in theory the smoothing step is necessary anyway, no extra computational effort is required. We find in fact that the smoothing function is determining the performance of the subsequent edge detector, and the use of Gaussian smoothing should give near optimal step edge detection.

5.2. Gaussian Convolutions

It is perhaps surprising to see an entire section devoted to what seems a very straightforward and specific computation. However, there are several interesting properties of the two-dimensional Gaussian that suggest fast algorithms for convolution. In particular, the central limit theorem implies that repeated convolution with any finite filter tends in the limit to a Gaussian convolution. We begin with a review of discrete convolution.

5.2.1. Discrete Two-Dimensional Convolution

The output of the convolution of a discrete image $I(n, m)$ with a two-dimensional filter $f(i, j)$ is given by the double summation

$$O(n,m) = \sum_{i=-\frac{M}{2}}^{\frac{M}{2}} \sum_{j=-\frac{M}{2}}^{\frac{M}{2}} I(n-i, m-j) f(i,j)$$

assuming that the filter f has the same size M in both dimensions. This method requires M^2 multiplications and slightly fewer additions for each output point computed. It is a general method and will work with any two-dimensional finite impulse response filter.

5.2.2. Convolution using One-Dimensional Decomposition

We now consider a more specialized form of convolution which is applicable to a limited subclass of two-dimensional filters. The subclass is the class of separable two-dimensional filters. This class is characterized by the decomposition of their impulse responses into independent linear filters

$$f(i,j) = f_x(i,0) * f_y(0,j)$$

where the $*$ denotes convolution, and the filters f_x and f_y have only M non-zero components. By using the associativity of convolution, we break the convolution of an image with the two-dimensional filter into two convolutions with linear filters

$$I * f = I * [f_x * f_y] = [I * f_x] * f_y$$

This method requires only $2M$ multiplications and about the same number of additions per point. For large operator sizes (values of M of 64 are common) this method is substantially faster than the naive method, but is limited to separable filters. The number of useful members of this class is actually quite small, and the Gaussian is in fact the only two-dimensional symmetric function which can be decomposed in this way. Other useful separable functions include the first directional derivatives of the Gaussian in the x and y directions.

5.2.3. Recursive Filterring

So far we have been approximating the infinite Gaussian function with finite impulse response filters. It seems that the approximation could be more accurate

if we were to use infinite impulse response (recursive) filters instead. We can again make use of the separability of the two-dimensional Gaussian, and can therefore reduce the filter design problem to that of designing a one-dimensional filter which approximates a Gaussian. The infinite impulse response (IIR) filter can be characterized by the equation

$$y(n) = \sum_{i=0}^{Z} a_i x(n-i) + \sum_{j=1}^{P} b_j y(n-j) \tag{5.2}$$

where $x(n)$ and $y(n)$ are the input and output respectively at the n^{th} point. This filter is roughly equivalent to a continuous filter having P poles and Z zeros. The positions of the poles are determined by the coefficients b_j while the zeros are determined by the a_i.

The immediate drawback of using such a filter to approximate a Gaussian is that the filter is infinite "in one direction only", and that the Gaussian has an impulse response that extends to infinity in both directions. The solution to this problem is illustrated in figure (5.1). We employ two recursive filters moving in *opposite directions, each of which has an impulse response which is* approximately a half-Gaussian. We then sum the two responses (and subtract a component at the centre point which is doubled) and are left with a first approximation to the symmetric Gaussian. We can if we wish repeat this process on the filtered image and (by the central limit theorem) we will obtain a very close approximation to the Gaussian, as shown in the last frame of figure (5.1).

The half-Gaussian is approximated by a damped exponential cosine, which requires two poles and two zeros in the recursive filter. The b coefficients are derived by considering four discrete output values near a zero-crossing of the response. We choose the values to be

$$\exp(\alpha\tau)\sin(-\omega\tau) \qquad 0 \qquad \exp(-\alpha\tau)\sin(\omega\tau) \qquad \exp(-2\alpha\tau)\sin(2\omega\tau)$$

Application of equation (5.2) to the first three and last three values gives two equations each of which involves only one of the b_j,and the solution is

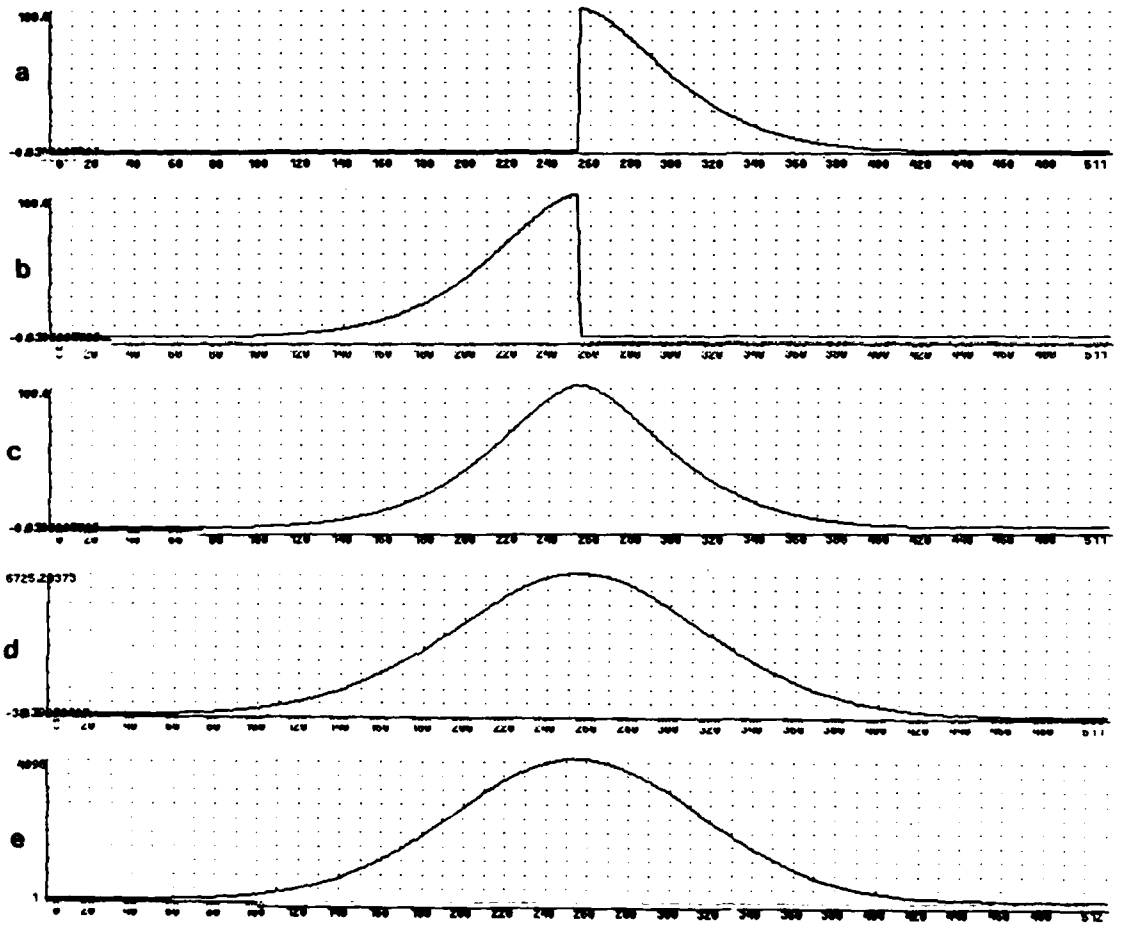

Figure 5.1. (a) and (b) Recursive Half-Gaussian filters moving from left to right and from right to left respectively, (c) sum of these, (d) Result of two applications of recursive filter and (e) True Gaussian.

$$b_1 = 2\exp(\alpha\tau)\cos(\omega\tau) \qquad b_2 = -\exp(2\alpha\tau)$$

where α and ω are the decay constant and angular frequency respectively, of the damped exponential cosine response. Typical values for α and ω are

$$\alpha = \frac{1}{\sigma} \qquad \omega = 0.8\alpha \tag{5.3}$$

where σ is the standard deviation of the equivalent Gaussian. The a_i determine the gain of the filter and its first derivative at the origin. For unit gain and best approximation to the slope of a Gaussian we use

$$a_0 = 1.0 \qquad a_1 = \exp\left(\frac{\alpha^2\tau^2}{2}\right) - b_1 \tag{5.4}$$

The interesting feature of this method is that its complexity is independent of σ. In fact for a single pass approximation, it requires only 12 multiplications and additions per point (3 each for filtering in four directions). It also requires an extremely small number of array references, and the number may be reduced even further by saving previous x and y values in registers (only three are needed). It is possible to implement the algorithm using only 4 references per point. In practice, it is usually better to make two passes over the image, so the above figures should be doubled.

This particular method is of course even more specialized than the previous methods, and is only useful for Gaussians and certain other infinite functions. However it has the lowest complexity of any algorithm discussed, and is very economical with regard to memory references. It has the additional advantage that the filter size can be varied by simply changing the value of some parameters, without affecting execution of the algorithm. It would seem to be the first choice for any future implementations.

5.2.4. Binomial Approximation

In the last two sub-sections we saw that by using the special properties of Gaussians we were able to reduce the number of multiplications required to perform convolution. The resulting algorithms were no longer general convolutions but were restricted to subclasses of two-dimensional filters. It is possible by exploiting the full power of the central limit theorem to produce an algorithm that requires no multiplication at all. Recall that repeated convolution with any spatially limited filter tends to an equivalent Gaussian convolution. If we choose the filter to be addition of two adjacent points, and if we repeat the addition many times, we can obtain a Gaussian approximation without multiplication.

A useful analogy to this method exploits the equivalence of discrete convolution and polynomial multiplication. The filter produced by the addition of two consecutive samples is isomorphic to multiplication by the polynomial $(x + 1)$. If the filter is applied n times it is equivalent to multiplication by the polynomial $(x + 1)^n$. The coefficients of this polynomial are given by the binomial theorem. We then use the fact that for large n, the binomial distribution may be approximated by a Gaussian. This method is economical in terms of multiplication, but its complexity is relatively high. Since the variance of two distributions add when the distributions are convolved, the standard deviation σ only increases as the square root of the number of convolutions. The value of σ after n applications of the addition filter is

$$\sigma = \frac{1}{3}\sqrt{n}$$

To phrase this result in the terms used in the rest of this section, we find the number of samples M required for an equivalent discrete convolution. Since M is typically 8σ, the relationship between the number of additions per point n and the equivalent mask size is

$$n = \frac{9}{64}M^2$$

The overall complexity of this algorithm for two-dimensional convolution (assuming it is used with decomposition) is $\frac{9}{32}M^2$ additions per point, with the

number of memory references being roughly the same. This may sound like a very small number, but the exponent is high. The smallest value of M that is ever likely to be used is 8, and so the minimum number of additions using this method is 18. However, both the number of additions and the number of memory references grows with M^2 even though we are exploiting separability. Since the time required for floating point addition is often not much lower than the time for a multiply, this method rapidly becomes unattractive as M increases.

5.2.5. Fast Convolution

In recent years, very fast algorithms have been developed for integer or polynomial multiplication (Schonhage and Strassen 1971). Asymptotically these algorithms are $O(n)$ in the length of the integers being multiplied. In the case of convolution, we typically use a filter that is much shorter than the length of the input, and we should therefore expect the asymptotic time for convolution to be independent of the filter length. Attempting to achieve anywhere near the asymptotic complexity however, would introduce prohibitively high constants.

But all is not lost. By using the simplest form of fast multiply, we can gain a very useful speedup with relatively low overhead. Consider two sequences of numbers which are to be convolved. We assume w.l.o.g. that the length of the sequences is $2n$, and we break each sequence into two subsequences of length n. Let the two sequences be x and y, and denote the subsequences as x_1, x_2 and y_1 and y_2. Then

$$x = x_1 \uparrow_n + x_2 \qquad \text{and} \qquad y = y_1 \uparrow_n + y_2$$

where $\uparrow_n$ denotes left-shifting of the sequence by n. We then use the distributivity of convolution over addition, and we have

$$x * y = (x_1 \uparrow_n + x_2) * (y_1 \uparrow_n + y_2) = x_1 * y_1 \uparrow_{2n} + (x_1 * y_2 + x_2 * y_1) \uparrow_n + x_2 * y_2$$

From which it would seem that computation of a $2n$ length convolution requires 4 convolutions of length n, implying an order of growth of n^2. But the above expression can also be written as

$$x * y = x_1 * y_1 \circlearrowleft_{2n} + [(x_1 - x_2) * (y_2 - y_1) + x_1 * y_1 + x_2 * y_2)] \circlearrowleft_n + x_2 * y_2$$

Which requires only 3 convolutions of length n, plus some extra addition and subtraction. We can recursively apply this technique to compute these shorter convolutions, and we arrive at an algorithm with lower order of growth than n^2. This leads to recurrence relationships for the number of multiplies and additions to perform a convolution of length n

$$C_m[n] = 3C_m\left[\frac{n}{2}\right]$$

$$C_a[n] = 3C_a\left[\frac{n}{2}\right] + 4n - 4$$

where C_m is the number of multiplications and C_a the number of additions for an n-point convolution. When these recurrences are expanded and simplified we obtain for the multiplication and addition complexity

$$C_m[n] = 3^L \approx 3^{\log_2(n)} = n^{\frac{\log 3}{\log 2}} \approx n^{1.6}$$

$$C_a[n] = 6 \cdot 3^L - 8 \cdot 2^L + 2 \approx 6n^{1.6} \qquad \text{for large } n \tag{5.5}$$

where L is the smallest integer greater than or equal to $\log_2(n)$. To translate these results into the context of convolution of a long sequence (say length n_1) with a much shorter one (length n_2), we assume $n = n_2$. We will require $\frac{n_1}{n_2}$ such convolutions, and each one will require about $n_2^{1.6}$ multiplies. The resultant complexity is $\frac{n_1}{n_2} n_2^{1.6} = n_1 n_2^{0.6}$, so we find that the complexity is linear in the

length of the longer sequence but only varies as the square root (roughly) of the shorter sequence. For two-dimensional convolution, similar results hold, and the multiplication complexity is $M^{1.2}$ multiplies per point while the addition complexity is about six times this.

Thus we have the remarkable result that this method has almost the same complexity as convolution with one-dimensional decomposition, but uses a completely general two-dimensional mask. The algorithm has been implemented and early tests indicate that it starts to exhibit its reduced complexity over naive convolution at about $n = 16$. At $n = 1024$, the speedup is five to six fold. It can be implemented in $6n$ space, and the number of memory references is about the same as the number of additions.

The low value of the complexity constants make this method faster than convolution employing fast Fourier transforms for values of n less than about 16000 (caution: this number is *very* hardware-dependent). It is also somewhat easier to encode than the FFT, since it has a natural recursive definition. It is quite likely that it is the fastest way to do general convolution for n in the range 16 to 16000. The method makes it possible to use two-dimensional masks that have exactly the form of the optimal edge detection operator, rather than Gaussian approximations. While the fast convolution algorithm has not yet been incorporated into the edge detector, it is certainly worthy of further experiment.

5.2.6. Sub-Summary

Hopefully this section has highlighted the fact that there are frequently manifold interesting implementations of seemingly mundane operations, e.g. convolution. But it has another purpose. When trying to solve a vision problem the first consideration should be motivational, i.e. what should this algorithm compute. The second is feasibility, e.g. what can be computed from an image. Only after these two have been treated should there be any constraints imposed by tractability, i.e. what can be computed in reasonable time. The choice of algorithm should not be prejudiced by considerations of efficiency until much consideration has been given to implementation, and only if it seems likely that no efficient algorithms exist for the computation. This theme is characteristic of the work of Marr (1976) who

argued strongly for a breakdown of image processing problems using the above considerations.

5.3. Non-Maximum Suppression

The optimal edge operator was derived under the assumption that edges would be marked at maxima in its output. For two-dimensional images, finding these directional maxima is straightforward but there has been quite a bit of experimentation with various non-maximum suppression schemes. The operation should be as local as possible i.e. it should rely on pixels that are close to the potential edge point, but it should also be robust and accurate.

The non-maximum suppression scheme described here may be used in either of two ways. In the first instance the edge direction is estimated from the gradient of a Gaussian-smoothed image surface by simply differentiating in the x and y directions. The gradient magnitude is then non-maximum suppressed in the gradient direction. This is just a possible implementation of equation (3.1). In the second case, the algorithm is used for non-maximum suppression of the outputs of directional masks. Here the gradient direction is fixed and is a property of the operator. We again non-maximum suppress the gradient magnitude, which in this case is the magnitude of the response of that operator.

In either case the algorithm is the same. It uses a nine-pixel neighbourhood as shown in figure (5.2). The normal to the edge direction (either the gradient or the prefered operator direction) is shown as an arrow, and it has components (u_x, u_y). We wish to non-maximum suppress the gradient magnitude in this direction, but we have only discrete values of the gradient at points $P_{i,j}$. We require three points for non-maximum suppression, one of which will be $P_{x,y}$ and the other two should be estimates of the gradient magnitude at points displaced from $P_{x,y}$ by the vector **u**.

Now for any **u** we consider the two points in the 8-pixel neighbourhood of $P_{x,y}$ which lie closest to the line through $P_{x,y}$ in direction **u**. The gradient magnitude at these two points together with the gradient at the point $P_{x,y}$ define a plane which cuts the gradient magnitude surface at these points. We use this plane to

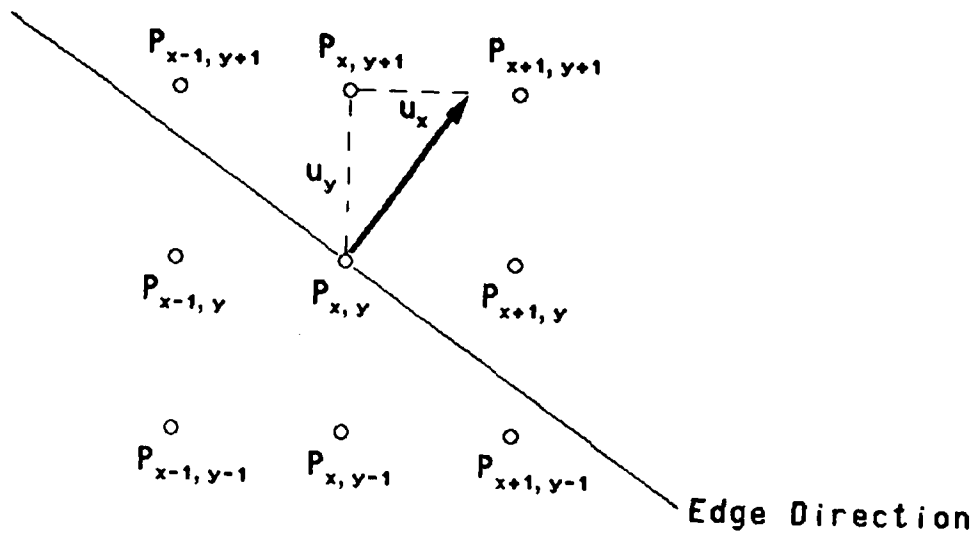

Figure 5.2. Support of the non-maximum suppression operator

---

locally approximate the surface, and to estimate the value at a point on the line. For example, in figure (5.2) we estimate the value of a point in between $P_{x,y+1}$ and $P_{x+1,y+1}$ that lies on the line. The value of the interpolated gradient is

$$G_1 = \frac{u_x}{u_y} G(x+1, y+1) + \frac{u_y - u_x}{u_y} G(x, y+1)$$

Similarly the interpolated gradient at a point on the opposite side of $P_{x,y}$ is

$$G_2 = \frac{u_x}{u_y} G(x-1, y-1) + \frac{u_y - u_x}{u_y} G(x, y-1)$$

We mark the point $P_{x,y}$ as a maximum if $G(x,y) > G_1$ and $G(x,y) > G_2$. The interpolation is similar for other gradient directions, and it will always involve one diagonal and one non-diagonal point. In practice, we can avoid the divisions by multiplying through by u_y.

This scheme involves five multiplications per point, but this is not excessive, and it performs much better than a simpler scheme which compares the point $P_{x,y}$ with two of its neighbours. It also performs better than a scheme which used an averaged value for the gradient along the edge, rather than just the value at $P_{x,y}$.

5.4. Mapping Functions

We close this chapter with a brief discussion of a general approach to program structure for image processing algorithms. The development of a low-level vision program requires many repetitive operations on each point of the image. There will be some set of dependencies between the results of these computations, which implies that there is a natural (partial) ordering of computations, and that some intermediate results must be computed and saved somewhere. Aside from any hardware (or object code) considerations, there are two basic ways of implementing a software interface for this kind of processing.

The first and most obvious way is to provide a set of primitive array operations, such as addition or convolution, which take arrays as arguments and store results into arrays. Programs written using these primitives look like normal sequential assembly code, unless there is some complex function (built from the primitives) which must move over the array in a non-standard way. In this case the arguments describing the way the function is to be moved must be repeated in each call to a primitive. This leads to cumbersome and non-orthogonal code.

The second approach is to provide a mapping function which takes a local image processing function as an argument and moves it over some number of arrays, with the motion specified by other arguments. The two operations of mapping and local computation are now handled by separate functions. This method is

reminiscent of the MAP- functions in Lisp, (Moon, Stallman and Weinreb 1983) and is similar in philosophy to the concept of iterators in CLU (Liskov et al. 1979). It has a number of advantages at the user level. The first is that the local function can be written in the source language e.g. Lisp (even if the mapping function turns it into something quite different) and tested on a sample set of arguments, without having to generate test images. The source code is more compact and less error-prone, and subjectively more readable. If parallel processing hardware is available, the source code would compile into something like the code using the first method. There would be no significant differences in the execution efficiencies of the two methods.

For a serial machine though, there are concrete advantages in directly implementing something like the second method. Since the local function is evaluated completely at one point before moving to the next, there is only one storage location required for each intermediate result. This contrasts with the former method which needs a block of storage for each intermediate result. The intermediate values may be held in high-speed storage (registers or cache) which greatly reduces the number of memory accesses required to apply the function to a full image. There is also a very considerable speedup possible when the local function uses conditional branching, such that the time to process an image point depends strongly on the data values at that point. For (most) parallel machines the time to apply the function to n points will be the worst case time for a one-point application. Conditional branching must be accomplished by setting a non-execution flag for the length of the code to be skipped. No advantage can be taken of sparse data, or computional shortcuts such as recursive filtering.

It is the author's experience that the latter style makes code development much easier (this was a serious consideration in the implementation of the algorithm, much of which is written in Lisp machine microcode). This is true to the extent that some of the more complicated functions, such as the sparse directional masks, could probably not have been implemented using the first approach because of the sheer amount of code. The edge detector has been implemented partially using the first approach, and fully using a mapping function (which is itself microcoded). The

mapping function maps over any number of arrays, with arbitrary increments for each array, and can store results into several output arrays if the function being mapped returns multiple values. The difference in execution times between the two methods is small, but the second method uses much less array storage, and has a much shorter source.

6. Experiments

It has been stressed that edge detection is only the first stage in a vision system and that the performance of the detector can only be gauged in its context. It has also been argued that the requirements of many of the later modules are similar to the extent that it should be possible to design a detector that will work well in several contexts. Starting from this assumption we proceeded to design a detector based on a precise set of performance criteria which seemed to be common to these later modules. We saw in chapters 2 and 4 that it was difficult to capture exactly the "intuitive" criteria that we originally defined. It is virtually impossible to capture all of the desirable properties of edge detection in a finite set of criteria and in the final analysis the only valid criterion is the performance of the detector on real data. This chapter is concerned with evaluating performance at the experimental level, and will include comparisons with some other edge detection algorithms. The evaluation is in three stages:

(i) Validation of the analytic performance criteria. The operator has been designed to optimally detect step edges in Gaussian noise. It should perform well on synthetic images of steps.

(ii) Subjective evaluation of performance on real images. The intention here is to verify the operation of various parts of the algorithm, in particular the integration of different operator widths and orientations. It is not possible to validate these by inspection of the detector output, but defects in their operation can often be isolated in this way. That is, we cannot tell by looking at the output whether the detector is working perfectly, but we can often tell where it is failing.

(iii) Evaluation of detector performance in some context. Since an edge detector is the first stage in many vision programs, it is appropriate to compare edge detectors by comparing the performance of the program which uses the two detectors. If the original assumption that many vision modules have similar requirements is valid, a detector designed using these criteria should perform well with all modules.

Finally we will present some simple demonstrations of properties of the human visual system which are consistent with the edge detector presented here. While this does not prove that the human visual system performs the same computations, it does suggest that the two systems share a common set of goals. It reinforces the choice of performance criteria and gives evidence that an edge detector designed using these criteria can perform well on a great variety of images.

6.1. Step Edges in Noise

In chapter 7 we will demonstrate that a directional second derivative edge operator gives better localization than the Laplacian when applied to a Gaussian smoothed image. We have also claimed (chapter 2) that a difference of boxes operator gives unacceptable multiple response performance to a noisy step edge. We should test those results experimentally now. In figure (6.1) We have a two-dimensional step edge with additive white Gaussian noise. The successive frames show the responses of difference of boxes, Laplacian of Gaussian and directional first derivative of Gaussian operators. The signal to noise ratio of the image, defined as the ratio of the amplitude of the step to the standard deviation of the noise at each pixel, is about 0.2, and the image is 256 by 256. The Gaussians for the Laplacian and first derivative operators both have a σ of 8.0 pixels, while the box masks have a length of 32 pixels in x and y.

Processing of the output of the difference of boxes operator after the convolution step is identical with the directional first derivative operator, that is, it is non-maximum suppressed and thresholded with hysteresis. For the Laplacian of Gaussian, the sequence is slightly different. Edges are initially marked at the zero-crossings in the convolution output, then the gradients of the convolution output are computed and the gradient magnitude is thresholded with hysteresis.

For each operator there are two thresholds that are set empirically to give the best subjective output. Figure (6.1) gives a guide to the localizing and multiple response performance of each of the operators. As we would expect, the directional first derivative operator gives subjectively better localization than the Laplacian, and the difference of boxes produces several contours in response to the single edge.

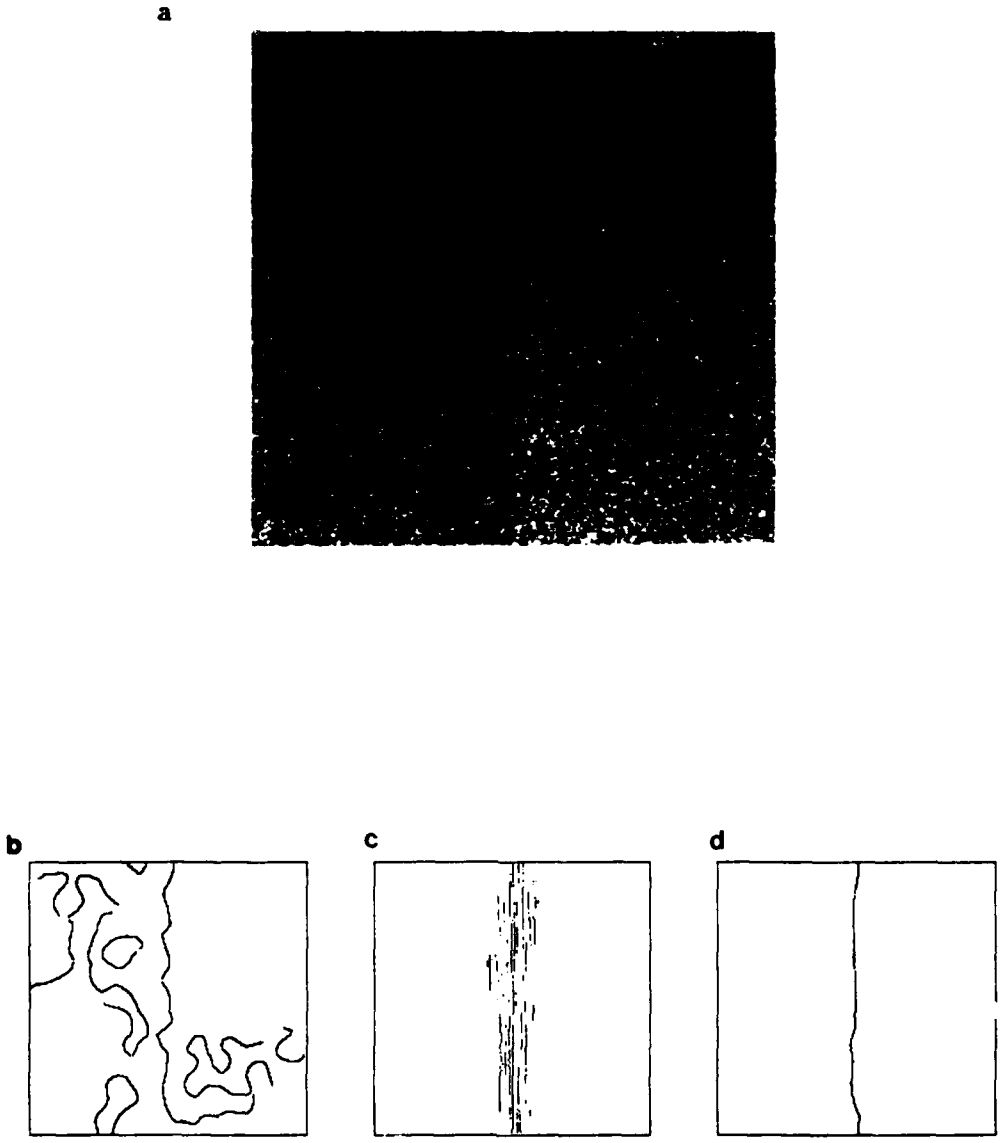

Figure 6.1. (a) Two dimensional step edge with additive white Gaussian noise, and outputs of (b) Laplacian of Gaussian, (c) difference of boxes and (d) first derivative of Gaussian operators.

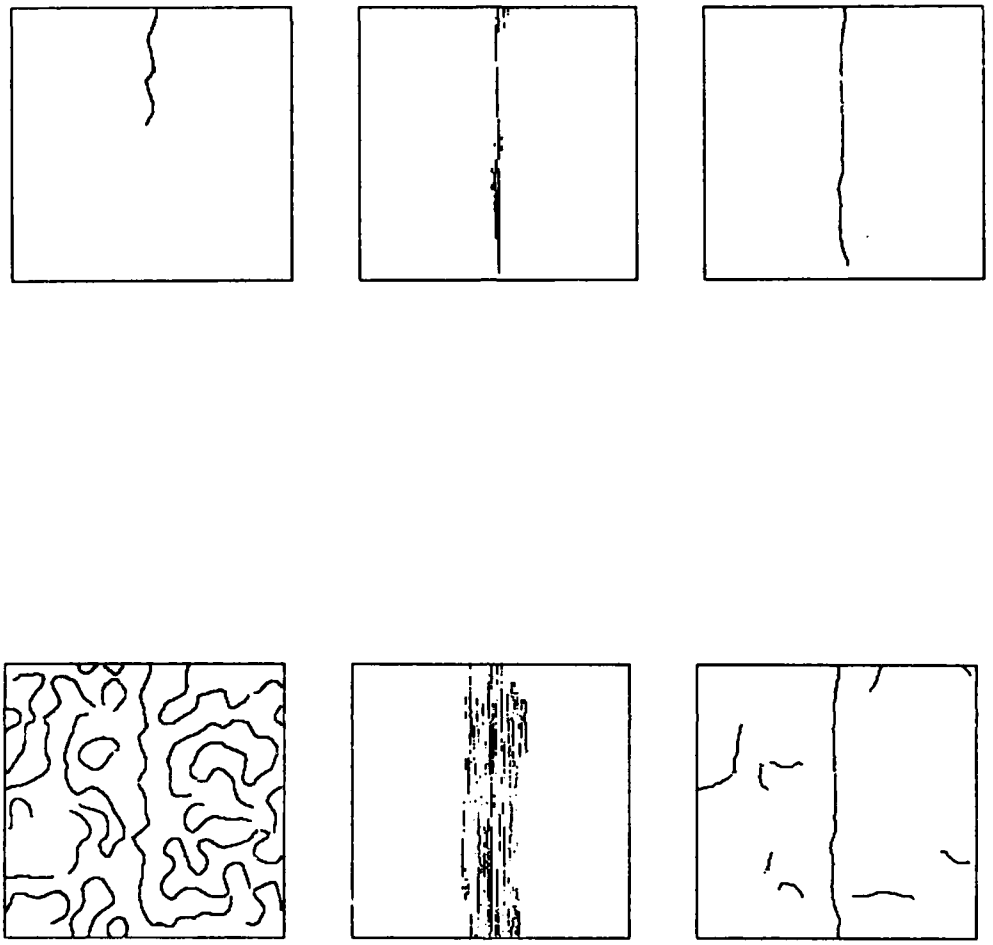

Figure 6.2. Effect of changing operator thresholds. In the first row, the thresholds are increased by 50% , and in the second row they are reduced by 50%. The order of operator outputs is (from left to right), (i) Laplacian of Gaussian, (ii) difference of boxes and (iii) first derivative of Gaussian.

To gain some idea of the detection performance (i.e. signal to noise ratio) of the operators, we can see how their outputs vary as we change the thresholds from the optimum values. The first row of figure (6.2) shows the result of increasing all thresholds by 50%, and in the second row the thresholds are reduced from from the optimum levels by 50%. From these we can infer that the difference of boxes operator has the best signal to noise ratio, since for all threshold levels, it marks edges only in the vicinity of the step. Of course signal to noise ratio is only one component of detection performance, and lack of multiple responses is the other. In this respect the difference of boxes performs very poorly, and worse as the thresholds are lowered. The Laplacian of Gaussian exhibits poor signal to noise ratio compared to the other two, and it is not possible to set the thresholds so that the full length of the edge contour is marked without introducing contours due to noise.

It may be argued that the problems with Laplacian of Gaussian or difference of boxes operators can be circumvented by applying "pruning" heuristics to their outputs. For example, it may be argued that it is possible to eliminate erroneous maxima in the difference of boxes output that are "near" the edge, or to use the outputs of different Laplacian of Gaussian channels to reinforce the evidence of an edge. This argument misses the point. The optimal operator derived here, or the first derivative of Gaussian approximation to it, gives the best performance for a *single* linear operator when followed by non-maximum suppression. In order to improve the performance of the other operators, non-local predicates have to be applied which in a sense make the filtering step redundant.

6.2. Operator Integration

We have argued that in order to handle a variety of images, an edge detector should incorporate operators of different widths. We have also argued for highly directional masks when they are applicable. All of these operators respond to the same type of feature, a step edge, and where several of them respond to the same edge, the detector must mark a single edge only. The problems with the integration of different operator outputs are very great. In fact many of the arguments against directional operators have been pragmatic, that it is difficult to combine oriented

operators and produce a coherent output. The problems with combining operator outputs of different widths are even worse, because maxima in the outputs of two operators responding to a single edge may be displaced from each other. Chapter 3 described feature synthesis as a method for combining several feature detector outputs. This method is used in the implementation of the edge detector, and we now explore how well it performs on some test images.

6.2.1. Integration of Different Mask Widths

The reader can readily gain an appreciation of the variety of detail that occurs at different scales in an image by reference to figure (6.4). This figure shows the edges marked by two operators on an image of a perforated cleaning cloth. The mask widths are $\sigma = 1.0$ and $\sigma = 5.0$ respectively. The edges at the two scales are virtually independent. In contrast, figure (6.7) shows the edges marked by operators with $\sigma = 1.0$ and $\sigma = 2.0$ on an image of some mechanical parts. In this image, almost all of the detail is picked up by the smaller operator, and it only fails on some of the shadow boundaries. These two figures capture the essence of the feature integration problem. Ideally every feature in the image should be marked, but only once.

Our basic width selection criterion, that is using the smallest operator that has sufficient signal to noise ratio, should do the right thing on the parts image. The edges at the smaller scale will first be marked, then the larger operator output will be synthesized from them, and finally any edges in the large operator output that are not consistent with the synthesized output will be added. The result is shown in the figure (6.8a). The only difference between this and the figure (6.7a) is the addition of some shadow edges, and the extension of some shading edges. Similarly the figure (6.5a) shows the combined output from the edges in figure (6.3). Since the long shading lines in the image are not seen by the smaller operators, the large operator features that correspond to them are not synthesized. When they appear in the actual large operator output they are marked in the detector output.

There is some freedom with the feature synthesis approach as to the "inhibition" effect of the synthesized operator outputs. Recall that the actual operator output had to be significantly greater than the synthesized output for an edge to be

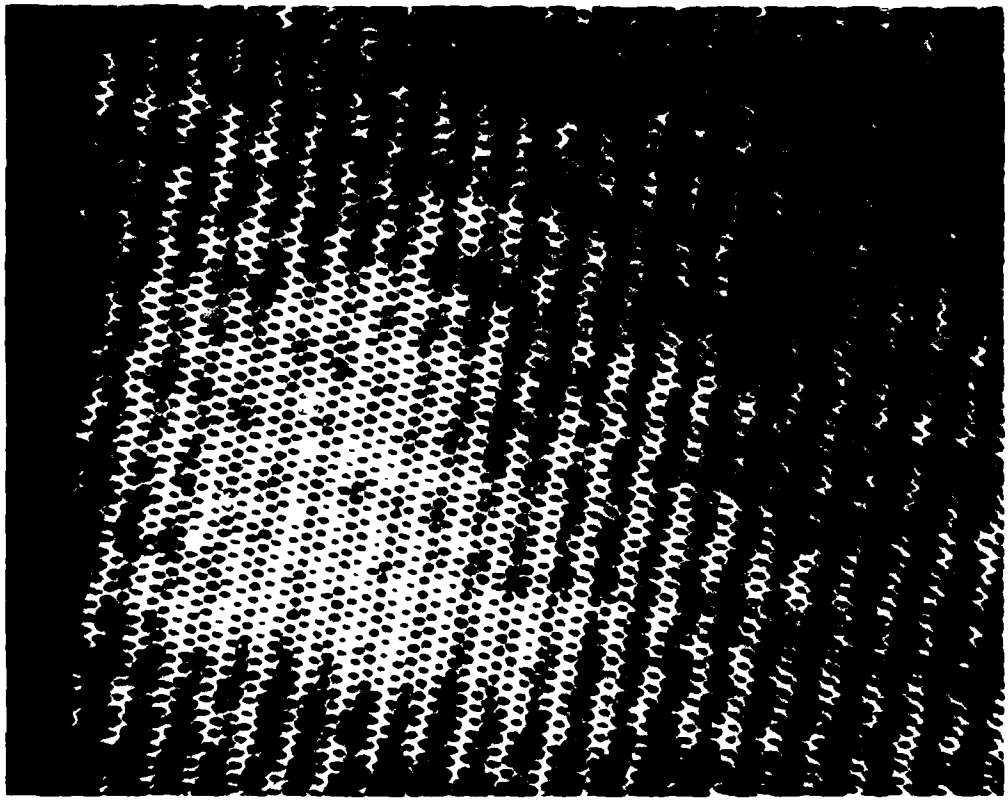

Figure 6.3. (a) Cleaning cloth image

AD-A130 824 FINDING EDGES AND LINES IN IMAGES(U) MASSACHUSETTS INST 2/2
OF TECH CAMBRIDGE ARTIFICIAL INTELLIGENCE LAB
J F CANNY JUN 83 AI-TR-720 N00014-80-C-0505

UNCLASSIFIED F/G 20/6 NL

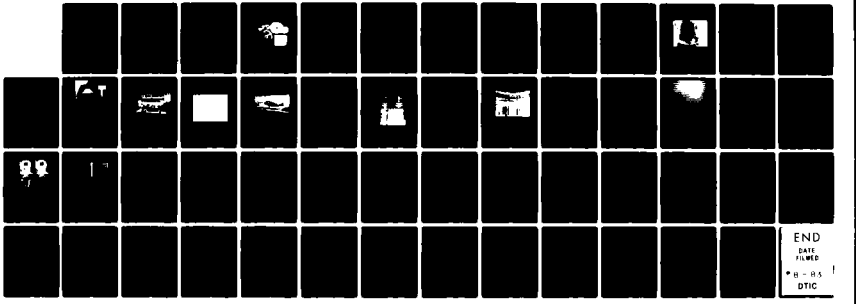

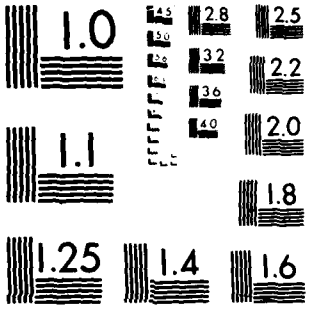

MICROCOPY RESOLUTION TEST CHART
NATIONAL BUREAU OF STANDARDS 1963 A

a

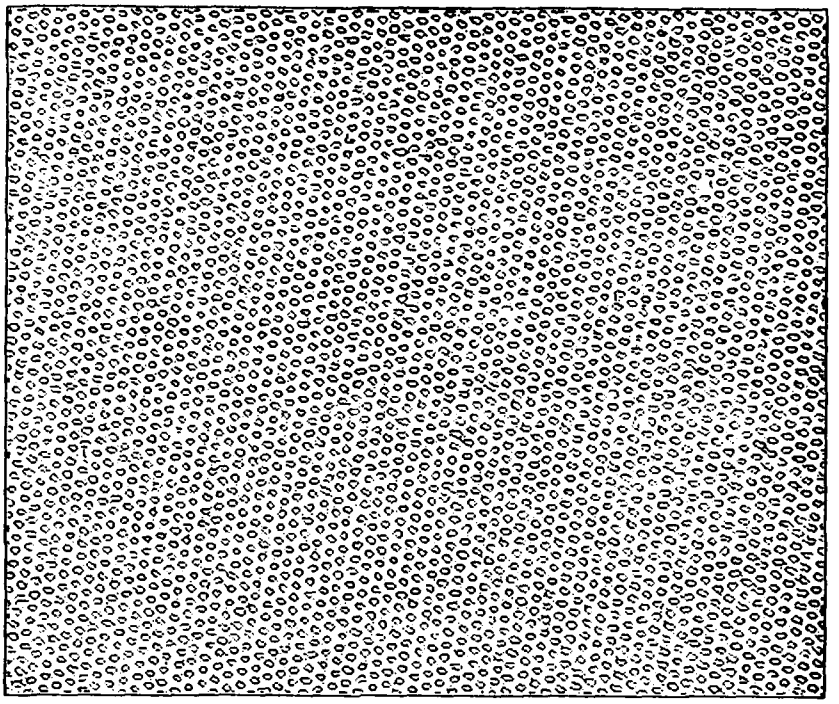

b

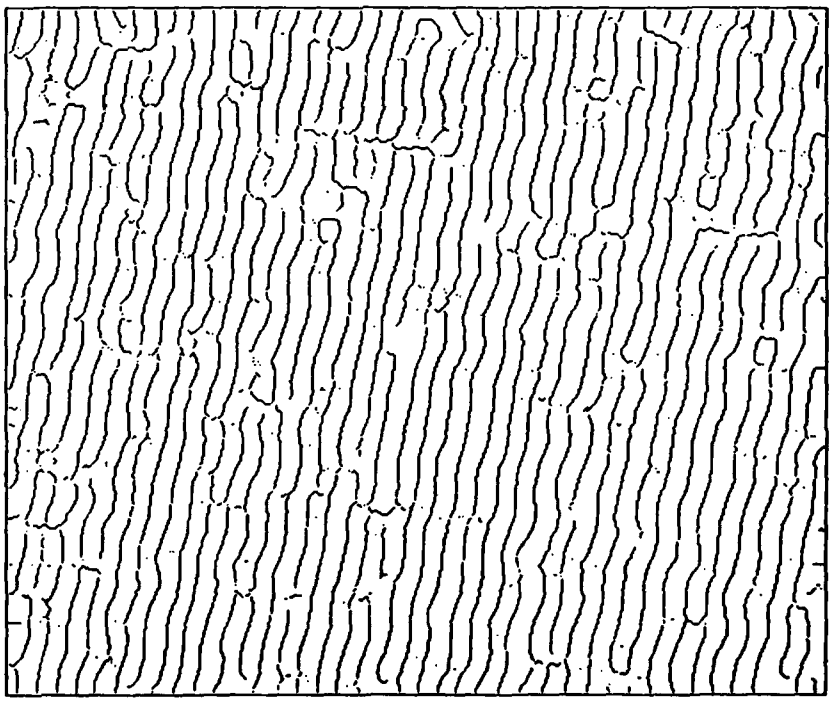

Figure 6.4. (a) Edges from cleaning cloth image with operator width $\sigma = 1.0$ (b) edges from operator with $\sigma = 5.0$

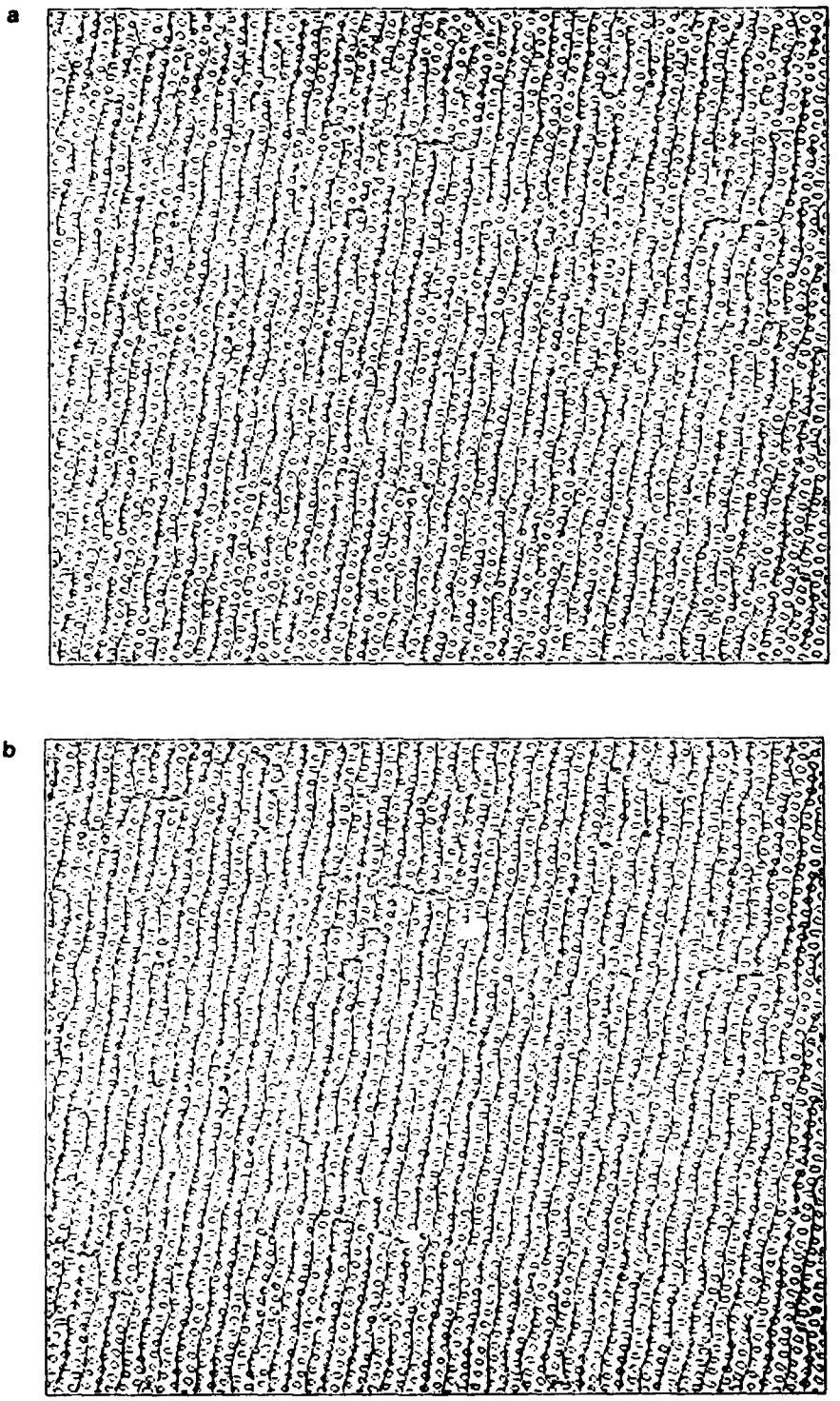

Figure 6.5. (a) Combined edges from cleaning cloth image using feature synthesis, (b) superposition of the two sets of edges

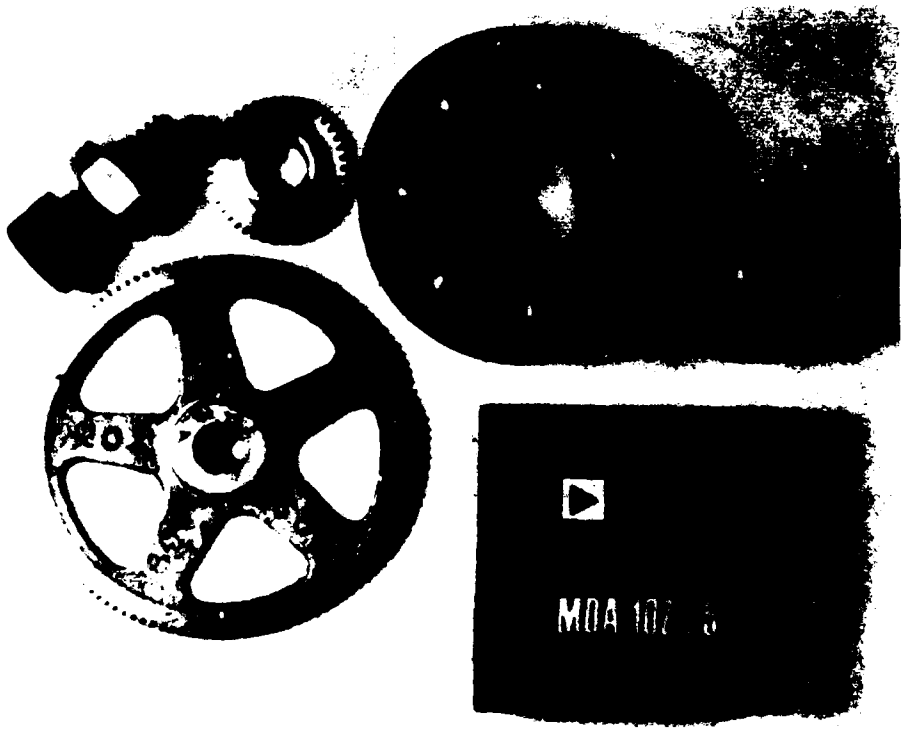

Figure 6.6. (a) Parts image

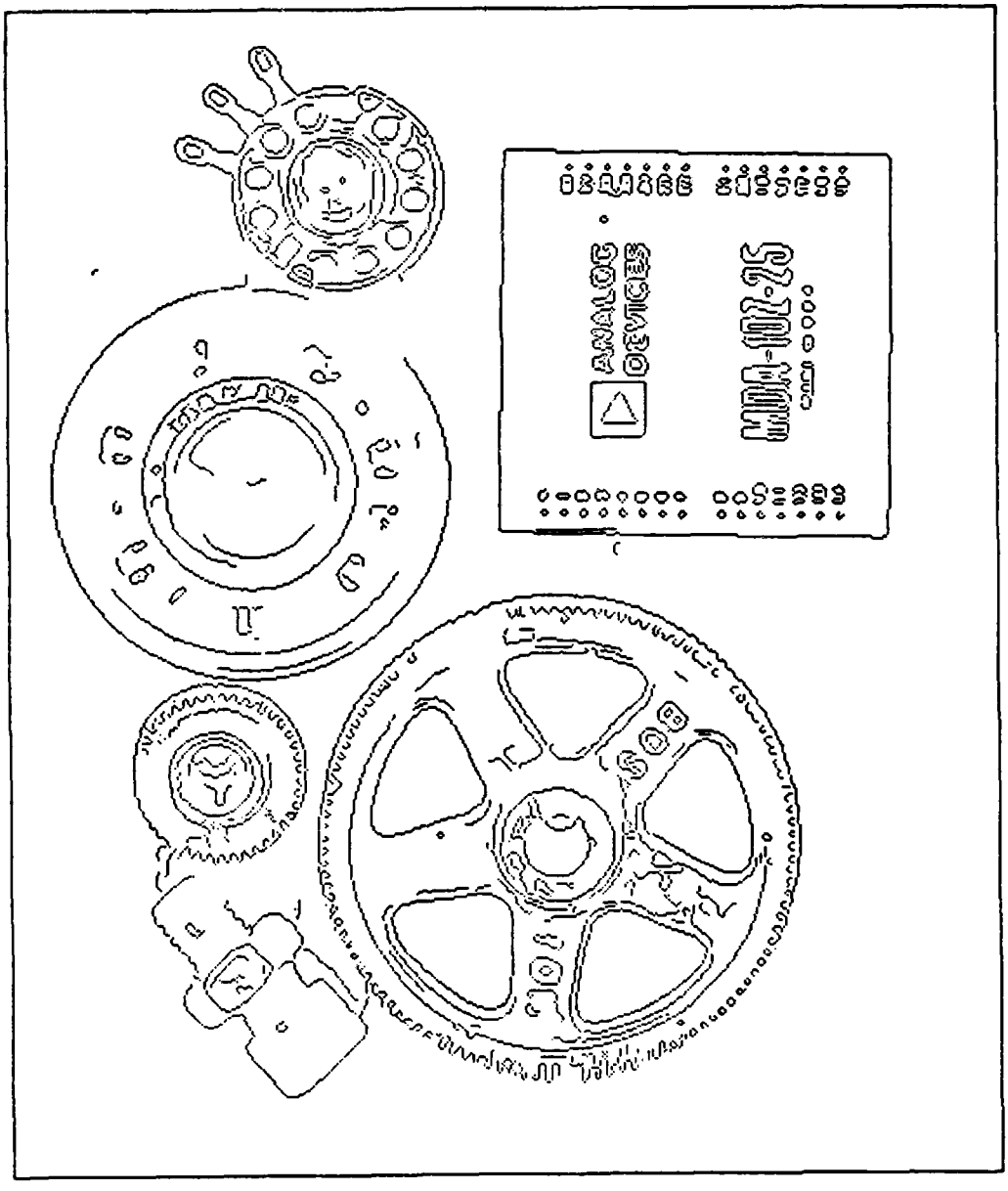

Figure 6.7a. Edges from parts image with operator width $\sigma = 1.0$

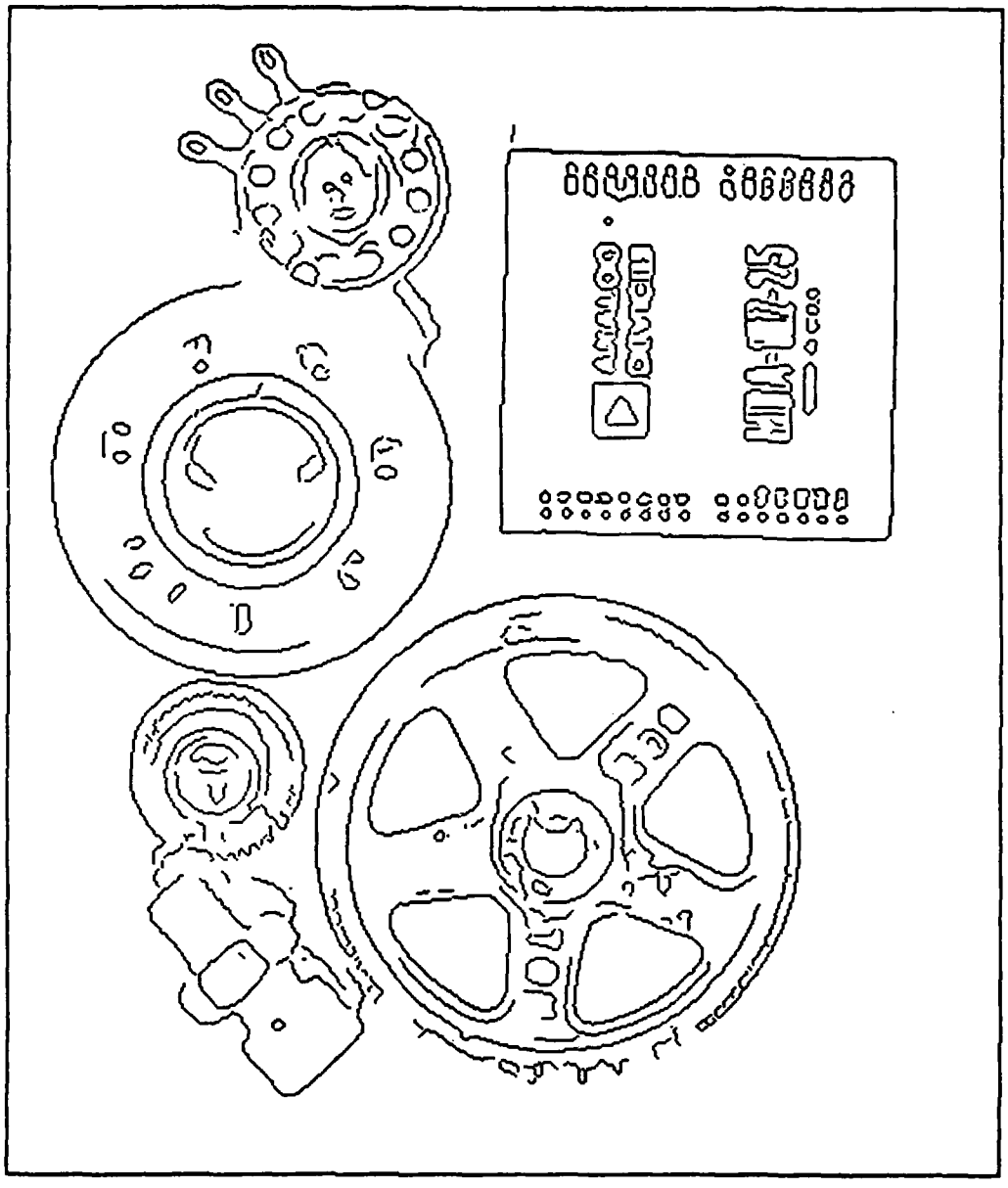

Figure 6.7b. Edges from parts image with operator width $\sigma = 2.0$

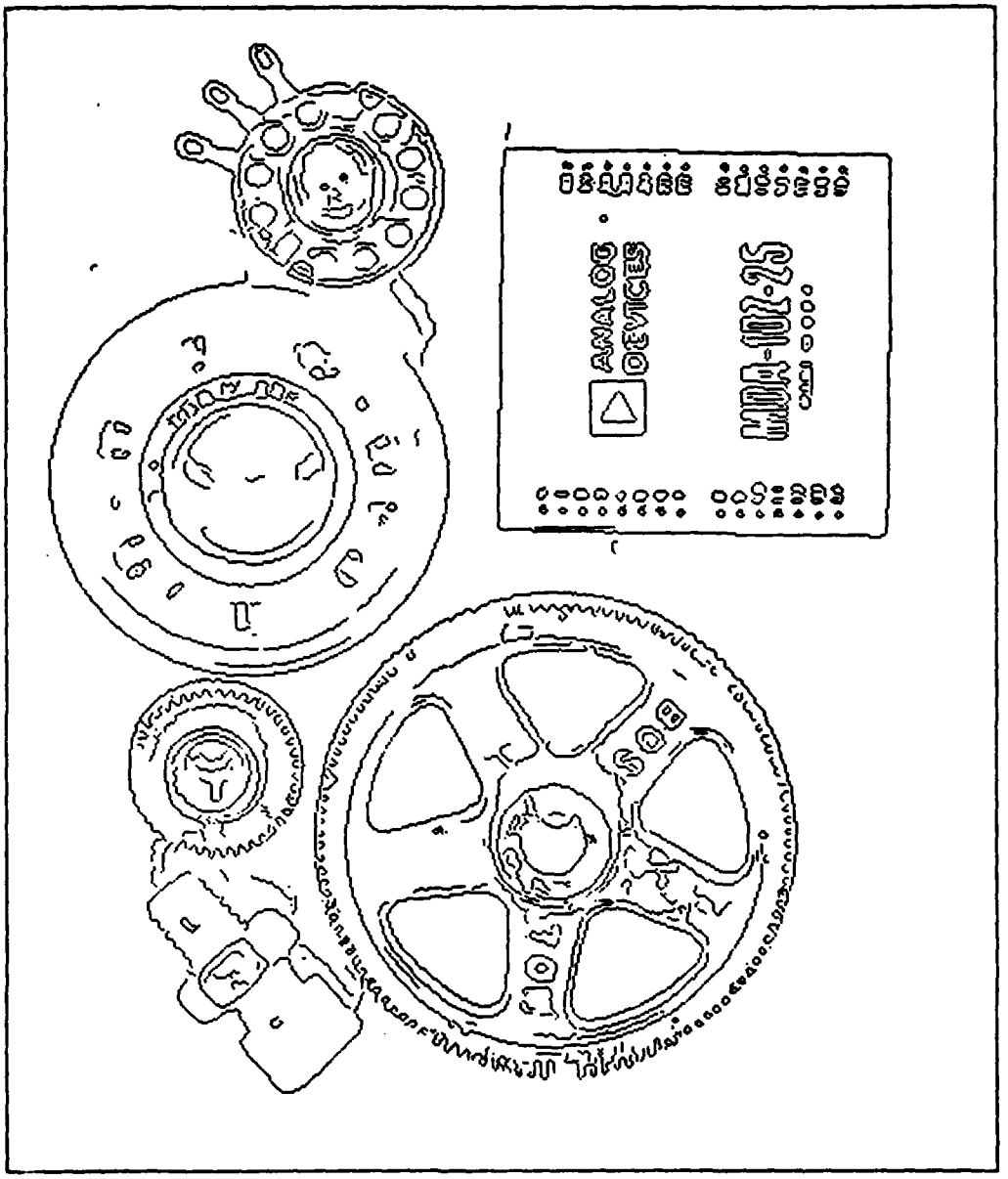

Figure 6.8a. Combined edges for parts image using feature synthesis

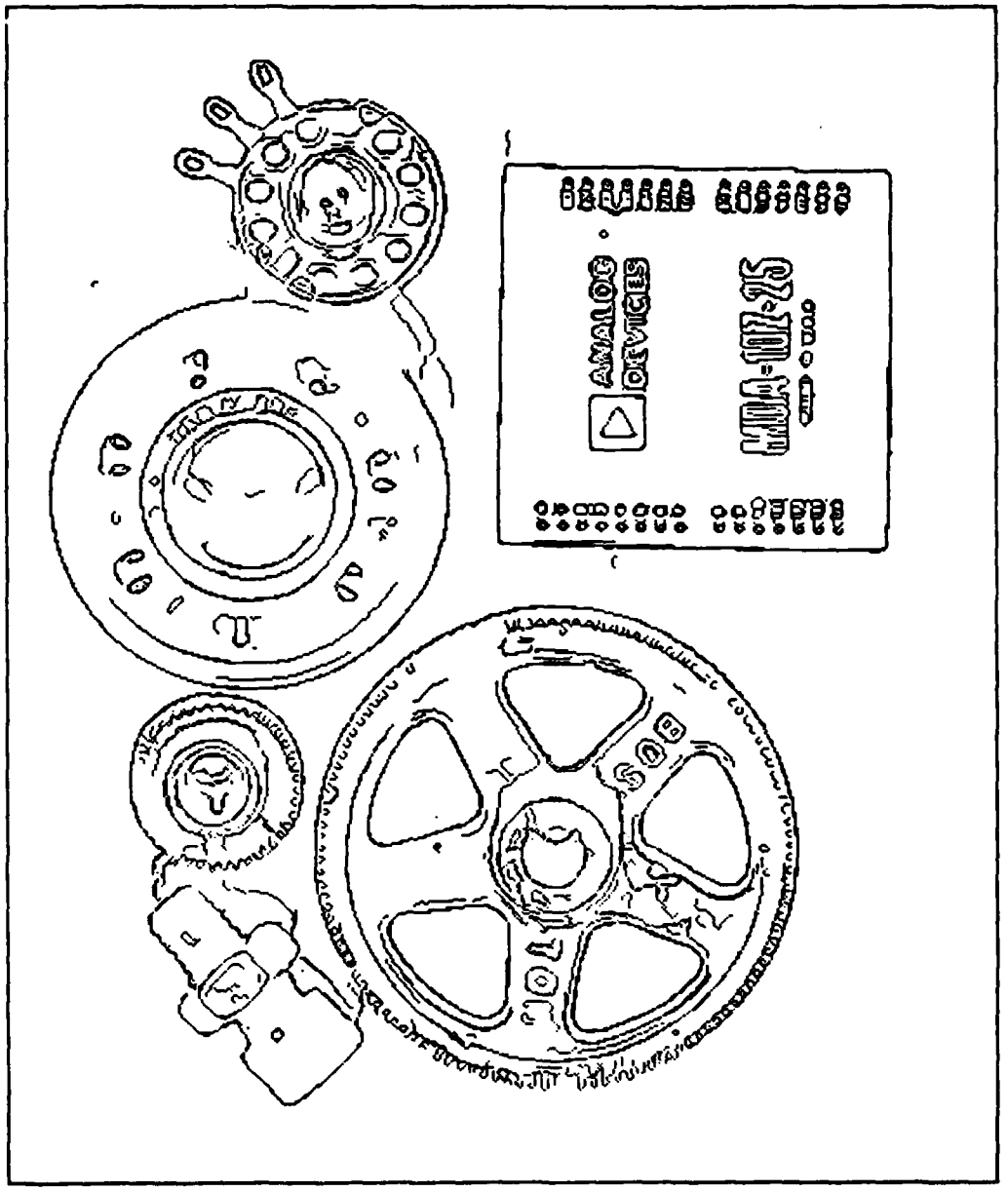

Figure 6.8b. Superposition of the edges for parts image

marked. In the present implementation the vector difference between the actual and synthesized gradient is first taken and if the magnitude of this difference is greater than the magnitude of the synthesized gradient, a new edge is marked. By introducing a scale factor into the comparison, the likelihood of a new edge being marked can be varied. This factor must be determined empirically. The above two images place conflicting requirements on the factor. If it is too large, the fuzzy edges in the cloth texture are missed. If it is small, there is duplication of edge points in the parts image, and consequent smearing of the edge contours. A single value was found which gave the results shown in the two figures. This value has given good results on all the images tried, and does not require "tuning" for a particular image. For comparison, below each of the combined edge maps in figures (6.5) and (6.8) is the superposition of the edges from which the maps were formed.

Two final notes. In order for feature synthesis to be effective on the cloth texture image, the edges at the smaller scale should be produced by an operator which is insensitive to slow gradients as described in section (3.5). Otherwise the synthesized large operator output will contain a slowly varying component that will prevent new edges from being marked, even though the small operator did not mark the slow edges. This component is due to the slow gradient "leaking through" the large number of closely spaced edges from the smaller operator. In general feature synthesis is most effective when the two features are independent.

Also the combined output exhibits streaking of the long contours. This is because a single scale factor is presently being used for comparison of real and synthesized outputs. This factor may be viewed as a kind of threshold, and therefore improved performance should be possible by using two values, i.e. by thresholding with hysteresis. This has yet to be tried at the time of writing.

6.2.2. Integration of Directional Masks

Recall from section (3.2) that highly elongated directional operators are preferred whenever they have sufficient goodness of fit to the image. The goodness of fit measure is simply the standard deviation of the gradient values at several points along the length of the directional mask. A directional operator can only mark an edge if the sum of these values exceeds some fixed multiple of their

standard deviation. This prevents a directional operator from responding to curved edges or from extending edge contours beyond corners.

It also makes operator integration much easier. For one thing there will seldom be more than two directional operators responding to an edge of a particular orientation. Also the edges points produced by directional operators will not be displaced significantly from the edges produced by less directional operators if both have the same width. This is because the only way an edge point can be displaced is if the edge is significantly curved, but this will immediately prevent a directional operator from responding to it. Feature synthesis is not necessary for directional operator integration, and a simple non-maximum scheme suffices.

The *non-maximum* suppression scheme was described in section (5.3). The only peculiarity of non-maximum suppression for directional operators is that the direction of non-maximum suppression is fixed a priori for each mask. It is normal to the long axis of the mask. Once all edges have been marked by the directional operators, the simple gradient magnitude is computed. A composite gradient is formed as the maximum of the simple gradient and the magnitude of the directional gradient. This composite gradient is then non-maximum suppressed in the gradient direction. The effect of forming a composite gradient is to prevent simple (non-directional) edges from being marked adjacent to directional ones. An example of the performance of this scheme is given in figure (6.10). The first frame of (6.10) shows the edges marked using simple gradient non-maximum suppression. The second frame shows the addition of directional operators at the same scale. Several additional elongated edges are visible in the second frame. There is no evidence of straightening of curved edges or extension of edges beyond corners.

The edge detector has been used quite extensively by the author in practical systems. The first of these is a contour tracker which locates an edge contour in an image from a television camera, and plans a trajectory for a robot manipulator which follows the contour. The second system forms polygonal approximations to the bounding contours of objects in an overhead image of a robot's workspace. An example of this system is given in figure (6.11). These are then used to plan paths through the workspace which avoid the obstacles. It has also been used by others

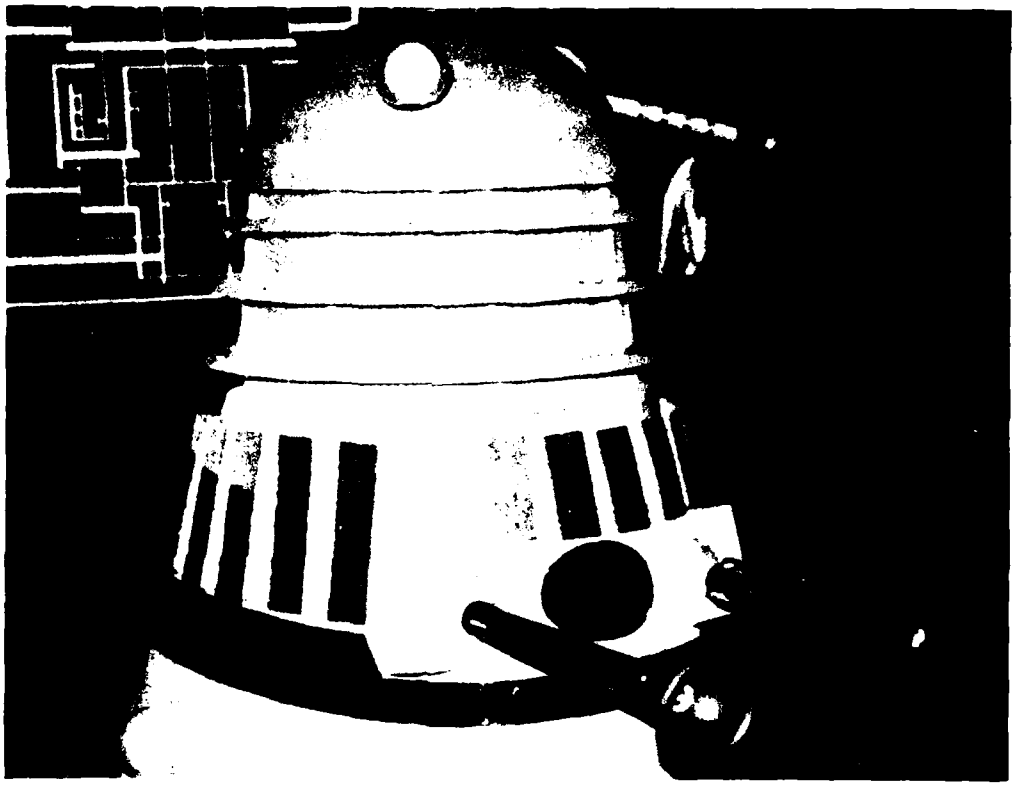

Figure 6.9. Dalek image, approximately 700 by 500 pixels

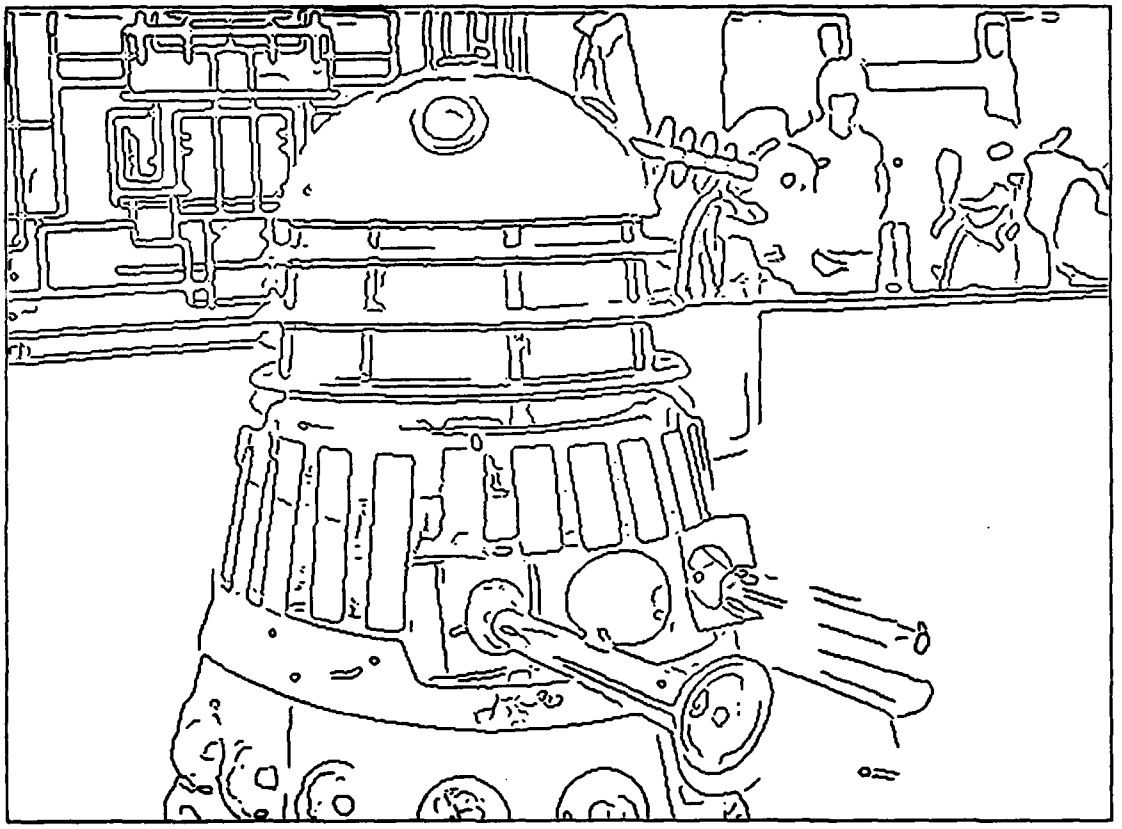

Figure 6.10a. Edges from Dalek image at $\sigma = 2.0$

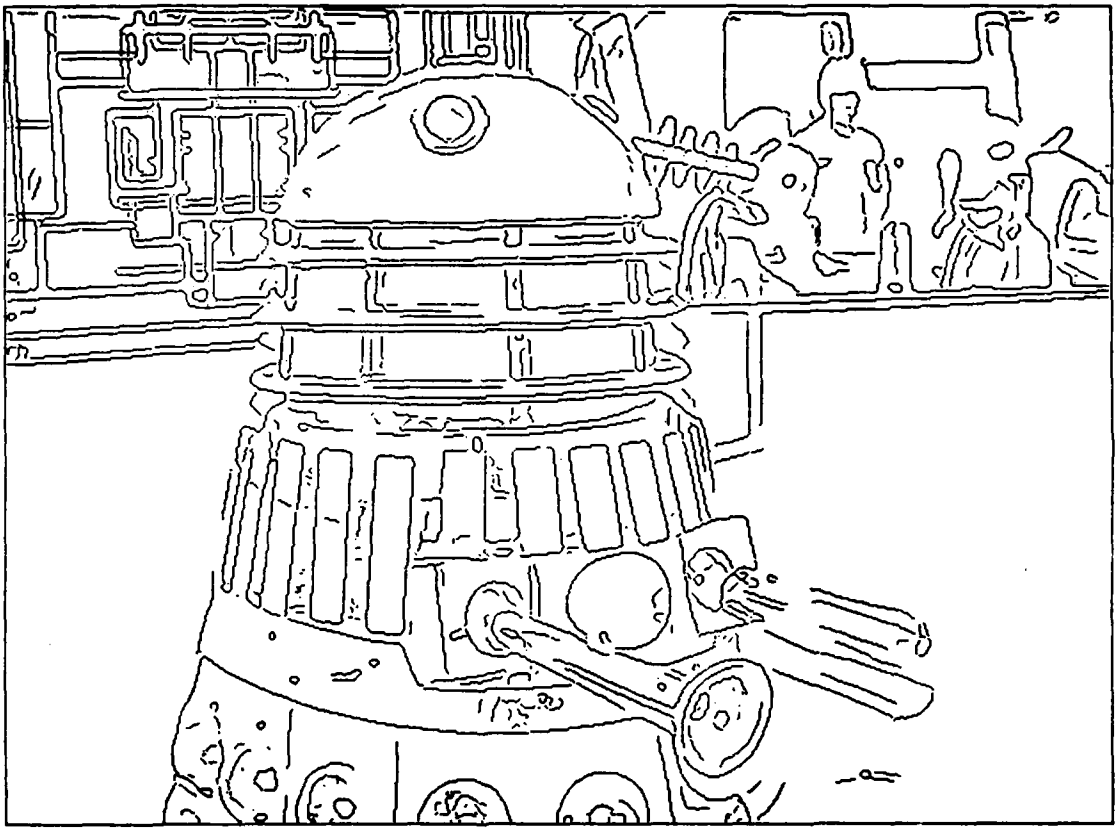

Figure 6.10b. Directional edges from Dalek image at $\sigma = 2.0$, with operators in six directions

in the context of shape description (Brady and Asada 1983). It has been used as a front end for an implementation of the Marr Poggio stereo algorithm (Grimson 1981) but a quantitative comparison with Laplacian of Gaussian zero-crossings in this application has not yet been done. We close this section with examples of the edge detector output on (as promised) a variety of images. These appear in figures (6.12) through (6.15). The images are all roughly 700 by 500 pixels and the time to process each one was about 10 minutes on an MIT Lisp machine with no special hardware.

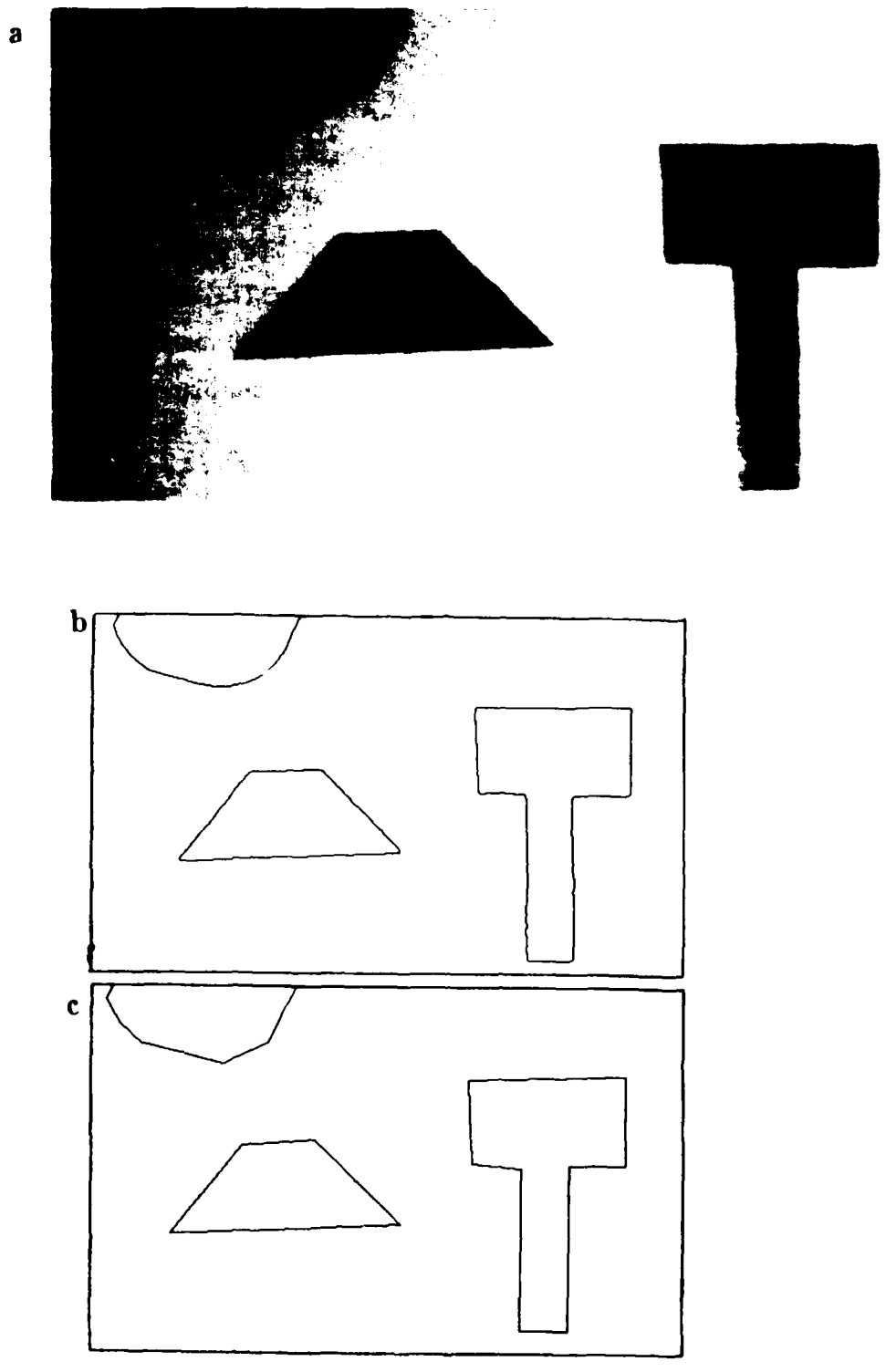

Figure 6.11. (a) Image of some paper shapes, (b) edges from operator width σ = 1.0, (c) bounding polygonal approximation to the edges

Figure 6.12a. Quasimodo image

Figure 6.12b. Edges from Quasimodo image using operator width $\sigma = 1.0$, where edge strength is represented by increasing brightness.

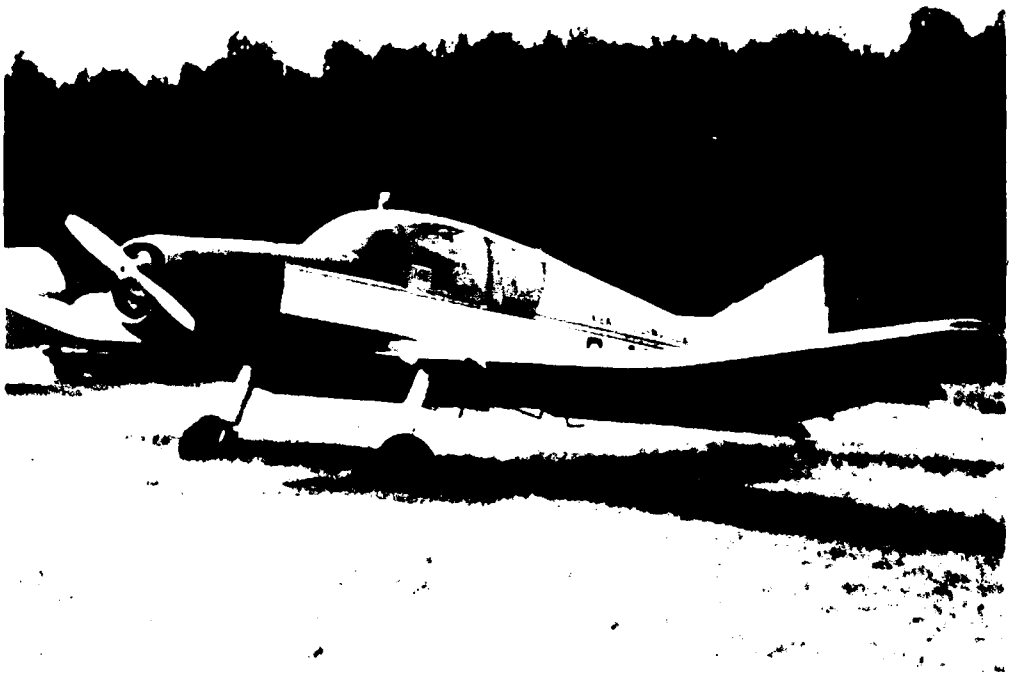

Figure 6.13a. Kent image

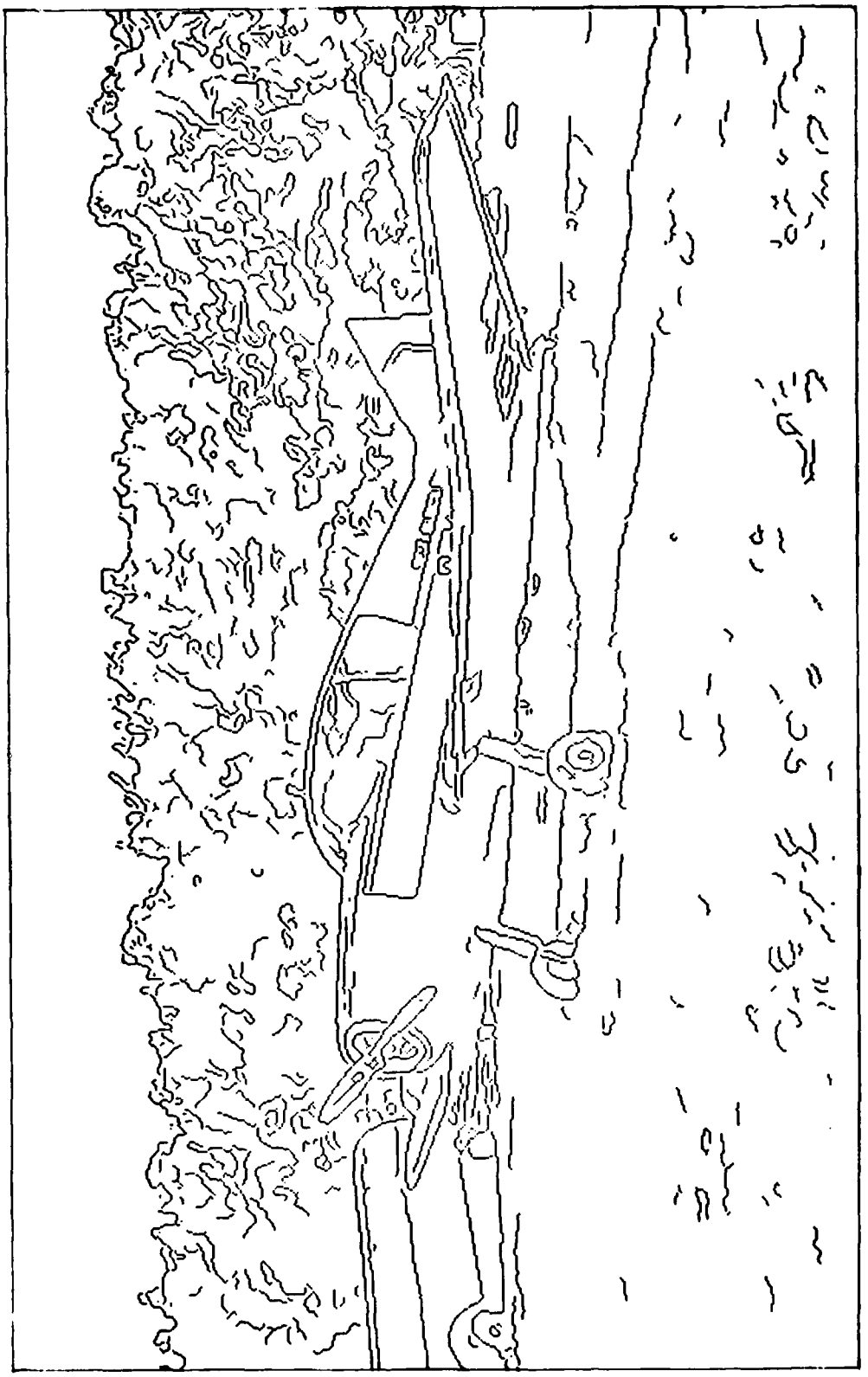

Figure 6.13b. Edges from Kent image using operator width $\sigma = 1.0$

Figure 6.14a. Westminster image

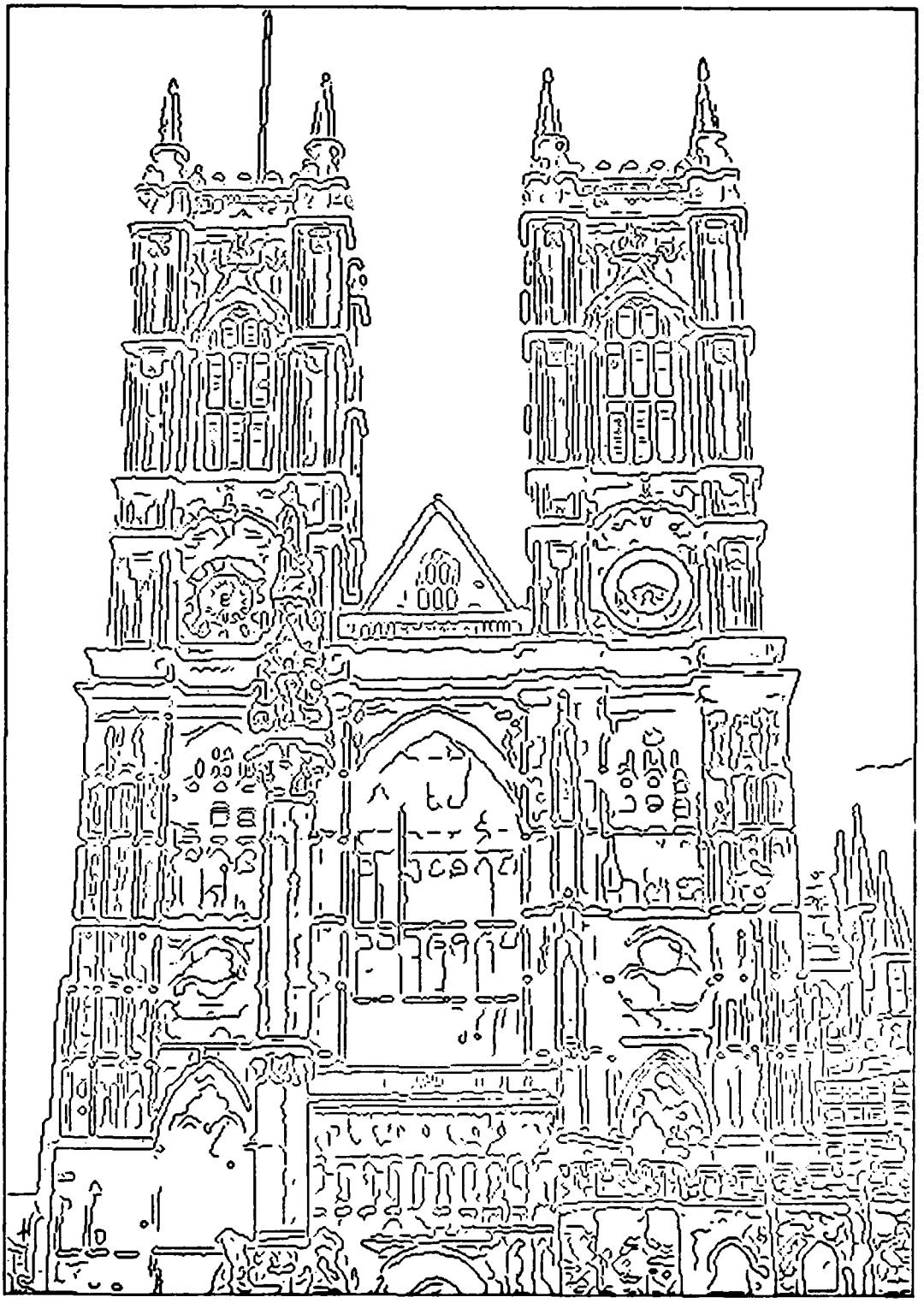

Figure 6.14b. Edges from Westminster image, operator width $\sigma = 1.0$

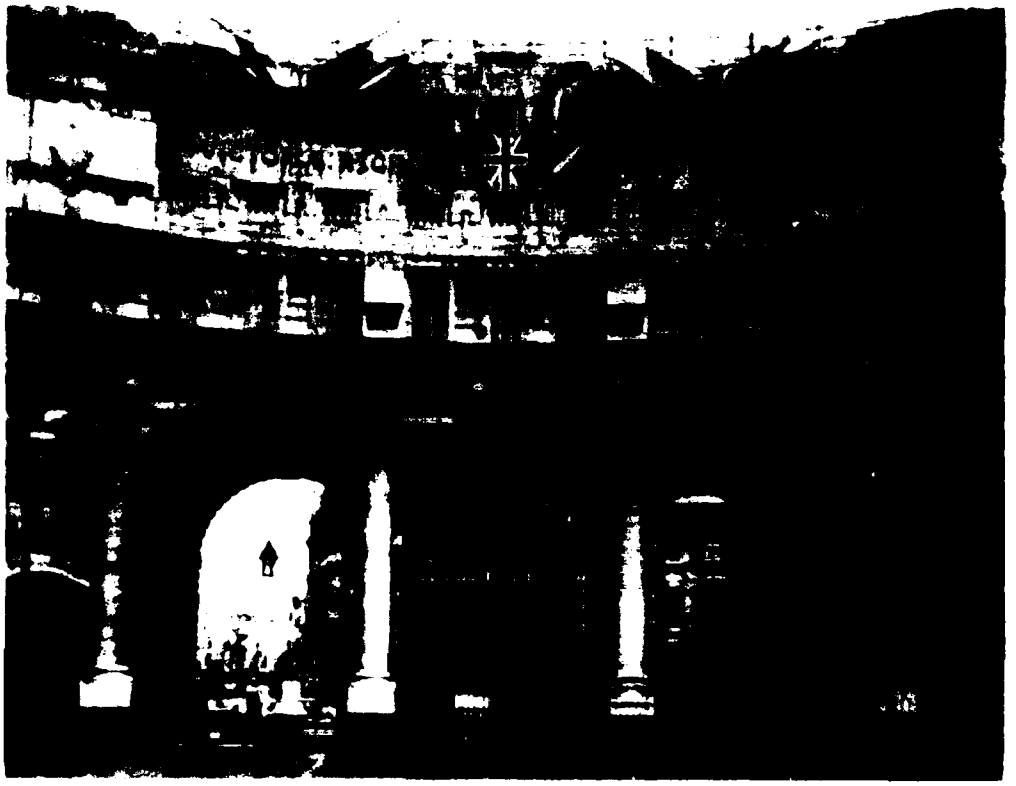

Figure 6.15a. Marine image

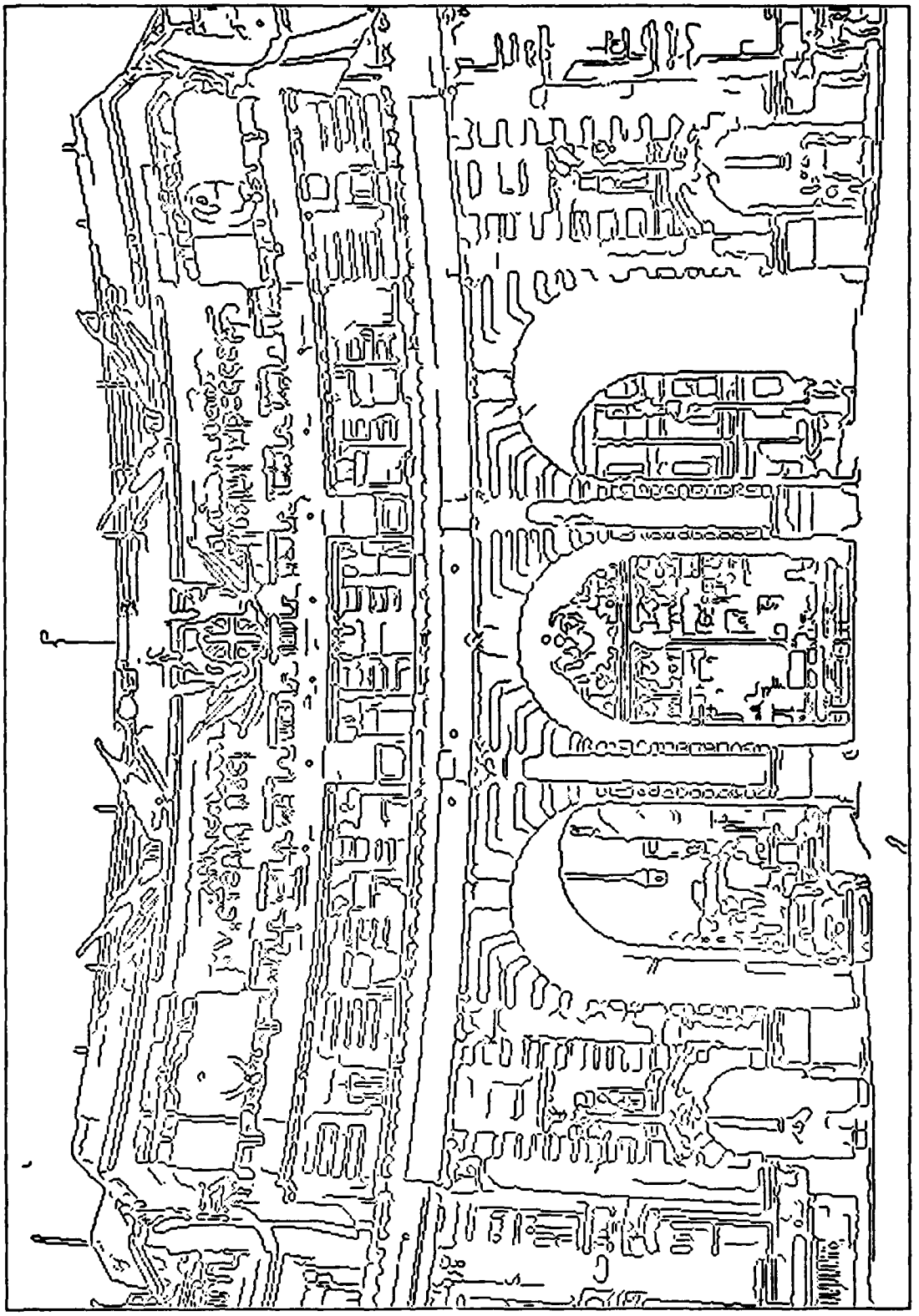

Figure 6.15b. Edges from operator width $\sigma = 1.0$

6.3. The Line Finder

An optimal operator for ridges was derived in chapter 4. It was pointed out that the extension of this operator to two dimensions was more difficult than the edge detector because of the lack of a natural property (such as the gradient) which could be used to determine the ridge orientation. The ridge detector must rely on a much more noisy quantity (which is approximately the direction of maximum curvature) to perform non-maximum suppression. Printed text is a difficult test case for a ridge detector because of the variation in orientation and width, and the presence of junctions. The ridge detector output on some printed text is given in figure (6.16). It uses a second derivative of a Gaussian to approximate the optimal operator derived in section (4.1). For reference, the edge detector output on the same image is given in figure (6.17). The ridge detector output is subjectively more legible, but in many places sections of contour are missing.

In principle it should be possible to incorporate the ridge detector output in the step edge detector using feature synthesis (or some other feature integration approach). This has not been done to the present time and remains a challenge to low level vision schemes.

a

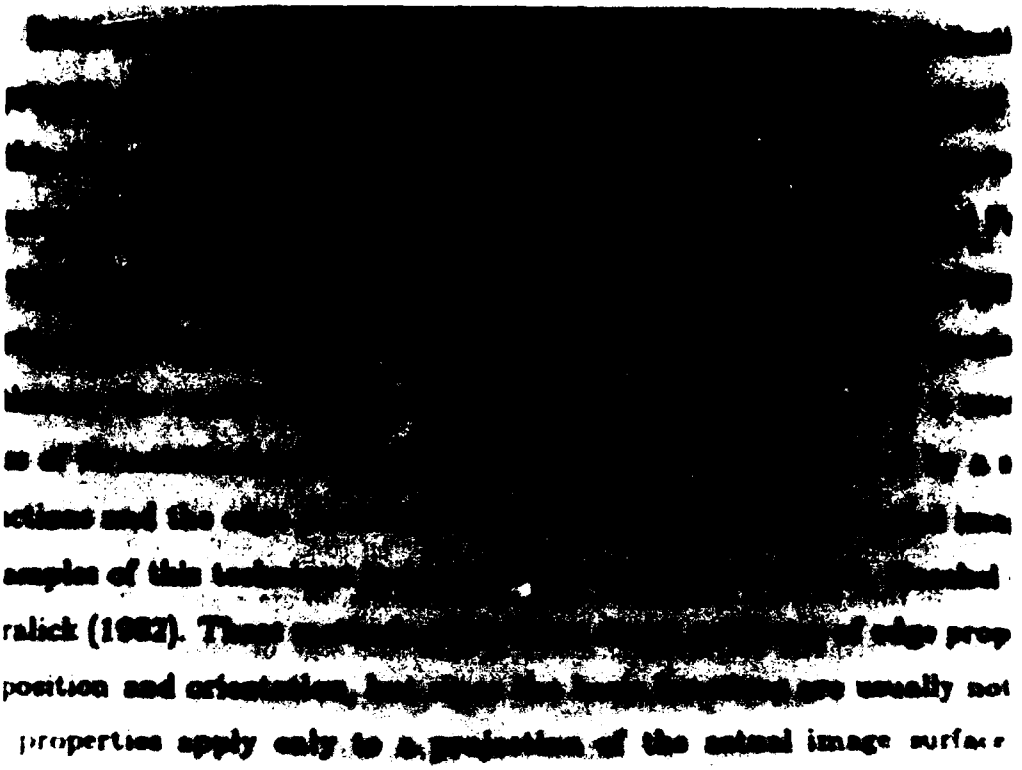

b

Some previous formulations have chosen the first or second derivati
ppropriate quantity to characterize step edges, and have formed optimal
f this derivative over some support. Examples of first derivative operato
perators of Roberts (1965) and Macleod (1970), while Modestino and Fr
ormed an optimal estimate of the two-dimensional Laplacian over a large
lam and Hildreth (1980) suggested the Laplacian of a broad Gaussian
ptimizes the trade-off in localization and bandwidth. There is a seco
lass of formulations in which the image surface is approximated by a s
unctions and the edge parameters are estimated from the modelled imag
Examples of this technique include the work of Prewitt (1970), Hueckel (
Haralick (1982). These methods allow more direct estimates of edge prop
s position and orientation, but since the basis functions are usually not
he properties apply only to a projection of the actual image surface

Figure 6.16. (a) Text image, (b) negative ridge detector output using $\sigma = 0.7$

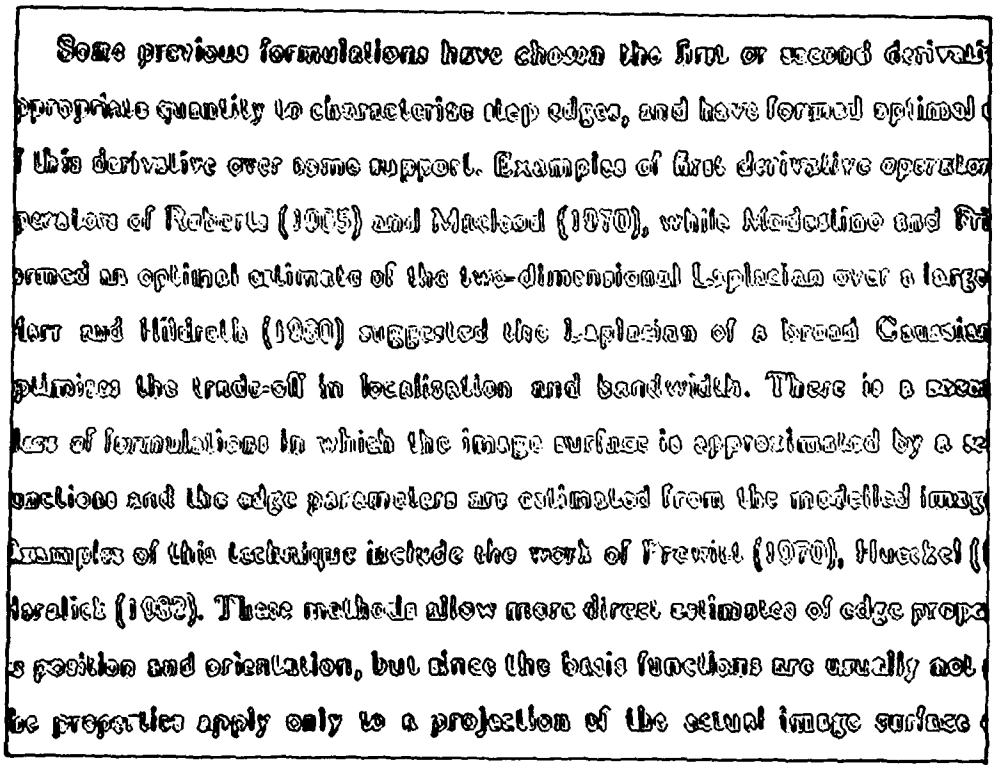

Figure 6.17. Output of the edge detector on the text image, $\sigma = 1.0$

6.4. Psychophysics

We have made a case for a particular set of criteria on effective edge detector and we have claimed that these criteria are common to a variety of applications. In theory any edge detector which is used in these applications should use similar criteria, and an algorithm which is consistent with these criteria. The human visual system provides structural information about the visual field to later processes, and human beings are adept at stereoscopic depth perception. It is reasonable to argue that it should perform edge detection at an early stage.

It is also reasonable (from the arguments given in chapter 3) to suggest that it should use a variety of operator widths and orientations. It should therefore give preference to small operators whenever they have sufficient signal to noise ratio. To test this hypothesis we need somehow to produce an image which has different detail at two scales, and then add noise to see if the percept changes. Such an image is the coarsely sampled picture of Abraham Lincoln used by Harmon and Julesz (1973). The effect of the coarse sampling is to introduce irrelevant detail at small scales. The detail makes the image difficult to perceive unless blurred.

The same effect should be observed if we add noise to the image, because the signal to noise ratio of the small operators will become intolerable before the larger ones. Therefore the smaller channels should be ignored at high noise levels, while the larger channels will still contain coherent information. A coarsely sampled image of a well-known stereo-type (not Lincoln) is shown in figure (6.18). The successive frames have not been blurred but contain increasing amounts of additive *white* Gaussian noise. The later frames are easier to perceive as a human face. We therefore have the remarkable situation that adding incoherent noise to such an image makes it more perceptible.

A second result of the analysis in chapter 3 is that highly directional operators have better signal to noise ratio than less directional operators. The highly directional operators will not be as sensitive to rapid changes in the orientation of an edge contour, and will tend to make a rapidly changing contour appear straighter. Figure (6.19) contains an series of parallel lines which are locally curved but globally straight along their length. The lines are closely spaced so that larger channel

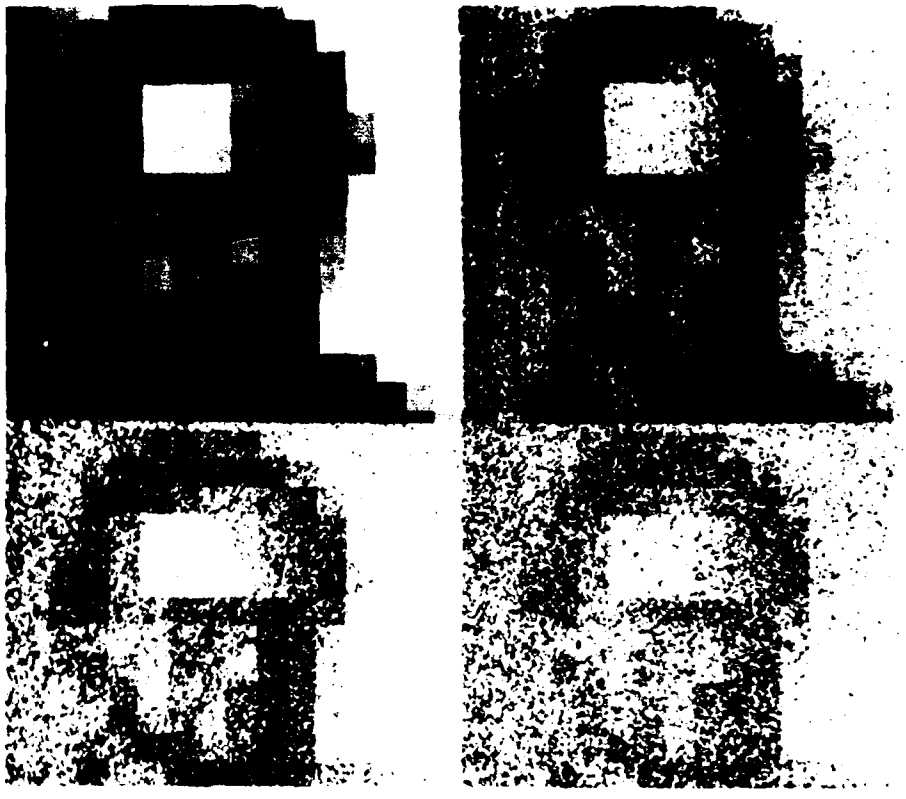

Figure 6.18. Image of a human face with varying amounts of additive white Gaussian noise.

---

widths (which would also tend to give a subjective straightening of the contour) will have poor signal to noise ratio. When noise is added to this image, there is an apparent straightening of the lines.

This would indicate a scheme which, in contrast with the present detector, gives preference to less directional operators when they have sufficient signal to noise ratio. However the apparent inconsistency can be resolved if we use a more sophisticated applicability test for the directional operators. In the present algorithm, directional operators would not be applicable in either of the frames in

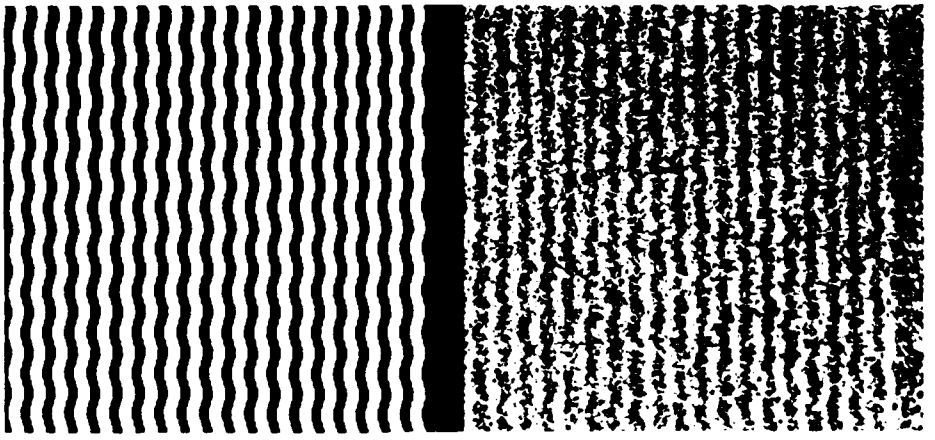

Figure 6.19. Image of approximately parallel lines with sinusoidal variation in direction and additive Gaussian noise

figure (6.19) because of the poor approximation of the contours to straight line The simple standard deviation applicability measure is poor if the edge contour is not straight or breaks at a corner. It is also poor if the image is noisy, but in this case a directional operator is no less applicable. If image noise is taken into account in the applicability metric, we would expect the addition of noise to enhance the applicability of directional operators, consistent with (6.19).

7. Related Work

Now that we have examined in some detail the design of an edge detector using variational techniques, we can contrast it with other schemes with respect to both its design goals and the methods used to attain those goals. In order to consider any appreciable fraction of the great variety of edge detection schemes that have been proposed it is necessary to form a categorization of these schemes. Most schemes in fact do not lie wholly within one of these categories, but retain aspects of several. We will examine several detectors based on their apparent commitment to the following goals

(i) A decision as to the presence of an edge and an estimate of its location from a best-fitting surface that approximates the real image surface.

(ii) To optimally estimate some derivative, usually first or second, at each point in the image and mark edges at local features in these derivative outputs, e.g. zero-crossings in second derivative or maxima in first derivative.

(iii) Frequency domain techniques, which attempt to enhance edges by filtering. Here the filters are designed using frequency domain techniques to optimally discriminate step edges from the background, by assuming some frequency distribution for the background.

All comparisons will be theoretical and generally quantitative, since for early vision level of performance of an algorithm can be crucial. For a more extensive survey the reader is referred to Davis (1975). For experimental comparisons the reader should see Fram and Deutsch (1975), which compares several operators applied to step edges in noise, and includes a comparison with human performance on the same synthetic images. Abdou and Pratt (1979) compare local differential and template matching operators based on a figure of merit which is very similar to the performance criterion used in the present detector. This figure of merit was introduced by Pratt (1978, p495) and is given by

$$F = \frac{1}{\max(I_I, I_A)} \sum_{i=1}^{I_A} \frac{1}{1 + \alpha d^2(i)}$$

where I_I and I_A are the number of ideal and actual edge points, $d(i)$ is the distance of the i^{th} pixel from the true edge, and α is a scaling constant which determines the trade-off between detection and localization.

7.1. Surface Fitting

There are a number of edge detectors that are based on some kind of image surface modelling. These methods usually involve an initial parametrization of the image surface in terms of some set of basis functions followed by the estimation of the amplitude and position of the best-fitting step edge from the parameters. One of the earliest examples of this method was the Prewitt operator (1970), which used a quadratic set of basis functions. Another early example is the detector of Hueckel (1971). Hueckel's method uses basis functions with circular support, and tries to fit a single step edge to each circular area. The basis functions are chosen so as to give an approximate Fourier Transform of the circular region. However, as with most surface fitting schemes, the basis set is not complete (there are only 8 basis functions over a support of 52 pixels) and an edge is actually fitted to a smoothed version of the original surface. An argument is presented to the effect that the choice of a low-frequency subset of the complete space of basis functions does not prejudice the ability of the operator to detect and localize edges, but proof of this is not given. Instead it is argued that the high-frequency components should be ignored because they will contain much of the image noise.

Another example of this approach is the work of Haralick. In Haralick's 1980 article, he proposes a fitting of the image by small planar surfaces or "facets". Edges are marked at points which belong to two such facets when the parameters of the two surfaces are inconsistent. The test for consistency is based on the goodness of fit of each surface within its neighbourhood and uses a χ-squared statistic. Again the initial surface fitting involves a set of parameters which do not completely represent the image surface. In this case there are 3 parameters over a square support of somewhere between 4 and 25 pixels. The three parameters are in fact estimates of the x and y slope and the average value over the support.

In subsequent work on edge detection using a more general surface fitting

technique, Haralick (1982) has used higher order polynomial basis functions with larger operator supports. The later scheme locates edges at zero-crossings in the second derivative of the modelled image surface in the image gradient direction. It uses cubic polynomials (in x and y) as the basis functions over a square support of (typically) 121 pixels. Interestingly, this choice of basis functions yields an operator which can be shown to be quite similar to the operator described in this report. However, if higher order or lower order polynomials are used, performance will be worse. We now demonstrate this similarity.

The polynomials used are the discrete Chebychev polynomials, denoted $P_i(r)$, and for simplicity we will consider a one-dimensional problem. The objective of surface fitting is to find the coefficients a_i such that the sum

$$Q(r) = \sum_{i=0}^{n} a_i P_i(r) \tag{7.8}$$

gives the best square-error fit to the actual sampled image surface $I(r)$. That is we seek to minimize the value of

$$e^2 = \sum_{r=-R}^{R} \Big(I(r) - \sum_{i=0}^{n} a_i P_i(r) \Big)^2 \tag{7.9}$$

We do this by setting to zero the partial derivatives of e^2 with respect to each of the a_j.

$$\sum_{r=-R}^{R} \Big(I(r) - \sum_{i=0}^{n} a_i P_i(r) \Big) P_j(r) = 0$$

This leads to the solution of a system of linear equations in the a_j, but in the case where the polynomials are orthogonal the system is diagonal and the solution is simply

$$a_j = \frac{1}{\rho_j} \sum_{r=-R}^{R} P_j(r) I(r) \tag{7.10}$$

where

$$\rho_j = \sum_{r=-R}^{R} P_j^2(r)$$

The method then estimates the first and second partial derivatives of this modelled surface. For example the first derivative is

$$\frac{d}{dr}Q(r_0) = \sum_{i=0}^{n} a_i \frac{d}{dr}P_i(r_0) \tag{7.11}$$

Substituting equation (7.10) into (7.11) we obtain

$$\frac{d}{dr}Q(0) = \sum_{j=0}^{n} \frac{1}{\rho_j} \sum_{r=-R}^{R} P_j(r)I(r)\frac{d}{dr}P_j(0) \tag{7.12}$$

The important thing to note about this equation is that it is linear in the sampled image intensity, and that therefore the operation of surface fitting followed by derivative estimation can be represented as a single convolution. We find the equivalent filter for this convolution from (7.12). Since this expression has the form of a discrete convolution over r, by removing the summation over r and the input term $I(r)$, we obtain the impulse response of the equivalent filter

$$f(r) = \sum_{j=0}^{n} \frac{1}{\rho_j} P_j(r)\frac{d}{dr}P_j(r_0) \tag{7.13}$$

The derivation of the expression for the second directional derivative is similar. The next step in the surface fitting approach is to mark edges at zero-crossings in the second directional derivative. These will correspond to maxima in the first derivative given above. This puts us in the position of being able to directly compare the surface fitting approach to the variational approach described in this report. Both methods are effectively marking edges at the maxima in the output of the convolution of the image with some linear operator. We can use the optimality criteria that we defined for step edges to (analytically) evaluate the performance of the surface fitting operator.

The form of the equivalent filter depends directly on the choice of basis functions P_i. The equivalent filter for the Chebychev basis polynomials up to degree three is shown in figure (7.1). It turns out that the choice of cubic basis polynomials gives the best approximation to the optimal operator derived in this report. The perceptive reader may note that the surface fitting and gradient estimation procedure is equivalent to convolving with a function that is the best approximation to a derivative function (within the constraints imposed by the basis functions) i.e. the filter has an impulse response that is the first derivative of a delta function. Reference to (7.13) shows that as the order of the basis functions becomes large, the filter $f(r)$ tends to a simple local gradient estimator, similar to the 3-pixel Prewitt operator. The equivalent filter for $n = 7$ is shown in the second frame of figure (7.1).

Thus the 3-order Chebychev polynomials give the best performance with this approach, while higher order polynomials lead to operators that are approximations to local derivative operators. This answers one of the questions raised by Haralick in his article as to what order of polynomial functions is best. The answer to the other question raised, viz. what form of basis functions to use, can also be answered, since his criteria of performance are essentially the same as ours. Note that these criteria were used to experimentally evaluate the performance of the surface fitting operator, but did not appear explicity in the design. The optimal surface fitting operator for step edges would use a single basis function which is the first derivative of Gaussian derived here. Fitting and gradient estimation using this single basis function is equivalent to convolution with the same function.

So we see that the ultimate performance of the surface fitting approach is determined entirely by the choice of basis functions. However, no analysis was done in Haralick (1980) or in Hueckel (1970) as to the optimality of their respective sets of functions. Other advocates of the surface fitting approach have made more detailed analysis of the basis functions. For example Hummel (1978) suggested the use of Karhunen-Loeve principal components for the basis functions.

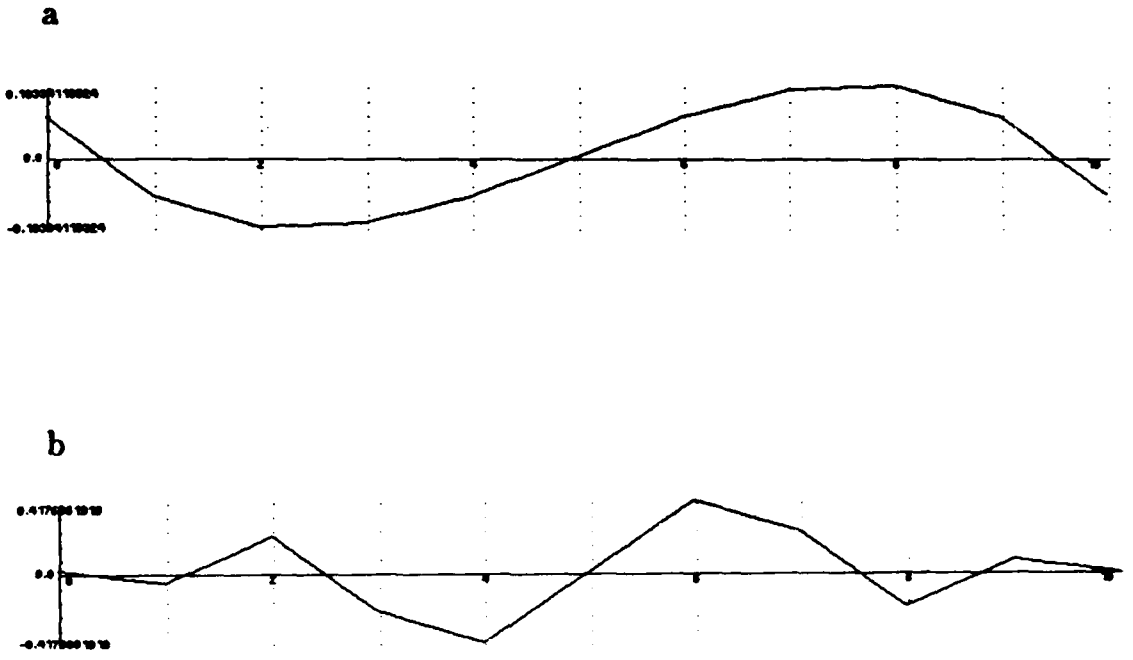

Figure 7.1. Equivalent filters for cubic basis functions (a) and for basis functions to degree 7 (b)

7.2. Derivative Estimation

Since an ideal step edge is a rapid transition from one intensity value to another, it seems that a reasonable way to detect edges is to estimate some derivative of the image intensity surface. First derivative detectors have been proposed by Roberts (1965), Prewitt (1970), Rosenfeld and Thurston (1971), Macleod (1970) and a variety of others. There has also been some interest in operators that estimate the second derivative of the image intensity. The operator of Modestino and Fries (1977) estimates a Gaussian smoothed Laplacian using a computationally efficient

recursive filtering algorithm. Herskovits and Binford (1970) used a form of lateral inhibition to reduce the sensitivity of their operator to slow gradients, and then followed with first and second derivative estimation to locate the edges. Recently there has been interest in operators which locate zero-crossings in the second directional derivative in the gradient direction, viz. Havens and Strikwerda (1983), Torre and Poggio (1983), Yuille (1983) and Haralick (1982).

We should note that the operator derived in chapters 2 and 3 has very strong similarities to two of the above operators. In particular, we have been using the first derivative of a Gaussian to approximate the optimal operator derived in chapter 2. The simplest two-dimensional extension of this used a Gaussian projection function, which results in a two-dimensional operator which is very similar to Macleod's. It also bears a strong resemblance to the Marr-Hildreth operator, at least in one dimension, as we shall see in a moment.

It has been argued in this report that the optimal edge detection function should be asymmetric (see section 2.1), and it may therefore be viewed as a first derivative operator. However, it was not designed to optimally estimate gradient, but to detect step edges. This distinction is subtle, but it should be stressed at this point. The argument for derivative estimation is that the image gradient attains a maximum at the centre of a step edge, and that therefore edges may be detected by finding maxima in gradient. However, it does not follow that gradient is the *best* measure to use to detect and localize edges. Marr and Hildreth (1980) suggest the use of the slope of the output of the Laplacian of Gaussian operator. Again the observation is that this quantity is proportional to the edge strength.

We should really be trying to estimate the "edgeness" of a potential edge. However such a measure can only be defined implicitly by a variational equation, such as equation (2.12). The tendency has been to use *a posteriori* measures, such as gradient or zero-crossings of some derivative, as evidence of edges. The fact that high gradients occur near edges do not mean that all points of high gradient correspond to edges.

Since in one dimension the zero-crossing of second derivative operator (Marr and Hildreth) is essentially the same (ignoring the thresholding question for the

moment) as a maximum of first derivative operator, and both employ Gaussian pre-convolution, we would expect similar performance from the two operators. In two dimensions the extensions are different and performance is noticeably different. We now show that the two dimensional Laplacian of Gaussian gives poorer localization than the directional operator described in chapter 3. Let the two-dimensional Laplacian of Gaussian be described by the equation

$$L(x,y) = \left(\frac{x^2+y^2}{\sigma^2} - 2\right)\exp\left(-\frac{x^2+y^2}{2\sigma^2}\right) \tag{7.14}$$

Now by the method of chapter 3, the standard deviation of the position of the zero-crossing is the quotient of the slope of the zero-crossing at the edge centre and the root mean squared noise in the operator output. Let the input be a step of amplitude A in the y direction, i.e. the equation of the input $S(x,y)$ is

$$S(x,y) = Au_{-1}(x)$$

Then the slope of the zero-crossing is

$$\frac{d}{dx_0}\int_{-\infty}^{x_0}\int_{-\infty}^{+\infty} AL(x,y)\,dy\,dx \tag{7.15}$$

and the root mean squared output noise is

$$n_{00}\left[\int_{-\infty}^{+\infty}\int_{-\infty}^{+\infty} L^2(x,y)\,dy\,dx\right]^{\frac{1}{2}} \tag{7.16}$$

Dividing (7.15) by (7.16) and substituting from (7.14) we find that the localization Λ_L of the Laplacian of Gaussian is just

$$\Lambda_L = 1$$

We compare this against the localization of a directional operator aligned with the edge. Let the point spread function of this operator be described by the equation

$$D_x(x,y) = \left(\frac{x^2}{\sigma^2} - 1\right)\exp\left(-\frac{x^2+y^2}{2\sigma^2}\right) \tag{7.17}$$

Again we find the quotient of (7.15) and (7.16) and substitute from (7.17) and we obtain for the localization of this operator

$$\Lambda_D = \sqrt{\frac{8}{3}} \approx 1.63$$

So on average we would expect the positional error of the Laplacian of Gaussian to be about 60% greater than that of a directional operator of the same σ.

It has been suggested that the strength of a zero-crossing may be estimated from the slope of the zero-crossing (normal to the edge direction). We should also compare the signal to noise ratio of this measure with signal to noise ratio of the first directional derivative. The slope of the zero-crossing of a Laplacian of Gaussian is again given by equation (7.15), while the noise in this value can be found from the integral

$$n_{00}\left[\int_{-\infty}^{+\infty}\int_{-\infty}^{+\infty}\left(\frac{d}{dx}L(x,y)\right)^2 dy\,dx\right]^{\frac{1}{2}} \tag{7.18}$$

This gives the Laplacian of Gaussian a signal to noise ratio Σ_L, formed from the quotient of equations (7.15) and (7.18), of

$$\Sigma_L = \sqrt{\frac{2}{3}}\sigma$$

Finally we compare this value with the signal to noise ratio of the two-dimensional directional derivative operator

$$D(x,y) = x\exp\left(-\frac{x^2+y^2}{2\sigma^2}\right)$$

which turns out to have a Σ value of

$$\Sigma_D = 2\sigma$$

This comparison shows that the directional first derivative operator betters the Laplacian of Gaussian (with slope estimation) by a factor of slightly greater than 2 with respect to signal to noise ratio, and by a factor of about 1.6 with respect to localization. In terms of the composite criterion $\Sigma\Lambda$ we find that

$$\Sigma_D\Lambda_D = 4\Sigma_L\Lambda_L$$

The above result shows that the slope of a zero-crossing is a very poor estimator for edge strength. While there are other possible choices for the edge amplitude estimator, we also find that the Laplacian of Gaussian still suffers in localization by comparison with a directional operator. The intuitive reason for this is that the two-dimensional Laplacian may be decomposed into the sum of second derivatives in (any) two orthogonal directions. If one of these is chosen to be normal to the edge direction, it is clear that this contribution is exactly that of a directional operator. But the second component, which will be parallel to the edge direction, contributes nothing to localization but will increase the amount of noise.

7.3. Frequency Domain Methods

In this (rather small) category, we find one particular example of an approach which used criteria very similar to ours, using a frequency domain derivation. We might expect this formulation to lead to an operator very similar to ours. In fact it did not, but this was due to a rather unfortunate restriction placed on the possible solution. When the restriction is removed, we again obtain a function which approximates a first derivative of a Gaussian.

The method is that of Shanmugam et al (1979), who proposed the use of a two-dimensional linear operator that approximates the Laplacian of a Gaussian. Their criteria of optimality were that the function maximize the proportion of total output energy confined to a fixed interval when it is convolved with a step edge. Also the function must be strictly band-limited. These two criteria approximately

capture those of the present design. Maximizing the proportion of total output energy in the interval will limit the range over which the maximum in the response to a step edge can occur. Band-limiting greatly improves output signal to noise ratio, since the spectrum of Gaussian noise is flat while the spectrum of a step edge varies as the inverse of frequency, i.e. most of the energy in the edge is concentrated at low frequencies.

Unfortunately, there are two steps in the method of Shanmugam et al which the present author finds hard to justify. The first is that they made no attempt to mark edge points, but instead thresholded filtered values were output. In fact their filter gives two peaks in its response to an ideal step, but these are on either side of the centre of the step, and the response at the centre is actually zero. This was rectified to some extent in the work of Marr and Hildreth (1980) who used the zero-crossings of the same filter, since these features occur at the centre of step edges.

A second problem is that they assumed a priori that the operator they were looking for would be trivially extensible to two dimensions by rotating it about an axis of symmetry. This immediately restricted them to symmetric operators, even in one dimension where the design was done. As we have seen in chapter 3, this restriction is unnecessary, and actually degrades performance. In fact if the restriction is removed, the same analysis leads to an operator that approximates the first derivative of a Gaussian, as used in the current design. We repeat their design without the assumption of symmetry now.

Once again we perform an optimization to find the function that extremizes one criterion while another is kept constant. In this case the bandwidth of the response Ω will be fixed while the fraction of total output energy in an interval $[-I/2, +I/2]$ is maximized. i.e. if the output response is $g(x)$ and the fraction of the energy in the interval is α, we maximize

$$\alpha = \frac{\int_{-I/2}^{+I/2} |g(x)|^2 \, dx}{\int_{-\infty}^{+\infty} |g(x)|^2 \, dx} \tag{7.1}$$

We can make use of the fact that there exists a set of functions $\psi_i(x)$ the

prolate spheroidal wave functions, that are band-limited, orthogonal over the interval $[-I/2, +I/2]$ and orthonormal over $(-\infty, +\infty)$. i.e.

$$\int_{-\infty}^{+\infty} \psi_i(x)\psi_j(x)\,dx = \begin{cases} 0, & i \neq j \\ 1, & i = j \end{cases} \qquad i, j = 0, 1, 2, \ldots \tag{7.2}$$

$$\int_{-I/2}^{+I/2} \psi_i(x)\psi_j(x)\,dx = \begin{cases} 0, & i \neq j \\ \lambda_i, & i = j \end{cases} \qquad i, j = 0, 1, 2, \ldots \tag{7.3}$$

with $\lambda_i \leq 1$ for all i, and $\lambda_0 > \lambda_1 > \lambda_2 > \ldots$

The prolate spheroidal wave functions are complete in the space of band-limited functions, and hence the output from any band-limited filter can be represented as

$$g(x) = \sum_{n=0}^{\infty} a_n \psi_n(c, x) \tag{7.4}$$

Where the constant c is a function of the bandwidth and the size of the interval

$$c = \frac{\Omega I}{2}$$

When the expansion for $g(x)$ is substituted into (7.1) using the results of (7.2) and (7.3), the value of α becomes

$$\alpha = \frac{\sum_{n=0}^{\infty} |a_n|^2 \lambda_n}{\sum_{n=0}^{\infty} |a_n|^2} \tag{7.5}$$

The λ_i are all positive and $\lambda_0 > \lambda_1 > \lambda_2 > \ldots$, so α is bounded by

$$0 < \alpha < \frac{\lambda_0 \sum_{n=0}^{\infty} |a_n|^2}{\sum_{n=0}^{\infty} |a_n|^2} = \lambda_0 < 1$$

The upper bound is attained when $a_n = 0$ for $n > 0$, so the optimal output is

$$g(x) = a_0 \psi_0(c, x) \tag{7.6}$$

Since this is the desired step response of the filter, we can obtain the impulse response $f(x)$ by differentiation.

$$f(x) = a_0 \frac{d}{dx} \psi_0(c, x) \tag{7.7}$$

An approximation to the functions $\psi_n(c, x)$ due to Slepian (1965) can be used to find a closed form expression for $f(x)$.

$$\psi_n(c, x) = (\frac{c}{2})^{\frac{1}{4}} 2^{-\frac{n}{2}} (n!)^{-\frac{1}{2}} H_n(c^{\frac{1}{2}} x) \exp\left(\frac{cx^2}{2}\right)$$

where $H_n(x)$ is a Hermite polynomial of degree n. This approximation is useful for $x < c^{-1/4}$ and $n < c$. So $\psi_0(c, x)$ may be approximated by a Gaussian for small x, and the optimal spatial function $f(x)$ will be the first derivative of a Gaussian as before

$$f(x) = (kx) \exp\left(\frac{-cx^2}{2}\right)$$

In their original article, when Shanmugam et al (1979) assumed that the function $f(x)$ should be symmetric, they were restricted to the odd prolate spheroidal functions ignoring $\psi_0(c, x)$ which in fact gives the best performance. The $\lambda_i(c)$ may be used as performance indices since they measure the fraction of the total energy in the specified region for the corresponding ψ_i. The values of λ_0 may be significantly higher than those of λ_1 for small values of c. The small values of c imply that the product of spatial and frequency extent are minimal. For example at $c = 0.5$ the value of λ_0 is about 0.3 while the value of λ_1 is 0.0086 (see Slepian 1960).

The intent of this chapter has been to put the present edge detector in context with several other well-known schemes. We have seen that there are strong similarities in analytic form with several of these schemes, in particular with the detectors of Marr and Hildreth, Macleod, Haralick and Shanmugam et al. There are also important differences, for example we have not yet considered the use of multiple operators or of highly directional masks. Rosenfeld (1971) used several

sizes of difference of boxes, and formed a composite edge map by giving preference to the largest operator which did not have a significantly lower response than the next smaller operator. Marr (1976) argued both for highly directional operators and for multiple scales, but reneged on the first requirement in later articles (1980) mostly because of the apparent difficulty in implementating them. The present design produces an edge map which is very similar in principle to the 1976 version of the primal sketch, which was motivated purely by computational considerations.

8. Conclusions and Suggestions for Further Work

We began this report with a precise definition of a set of goals for edge detection and proceeded to derive an operator which best achieved these goals. The goals were carefully chosen with minimal assumptions about the form of an optimal edge operator. The constraints imposed were that we would mark edges at the maxima in the output of a linear shift-invariant operator. By expressing the criteria as functionals on the impulse response of the edge detection operator, we were able to optimize over a large solution space, without imposing constraint on the form of the solution.

Using this technique with an initial model of a step edge in white Gaussian noise, in chapter 2 we found that there was a fundamental limit to the simultaneous detection and localization of step edges. This led to a natural uncertainty relationship between the localizing and detecting abilities of the edge detector. This relationship in turn led to a powerful constraint on the solution, i.e. that there is a class of optimal operators all of which can be obtained from a single operator by spatial scaling. By varying the width of this operator it is possible to vary the trade-off in signal to noise ratio versus localization, at the same time ensuring that for any value of one of the quantities, the other will be maximized.

It was then found that the goals as originally specified were not well defined, or rather that the analytic criteria did not articulate all that we expected of the edge detector. By adding an explicit criterion related to multiple responses, we were able to obtain an operator that met all of our intuitive design goals. The multiple response constraint did add considerable complexity to the form of the solution and in fact it was not possible to realize a solution in fully closed form. However, the analysis was able to constrain the solution to a finite (low) dimensional parameter space over which a numerical solution could be obtained. The impulse response of the operator is a sum of damped exponential cosines, and it can be approximated by the first derivative of a Gaussian.

We then extended the above operator to two dimensions and in doing so we followed the framework that was established for the one-dimensional formulation

in chapter 2. The basic criteria of detection and localization were the motivating concerns in the extension to two dimensions. It was found that multiple operator widths were necessary to deal with different signal to noise ratios in an *image* because of the trade-off described above. We also found that directional operators have clear advantages over non-directional operators, and that the more directional an operator is, the better its potential performance. The traditional problems associated with highly directional operators were dealt with by using a goodness of fit measure to decide whether each directional operator could be used. We then faced the considerable problem of combining all these feature descriptions into a coherent whole. Once again we used the same set of design goals to guide the heuristics for choosing the appropriate operator. Feature synthesis was presented as a means of combining the outputs of operators whose responses to the same feature are not necessarily spatially coincident.

The first selection heuristic was to give preference to operators of minimum width provided they had sufficient signal to noise ratio. This gives maximum resolution and localization for a given global signal to noise ratio. The combination of different operator widths was difficult because of the lack of spatial coincidence of different operator outputs. It was necessary to use feature synthesis (examples were given in chapter 6) for the operator integration.

The second heuristic was to favour highly directional operators whenever they have sufficient quality of fit to the image. The integration of different operator orientations was relatively simple and required only a slightly more complicated form of non-maximum suppression. Examples of this technique were given in chapter 6. It is unclear which goodness of fit measure should be used, and although an algorithm was presented which performs adequately, there was no demonstration of its optimality. In fact there is some evidence (section 6.4) that the human visual system, which in other respects demonstrates similarities to the detector described here, uses a different (or more complicated) decision procedure.

To make the convolution of images with the optimal operator more efficient, a first derivative of a Gaussian approximation was used. This allowed us to use any of the efficient algorithms presented in section 3.2 to speed things up. It was found

that there exists an approximately "linear" time (in the width of a square mask) algorithm for doing convolutions with arbitrary masks, and so efficient convolution is possible even without the approximation. Experiments are now being performed to determine the practicality of implementing this scheme in hardware.

In chapter 4 we were able to generalize the method used for step edges in white Gaussian noise to arbitrary features and to non-white but stationary random noise. In addition to a general form for the criteria, a fast numerical method for the solution was described. This technique was then used to find optimal operators for ridge and roof features. The ridge detector was extended to two dimensions, and this was found to be much more difficult than for the edge operator because of the lack of reliable information about the ridge direction. An example of the ridge detector output appears in section (6.3), and was compared to the edge detector on the same image.

Finally in chapters 6 and 7 some comparisons were made between the edge detector derived here, the Marr-Hildreth (1980) operator and the difference of boxes operator. There were both analytic and experimental comparisons. It was also compared to two other edge operators, those of Haralick (1982) and of Shanmugam et al. (1979), and was found to be similar to all of these in one dimension. Chapter 6 also included several examples of the edge detector output on some natural scenes. Finally we saw in section 6.5 some perceptual effects which seem to indicate that the human visual system uses a similar feature combination scheme.

There are several directions in which the work in this report could be continued. The most obvious is probably the area of integration of feature descriptions. The algorithm as described in this report includes a feature synthesis method to combine output of several operators of differing width. It could potentially be used to combine the outputs of detectors for different features, such as the ridge detector described in chapter 4. It may be possible to form criteria on the performance of a feature integration scheme. Two possible criteria are

(i) The integration scheme should not miss features. If a single feature is marked by one of the detectors, it should be marked in the integrator output. Also, if two feature detectors are responding at the same point in a way that is

not consistent with there being only a single feature in the image, then the integrator should mark both features on the output.

(ii) The integration scheme should produce an output with minimal redundancy. An obvious scheme which performs well according to criterion (i) would be to simply mark everything seen by any feature detector. In this case no integration of feature information is occurring, e.g. it is unnecessary to mark a ridge as two parallel closely spaced edges if it has already been identified for what it is. The feature integrator may be viewed as a filter on the outputs of all the feature detectors which removes redundant information.

Both of the above criteria require a scheme which is non-local, that is it must take into account the outputs of nearby feature detectors, not just those at a single point. Feature synthesis is a non-local scheme as is the surface fitting approach used in the Topographic Primal Sketch of Haralick (1983). It would be worth comparing the two schemes according to the above criteria. The difficulty with using an optimization scheme to find an optimal feature integrator is that a much more complicated image model would be necessary. At the very least it would need to include all those features for which the individual detectors were designed, and presumably all possible combinations of those features.

Another possible extension of the edge detector would be to 3 or more dimensions. We have already seen in chapter 3 that there is a simple extension of the optimal operator to n dimensions. This operator locates $n - 1$ surfaces (the n-dimensional extension of edge contours) where discontinuities in intensity occur. Using highly directional operators is more difficult in this domain because of the large number of directions needed to uniformly cover an n-sphere. Non-maximum suppression is also more complicated for the same reason.

In particular it is possible to consider the detection of moving edges as a three dimensional edge detection problem, where the third dimension is the time axis. Edges in this three dimensional space correspond to edges in the two-dimensional image or to points of rapidly changing irradiance. The direction of the edge in the three-space can be used to determine the velocity of the two-dimensional edge. There is a constraint that the time-space edge filter must be causal, that is it must

depend only on past and present intensity values. Using a filter that is broad in the time domain will introduce a delay into the velocity estimate. Thus the design of the time domain filter is a separate optimization problem which requires additional constraints of causality and minimal time delay.

One final generalization of the techniques described in this report would be to relax the restriction of linearity on the operator. Shift invariance is clearly a desirable property of an edge detection operator, but it is not clear that the optimal operator must be linear. In fact the composite operator derived in this report is non-linear because it involves a non-local predicate (from the feature synthesis scheme) applied to several operator outputs. Ideally this constraint should be either relaxed or it should be proven that linear operators can perform as well as non-linear operators. The restriction to linear operators here was necessary because of the sheer complexity of parametrizing a non-linear shift invariant operator in a form which would allow variational methods to be applied. It remains to be seen whether this restriction penalizes performance, and whether an unconstrained non-linear operator can do any better.

Appendix I. Definite Integrals used in the Derivations

These integrals were referred to in chapter 2 but were not included there because of their excessive length. There are 3 integrals required to evaluate (2.12), and an additional integral is neccesary for (2.24). Of these 4 integrals, 3 can be written in the same parametric form, because they all involve the integral of the square of a function of the form

$$g(x) = c_1 e^{ax} \sin \omega x + c_2 e^{ax} \cos \omega x + c_3 e^{-ax} \sin \omega x + c_4 e^{-ax} \cos \omega x$$

We now define

$$I_1(c_1, c_2, c_3, c_4) = \int_{-1}^{0} g(x)\, dx \qquad \text{and} \qquad I_2(c_1, c_2, c_3, c_4) = \int_{-1}^{+1} g^2(x)\, dx$$

And we find that all of the integrals in the performance criteria can be written in terms of I_1 and I_2 thus

$$\int_{-1}^{0} f(x)\, dx = I_1(a_1, a_2, a_3, a_4) + c$$

$$\int_{-1}^{+1} f^2(x)\, dx = I_2(a_1, a_2, a_3, a_4) + 4cI_1(a_1, a_2, a_3, a_4) + 2c^2$$

$$\int_{-1}^{+1} f'^2(x)\, dx = I_2(\alpha a_1 - \omega a_2,\ \alpha a_2 + \omega a_1,\ -\alpha a_3 - \omega a_4,\ -\alpha a_4 + \omega a_3)$$

$$\int_{-1}^{+1} f''^2(x)\, dx = I_2(\beta a_1 - \gamma a_2,\ \beta a_2 + \gamma a_1,\ \beta a_3 + \gamma a_4,\ \beta a_4 - \gamma a_3)$$

where

$$\beta = \alpha^2 - \omega^2 \qquad \text{and} \qquad \gamma = 2\alpha\omega$$

The closed form for the definite integral I_1 in terms of α, ω, and c_1 through c_4 and for a unit interval ($W = 1$) is

$$\begin{aligned} I_1(c_1, c_2, c_3, c_4) = \frac{1}{\alpha^2 + \omega^2}\Big(& c_1 e^{\alpha}(\alpha \sin\omega - \omega\cos\omega) + \omega c_1 \\ & + c_2 e^{\alpha}(\omega \sin\omega + \alpha\cos\omega) - \alpha c_2 \\ & + c_3 e^{-\alpha}(\alpha \sin\omega + \omega\cos\omega) - \omega c_3 \\ & + c_4 e^{-\alpha}(\omega \sin\omega - \alpha\cos\omega) + \alpha c_4 \Big) \end{aligned}$$

Similarly the closed form for I_2 over the unit interval is

$$\begin{aligned} I_2(c_1, c_2, c_3, c_4) = \frac{1}{2\alpha\omega^3 + 2\omega\alpha^3}\Big(& c_1^2 e^{2\alpha}(-\alpha\omega^2 \sin 2\omega - \alpha^2\omega\cos 2\omega + \omega^3 + \alpha^2\omega) - c_1^2\omega^3 \\ & + c_2^2 e^{2\alpha}(\alpha\omega^2 \sin 2\omega + \alpha^2\omega\cos 2\omega + \omega^3 + \alpha^2\omega) \\ & - c_2^2(\omega^3 + 2\alpha^2\omega) \\ & + c_3^2 e^{-2\alpha}(-\alpha\omega^2 \sin 2\omega + \alpha^2\omega\cos 2\omega - \omega^3 - \alpha^2\omega) + c_3^2\omega^3 \\ & + c_4^2 e^{-2\alpha}(\alpha\omega^2 \sin 2\omega - \alpha^2\omega\cos 2\omega - \omega^3 - \alpha^2\omega) \\ & + c_4^2(\omega^3 + 2\alpha^2\omega) \\ & + 2c_1c_2 e^{2\alpha}(\alpha^2\omega \sin 2\omega - \alpha\omega^2\cos 2\omega) + 2c_1c_2\alpha\omega^2 \\ & + 2c_1c_3(\alpha^3 + \alpha\omega^2)(2\omega - \sin 2\omega) \\ & - 4(c_1c_4 + c_2c_3)(\alpha^3 + \alpha\omega^2)\sin^2\omega \\ & + 2c_2c_4(\alpha^3 + \alpha\omega^2)(2\omega + \sin 2\omega) \\ & + 2c_3c_4 e^{-2\alpha}(-\alpha^2\omega \sin 2\omega - \alpha\omega^2\cos 2\omega) + 2c_3c_4\alpha\omega^2 \Big) \end{aligned}$$

9. References

Abdou I. E. and Pratt W. K. "Quantitative Design and Evaluation of Enhancement/Thresholding Edge Detectors," *IEEE Proc.* **67, No. 6** (1979), 753-763.

Binford T. O. "Inferring Surfaces from Images," *Artificial Intelligence* **17** (1981), 205-244.

Bingham C., Godfrey M.D., Tukey J.W. "Modern Techniques of Power Spectrum Estimation," *IEEE Trans. A.E.* **AU-15, No 2** (1967), 56-66.

Brady J. M. and Asada H. "Smoothed Local Symmetries and their Implementation," *To appear* (1983).

Courant R. and Hilbert D. *Methods of Mathematical Physics, vol. 1* , Wiley Interscience, New York, 1953.

Davis L. S. "A Survey of Edge Detection Techniques," *Computer Graphics and Image Processing* 4 (1975), 248-270.

Fram J. R. and Deutsch E. S. "On the Quantitative Evaluation of Edge Detection Schemes and Their Comparison with Human Performance," *IEEE Trans. Computers* **C-24, No. 6** (1975), 616-628.

Grimson W. E. L. *From Images to Surfaces* , MIT Press, Cambridge, Ma., 1981.

Hamming R. W. *Digital Filters* , Prentice Hall, New Jersey, 1983.

Haralick R. M. "Edge and Region analysis for Digital Image Data," *Computer Graphics and Image Processing* **12** (1980), 60-73.

Haralick R. M. "Zero-crossing of Second Directional Derivative Edge Operator," S.P.I.E. Proceedings on Robot Vision, Arlington Virginia, 1982.

Haralick R. M., Watson L. T. and Laffey T. L. "The Topographic Primal Sketch," *Robotics Research* **To appear (1983).**

Havens W. S. and Strikwerda J. C. "An Improved Operator for Edge Detection," *To appear* (1983).

Herskovits A. and Binford T. "On Boundary Detection," M.I.T. Artificial Intelligence Laboratory, Cambridge Mass., AI Memo 183, 1970.

Hildreth E. C. "Implementation of a Theory of Edge Detection," M.I.T. Artificial Intelligence Laboratory, Cambridge Mass., AI-TR-579, 1980.

Hildreth E. C. "The Measurement of Visual Motion," Ph.D. Thesis, Dept. of Electrical Engineering and Computer Science, MIT, Cambridge, Ma., 1983.

Horn B. K. P. "The Binford-Horn Line-Finder," M.I.T. Artificial Intelligence Laboratory, Cambridge Mass., AI Memo 285, 1971.

Horn B. K. P. "Obtaining Shape from Shading Information," *The Psychology of Computer Vision* P.H. Winston, ed., McGraw Hill, New York, pp 115-155, 1975.

Hueckel M. H. "An Operator Which Locates Edges in Digitized Pictures," *JACM* **18, No. 1** (1971), 113-125.

Hummel R. A. "Edge Detection Using Basis Functions," *Computer Graphics and Image Processing* **9** (1979), 40-55.

Jacobus C. J. and Chien R. T. "Two New Edge Detectors," *IEEE Trans. P.A.M.I.* **PAMI-3, No. 5** (1981), 581-592.

Liskov B., Atkinson R., Bloom T., Moss E., Schaffert C., Scheifler B., and Snyder A. "CLU Reference Manual," MIT Laboratory for Computer Science, TR-225, 1979.

Luenberger D. G. *Introduction to Linear and Non-Linear Programming* , Addison-Wesley, Reading, Ma., 1973.

Macleod I. D. G. "On Finding Structure in Pictures," *Picture Language Machines* S. Kaneff ed. Academic Press, New York, pp 231, 1970.

Marr D. C. "Early Processing of Visual Information," *Phil. Trans. R. Soc. Lond.* **B 275** (1976), 483-524.

Marr D. C. and Hildreth E. "Theory of Edge Detection," *Proc. R. Soc. Lond.* **B 207** (1980), 187-217.

Marr D. C. and Poggio T. "A Theory of Human Stereo Vision," *Proc. R. Soc. Lond.* **B 204** (1979), 301-328.

Modestino J. W. and Fries R. W. "Edge Detection in Noisy Images Using Recursive Digital Filtering," *Computer Graphics and Image Processing* **6** (1977), 409-433.

Moon D., Stallman R. M., Weinreb D. "Lisp Machine Manual," MIT Cambridge, Ma., 1983.

Pentland A. P. "Local Shape from Shading," Ph.D. Thesis, Dept. of Psychology, MIT, Cambridge, Ma., 1982.

Pratt W. K. *Digital Image Processing* , Wiley Interscience, New York, 1978.

Prewitt J. M. S. "Object Enhancement and Extraction," *Picture Processing and Psychopictorics* B. Lipkin & A. Rosenfeld Eds, Academic Press, New York, pp 75-149, 1970.

Rice S. O. "Mathematical Analysis of Random Noise," *Bell Sys. Tech. J.* **24** (1945), 46-156.

Roberts L. G. "Machine Perception of 3-Dimensional Solids," *Optical and Electro-Optical Information Processing* J. Tippett, D. Berkowitz, L. Clapp, C. Koester, A. Vanderbergh Eds, M.I.T. Press, Cambridge, pp 159-197, 1965.

Rosenfeld A. and Thurston M. "Edge and Curve Detection for Visual Scene Analysis," *IEEE Trans. Computers* **C-20, No. 5** (1971), 562-569.

Schonhage A., and Strassen V. "Schnelle Multiplikation grosser Zahlen," *Computing* **7** (1971), 281-292.

Shanmugam K. S., Dickey F. M. & Green J. A. "An Optimal Frequency Domain Filter for Edge Detection in Digital Pictures," *IEEE Trans. P.A.M.I.* **PAMI-1, No. 1** (1979), 37-49.

Slepian D. "Some Asymptotic Expansions for Prolate Spheroidal Wave Functions," *J. Math. Phys. MIT* **44** (1965), 99.

Stevens K. A. "Surface Perception from Local Analysis of Texture and Contour," M.I.T. Artificial Intelligence Laboratory, Cambridge Mass., AI-TR-512, 1980.

Torre V. and Poggio T. "A Directional Second Derivative Zero-crossing Operator," To appear, 1983.

Ullman S. *The Interpretation of Visual Motion* , MIT Press, Cambridge, Ma., 1979.

Wiener N. *Extrapolation, Interpolation and Smoothing of Stationary Time Series* , MIT Press, Cambridge, Mass., 1949.

Witkin A. P. "Shape from Contour," M.I.T. Artificial Intelligence Laboratory, Cambridge Mass., AI-TR-589, 1980.

Yuille A. "Zero-Crossings on Lines of Curvature," M.I.T. Artificial Intelligence Laboratory, Cambridge Mass., To appear, 1983.

END

DATE
FILMED

8 — 83

DTIC